Aalto University
School of Chemical
Technology

School of Chemical Technology
Degree Programme of Materials Science and Engineering

Essi Velin

THE EFFECT OF TEMPERATURE ON THE ZETA POTENTIAL OF MAGNETITE PARTICLES IN AMMONIA, MORPHOLINE AND ETHANOLAMINE SOLUTIONS

Master's thesis for the degree of Master of Science in Technology submitted for inspection, Espoo, 9 December, 2013.

Supervisor Professor Olof Forsén

Instructor D. Sc. (Tech.) Timo Saario

Aalto University
School of Chemical
Technology

Aalto University, P.O. BOX 11000, 00076 AALTO
www.aalto.fi
Abstract of master's thesis

Author Essi Velin

Title of thesis The Effect of Temperature on the Zeta Potential of Magnetite Particles in Ammonia, Morpholine and Ethanolamine Solutions

Department Material Science and Engineering

Professorship Corrosion and Hydrometallurgy **Code of professorship** MT-85

Thesis supervisor Professor Olof Forsén

Thesis advisor(s) / Thesis examiner(s) D. Sc. (Tech.) Timo Saario

Date 09.12.2013 **Number of pages** 97+8 **Language** English

Abstract

In nuclear power plants, flow accelerated corrosion releases magnetite particles from the surfaces of the feed water pipes. When these colloidal particles reach the steam generator, they can deposit to the surfaces of the steam generator and produce possibly dangerous and expensive material and thermal degradation phenomena. This deposition is presumed to be affected by the surface charge of the particles, which can be described with the zeta potential.

In this thesis, the zeta potential of magnetite particles in ammonia, morpholine and ethanolamine solutions were measured at the temperatures from 23˚C to 248˚C. The zeta potential measurements were conducted with a streaming potential measuring equipment designed for these measurements. The change in the pressure difference over the column containing magnetite powder and the change in the potential difference between platinum electrodes situated at the both ends of the column were measured as a function of the velocity of the water flow. The resulting $\Delta E/\Delta P$ was then multiplied with a calculation constant which consisted of the dimensions of the magnetite column, the resistance of the column and the viscosity and the actual permittivity of the solution. In order to conclude these measurements, the measuring equipment was first updated for higher measuring temperatures.

The aim of this thesis was to determine how the zeta potential of magnetite particles changes as a function of temperature when the pH at room temperature is 9.2. It was found out that at room temperature magnetite has a negative zeta potential in ammonia, morpholine and ethanolamine solutions. Increasing temperature resulted in a decrease of the zeta potential magnitude. Near the operational temperature of the steam generator, zeta potential seemed to approach a small but still negative value in all cases. A low zeta potential value can be interpreted as an indication of rather weak repulsive forces between the colloidal magnetite particles and an increased possibility for coagulation and deposition.

Keywords zeta potential, magnetite, steam generator, PWR, pressurized water reactor, electrical double layer, ethanolamine, morpholine, ammonia

Tekijä Essi Velin

Työn nimi Lämpötilan vaikutus magnetiitin zeta-potentiaaliin ammoniakki-, morfoliini- ja etanoliamiiniliuoksissa

Laitos Materiaalitekniikka

Professuuri Korroosio ja hydrometallurgia **Professuurikoodi** MT-85

Työn valvoja Professori Olof Forsén

Työn ohjaaja(t)/Työn tarkastaja(t) Timo Saario, TkT

Päivämäärä 09.12.2013 **Sivumäärä** 97+8 **Kieli** englanti

Tiivistelmä

Virtauksen kiihdyttämä eroosio-korroosio (FAC) irrottaa magnetiittipartikkeleita ydinvoimaloiden syöttövesiputkien pinnoilta. Kun nämä partikkelit kulkeutuvat voimalan höyrystimeen, ne voivat saostua höyrystimen pinnoille ja aiheuttaa monia mahdollisesti vaarallisia ja kalliita materiaalinvaurioitumismekanismeja ja hyötysuhteen huononemista. Partikkelien pintavarauksen uskotaan vaikuttavan saostumiseen. Tätä pintavarausta voidaan kuvata zeta-potentiaalilla.

Tässä diplomityössä magnetiittipartikkelien zeta-potentiaalia mitattiin ammoniakki-, morfoliini- ja etanoliamiiniliuoksissa huoneenlämpötilasta 248 °C:een. Zeta-potentiaalin mittaus suoritettiin streaming potential -mittauslaitteistolla, joka oli kehitetty näitä mittauksia varten. Mittausten aikana liuoksen virtausnopeutta vaihdeltiin samalla kun mitattiin aiheutunut muutos paine-erossa magnetiittipulverista muodostuneen pylvään päiden välillä sekä muutos pylvään päihin sijoitettujen platinaelektrodien välisessä potentiaalierossa. Saatu $\Delta E/\Delta P$ kerrottiin laskentavakiolla, joka koostuu magneettipylvään mitoista, pylvään resistanssista ja liuoksen viskositeetista ja permittiivisyydestä. Jotta mittaukset voitiin suorittaa, mittauslaitteisto päivitettiin toimimaan korkeammissa mittauslämpötiloissa kuin ennen.

Tämän diplomityön tarkoitus oli kyseisten mittausten perusteella määrittää, kuinka magnetiitin zeta-potentiaali muuttuu lämpötilan kasvaessa emäksisessä liuoksessa, jonka pH huoneenlämpötilassa on 9.2. Johtopäätöksenä voidaan esittää, että magnetiitilla oli huoneenlämpötilassa negatiivinen zeta-potentiaali sekä ammoniakkia, morfoliinia ja etanoliamiinia sisältävissä liuoksissa. Lämpötilan noustessa zeta-potentiaalin itseisarvo pieneni. Ydinvoimalan höyrystimen toimintalämpötiloja lähestyttäessä zeta-potentiaali vaikutti lähestyvän nollaa pysyen silti negatiivisena. Zeta-potentiaalin pienen itseisarvon voidaan tulkita tarkoittavan sitä, että kolloidisten magnetiittipartikkelien välillä on vain pieni hylkivä sähköstaattinen vuorovaikutus, jolloin koaguloitumisen ja saostumisen riski kasvaa.

Avainsanat Zeta-potentiaali, magnetiitti, höyrystin, PWR, painevesireaktori, sähköinen kaksoiskerros, etanoliamiini, morfoliini, ammoniakki

Foreword

The work for this thesis was conducted at the VTT Technical Research Centre of Finland, in the research group TK2024 Chemical environments in power plants, during a time period from June 2013 to December 2013. This thesis is part of the WAPA (Water Chemistry and Plant Operating Reliability) project of the SAFIR 2014 (Safety of Nuclear Power Plants – Finnish National Research Programme).

First, I would like to thank my supervisor Professor Olof Forsén for reviewing my thesis and giving me valuable advice and sincere support during this thesis and during all my studies at the Department of Material Science and Engineering. Professor Forsén's deep knowledge upon corrosion and electrochemistry has made a great impact on me.

I would like to express sincere gratitude to my instructor Dr Timo Saario as he shared his broad knowledge with me. I am thankful for his constant encouragement, help and guidance during the process. I also want to thank Dr Petri Kinnunen for providing me the opportunity to write this thesis at the VTT. Special thanks belong to Konsta Sipilä for providing me continuous help with all research equipment along with his own work.

I also want to thank Tiina Ikäläinen for helping me with calibrating the measuring equipment. Pasi Väisänen, Aki Toivonen and Jyrki Ranta are thanked for helping with everything in the research hall. Saija Väisänen earns my thanks for providing valuable proposals for improvement of the research equipment.

Johanna Lukin is acknowledged for preparing the magnetite samples for the measurements. I am also grateful for Seppo Peltonen and Tuomo Kinnunen for giving valuable advice concerning research equipment. Marketta Mattila, Taru Lehtikuusi and Asta Nurmela are being thanked from their kind help and guidance. I am thankful for Arto Nyholm for manufacturing necessary parts for the research equipment. All other co-workers are thanked as well for their help and advice and for taking me into the working community.

Finally, I would like to thank my family, relatives and friends. My warmest thanks go to my parents Ritva and Timo for their loving support and encouragement and to my dear brother Tuomo for his humor and words of wisdom. To conclude, I am deeply grateful for my fiancé Voitto for his love, support and patience.

Espoo, the 9th of December 2013

Essi Velin

Contents

Symbols and abbreviations

3MPA	3-methoxypropylamine
a	radius of the magnetite column
Ag/AgCl	silver / silver chloride
AMP	2-amino-2-methyl-propanol
AVT	all-volatile-treatment
CANDU	Canadian deuterium-uranium reactor
CPS	Condensate Polishing System
Cr	chromium
DMA	dimethylamine
ETA	monoethanolamine
FAC	flow accelerated corrosion
Fe	iron
Fe(OH)	iron hydroxide
Fe_3O_4	magnetite
H	hydrogen
H_2O	water
H-AVT	hydrazine based all-volatile-treatment
HNO_3	nitric acid
I_c	conduction current
IER	Ion Exchange Resin filter/bed
IGA	Intergranular Attack
I_s	streaming current
KNO_3	potassium nitrate

l	length of the magnetite column
Mo	molybdenum
Morph	morpholine
MPH	morpholine
MRPC	Multifrequency rotating pancake coil probe
N_2H_4	hydrazine
NaOH	sodium hydroxide
NaTr	sodium trifluoromethanesulfonate
NH3	ammonia
OD(I)A	Outer Diameter(-Intergranular) Attack
ODSCC	Outer Diameter Stress Corrosion Cracking
PAA	polyacrylic acid
Pb	lead
Pd	palladium
ppb	parts per billion
Pt	platinum
PTFE	Polytetrafluoroethylene
PWR	pressurized water reactor
PWSCC	Primary Water Stress Corrosion Cracking
R	inverse of the conductivity of the flow path; resistance of the magnetite column
SCC	stress corrosion cracking
SGBD	Steam generator Blowdown Demineralizer
WWER	(Russian) water moderated, water cooled energy reactor
Z	impedance
α-Fe_2O_3	hematite

γ-FeOOH	lepidocrocite
δ	phase shift
ΔE	change in the potentials of measuring electrodes
ΔP	change in the pressure difference over the magnetite column
ε_0	the permittivity of free space
ε_{rs}	relative permittivity
ζ	zeta
η	viscosity of the solution
ψ^d	potential of the outer Helmholtz plane: diffuse-layer potential: Stern potential
ψ^i	potential of the inner Helmholtz plane
ω	angular frequency

1. Introduction

Steam generators are an important component in the nuclear power plants as they limit the life time of the secondary circuit (EPRI 1997a). They create steam out of the water of the secondary circuit and this steam is used to produce electricity. However, the performance of the steam generators can be affected by several phenomena which are caused by corrosion product deposition.

One of these corrosion products is magnetite, Fe_3O_4. Magnetite forms a passive layer on the surfaces of carbon steel feed water pipes and is removed from there as particulates by flow accelerated corrosion. When these magnetite particles are circulated with feed water to the steam generator, they begin to form deposits on the steam generator tubes, tube support plates and other components. These deposits affect the performance of the steam generator mainly by two different ways: the deposits themselves hinder the heat transfer of the steam generator but they also make the impurities, such as chlorides and sulphates, concentrate, which can cause several types of corrosion phenomena.

An important way of preventing these thermal efficiency losses and corrosion problems is to maintain magnetite particles in a colloidal form so they will not attach to the surfaces of the steam generator. This can be achieved by altering water chemistry with certain amines. Some amines, like morpholine and ethanolamine, are used to increase the pH and simultaneously affect the surface charge of the magnetite particles and thus keeping them colloidal. Others are used as ‘filming amines’ which are supposed to improve the stability of the passive layer on the feed water line components and piping.

The surface charge of the particles is one of the most important aspects affecting the particle attachment to the surfaces. The sign and the magnitude of the surface charge of the particles can be described with zeta potential. The main purposes of this thesis are to measure zeta potential values for the magnetite particles in ammonia, morpholine and ethanolamine solutions at temperatures up to 248˚C, to develop the measuring equipment for that and to estimate how the temperature affects the zeta potential of the magnetite particles in those solutions.

In this thesis, the zeta potential is measured by using the method of streaming potential. This is accomplished by measuring the potential difference and the pressure difference over a column of magnetite particles when changing the velocity of water flow through the column. This information combined to the measurements of the impedance of the magnetite column is used for the calculations of the zeta potential. Measurements are repeated at different temperatures the highest of them being 248˚C which is the average temperature of some older steam generators, like the ones being used in the Loviisa nuclear power plant.

There have been several studies concerning the zeta potential of the magnetite particles but only few measurements have been made at higher temperatures (Wesolowski et al. 2000. Barale et al. 2008. Vidojkovic et al. 2011). There are no studies concerning the zeta potential of magnetite particles in ammonia, morpholine or ethanolamine solutions at high temperatures. Thus, there are no studies conducted at the temperatures of the steam generator in the solutions used in the nuclear power plants before this thesis.

This thesis also includes a literature survey which intends to describe dissolution and deposition of magnetite particles, to explain which kind of problems magnetite deposits can produce, and have produced, in the steam generators and how these problems can be minimized. Also the concepts of the electrical double layer and the electrokinetic phenomena are introduced shortly to explain the background of the experimental part of the thesis. The aim of the literature survey is to clarify the importance of the experiments and to justify the methods used in them.

This thesis is part of the WAPA (Water Chemistry and Plant Operating Reliability) project which is part of the national programme SAFIR 2014 (Safety of Nuclear Power Plants – Finnish National Research Programme). The purpose of the WAPA is to study dissolution and deposition of corrosion products both in the primary and secondary circuits of nuclear power plants.

2. Literature review

2.1 Steam generators

The steam generator makes steam by heating secondary side coolant with primary side coolant. This steam is used for electricity generating in the turbine generators. Therefore the steam generator is an essential component in the most of the nuclear power plants. In fact, steam generators are used in every power plant that has more than two circuits of cooling, i.e. the pressurized water reactor (PWR), the Canadian deuterium-uranium (CANDU) reactor and the Russian water moderated, water cooled energy reactor (WWER). Every reactor has normally two to six steam generators, but there have also been reactors with twelve steam generators. Each of these steam generators has several thousands of heat exchanging tubes. Primary water flows inside these tubes and boils the secondary coolant, which is outside of these tubes. (IAEA 2011, p. 1)

Besides its primary purpose of generating steam, the steam generator has an important radiation safety impact also, as it separates the primary coolant with radioactive species from the non-radioactive secondary coolant. As the primary coolant has higher pressure, it is necessary to maintain the integrity of steam generator tubes, in order to control radioactivity. (IAEA 2011, p. 2) This is not an easy task, as steam generator tubes have a very large surface; their surface area is typically in the range of several thousand square meters (Schwarz 2001). Because of that, over 60% of the area of the pressure-retaining boundary of the primary circuit is in the steam generator tubes (Tipping 1996. IAEA 2011, p. 2).

In the case of a fast depressurization of the secondary circuit, which may lead to severe damage in the steam generator tubes, it is even possible that there will be dangerous radiation transients and depressurization of the primary circuit which can lead to the melting of the core. Therefore steam generator tubes must not contain any cracks or other major material defects. (IAEA 2011, p. 2) This makes the steam generator an interesting component not only from the material science and engineering point of view but also from the safety point of view.

Several types of steam generators made by different manufacturers are in use. These types are divided to recirculating steam generators, once through steam generators, CANDU reactor steam generators and WWER steam generators. The recirculating steam generator is the most common steam generator type. In the recirculating steam generator (Figure 1), about 25 % of the secondary water is transformed to steam, and the rest is recirculated. In the once through model (Figure 2), the water goes through the steam generator only once. In the recirculating steam generator, the tubes are U-shaped; in the once through steam generator they are straight. (IAEA 2011, p. 3-16) The CANDU steam generators are very similar to the recirculating steam generators but they are smaller and have lower temperatures (Tapping et al. 2000. IAEA 2011, p. 11-13). The hot leg of the recirculating steam generator typically has the temperature of 315-330°C and the cold leg around 288°C. In the CANDU steam generators, the hot leg is normally between 290°C and 310°C. The WWER steam generators are positioned horizontally and they have special collector plates. The hot leg of the WWER steam generator is between 300°C and 330°C and the cold leg between 270°C and 300°C. (IAEA 2011, p. 3-17)

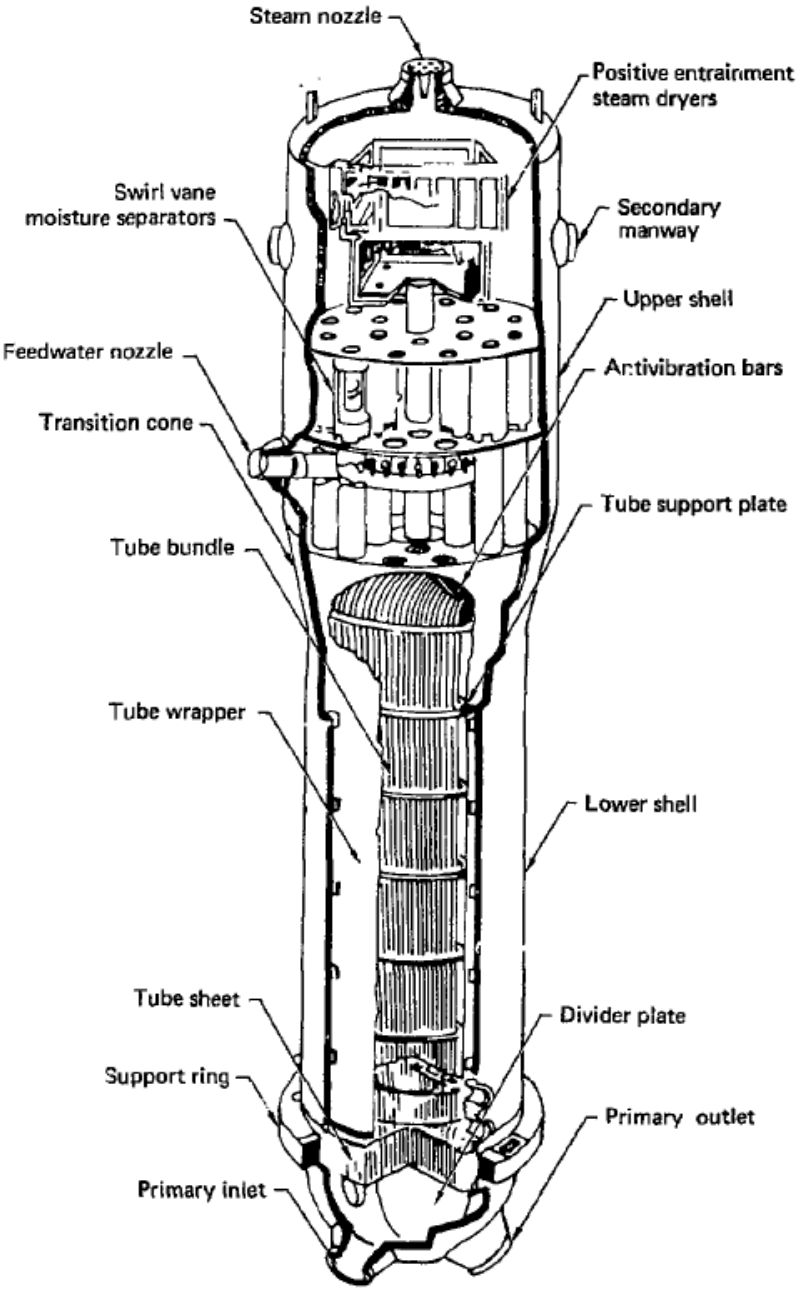

Figure 1: The recirculating steam generator (Woo & Lu 1981)

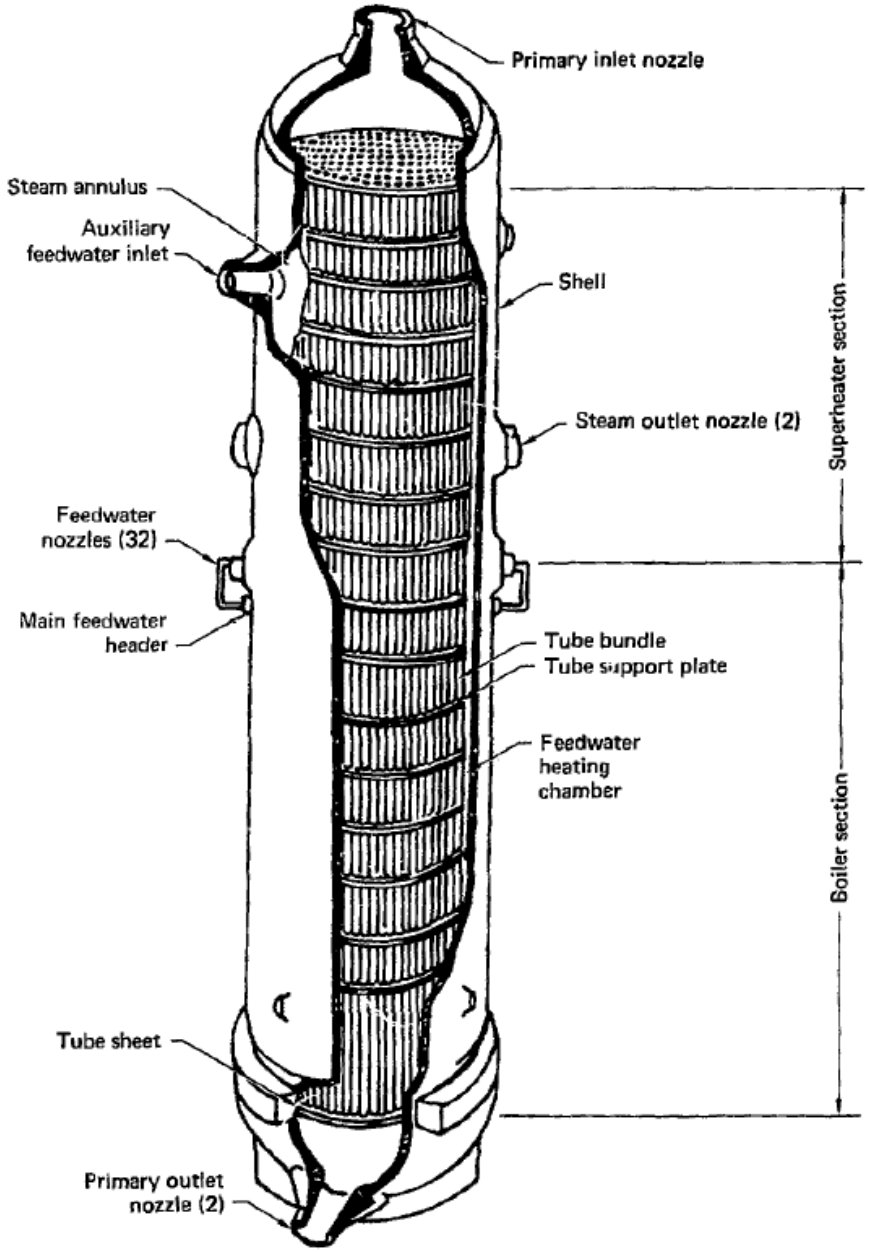

Figure 2: The once through steam generator (Woo & Lu 1981)

The very first steam generator tubes were made of austenitic stainless steels (Harrod et al. 2001). In the WWERs, like the Loviisa nuclear power plant, stainless steel steam generator tubes have been used successfully and are still in use (Wilam & Čermáková 1995. IAEA 2011, p. 21-23). Starting from the late 1960s, stainless steel was replaced in the PWRs mainly with nickel based Alloy 600 MA (Ni-16Cr-10Fe) because of its assumed immunity to chloride stress corrosion cracking (SCC) and other corrosion types (Harrod

et al. 2001). Soon after that almost all steam generator tubes in the western countries were made of Alloy 600 (Harrod et al. 2001. Odar & Nordman 2010. IAEA 2011, p. 22-23). Mill annealed Alloy 600 was then gradually replaced by thermally treated Alloy 600 in order to affect intergranular carbide precipitations (Harrod et al. 2001). German manufacturer Siemens changed in the early 1970s to Alloy 800NG (Fe-33Ni-22Cr) because of its better resistance to stress corrosion cracking (IAEA 2011, p. 21).

Today most new steam generator tubes are made from Alloy 690TT or Alloy 800NG. Alloy 690TT (Ni-30Cr-10Fe) has twice as much chromium as Alloy 600 and is much less susceptible to primary water stress corrosion cracking. (Harrod et al. 2001. IAEA 2011, p. 21-23) It also has better resistance towards secondary side corrosion. The other good alternative, Alloy 800NG is stabilized with titanium and has better corrosion properties than Alloy 600. Alloy 800NG is also used in the CANDU steam generators. WWER-440 steam generator tubing material is titanium-stabilized austenitic stainless steel 08Ch18N10T. (IAEA 2011, p. 21-23)

Also other materials must be considered when thinking of the steam generators, as the other materials in the secondary circuit affect to the steam generator. Traditionally plain carbon steels have been used for pipes and components on the secondary side. (Odar & Nordman 2010) The support plates of the steam generators are typically made from carbon steels as well, although recently some manufacturers have replaced carbon steels with stainless steels (IAEA 2011, p. 26). Condensers and feed water heat exchangers were made of copper alloys (Odar & Nordman 2010) and have been gradually replaced with more corrosion resistant materials, e.g. high-alloyed stainless steels or titanium alloys (IAEA 2011, p. 51).

Material selection and ensuring the integrity of materials of critical components are very important not only when considering the safety of the nuclear power plant but also when thinking of the economy. Changing of the steam generator is a hard and expensive task and it can cost $100-200 million (EPRI 1997a), when all the power losses and changing costs are considered. Steam generators are designed originally to have a life time of 40 years (EPRI 1997a). Therefore plant owners want to make sure that the degradation of materials stays at the level that can be managed. This has not always been easy.

2.2 History and current state of material degradation of steam generators

Problems in the steam generators have varied greatly in the history. Most problems have been caused by bad material and water chemistry choices, by bad design solutions and by lacking knowledge upon material behaviour and corrosion phenomena in certain environments. The very first steam generators were designed after the steam generators used in conventional, fossil fuelled power plants. Water chemistry and materials were also copied from there. At the very beginning of the history of the pressurized water reactors, sodium phosphates were the basis of water chemistry in the secondary circuit. This was due to the experience gained with sodium phosphates in the conventional power plants (EPRI 1997a. Odar & Nordman 2010. Wood 2012, p. 37).

The most serious problems occurred in the time span from the 1970s to end of the 1990s (Odar & Nordman 2010), see Figures 3 and 5. Until 1979, most failures were caused by tube wastage and denting (IAEA 2011, p. 31). Tube wastage is thinning of a tube caused by the phosphate chemistry adopted from fossil power plants (Green & Hetsroni 1995. Odar & Nordman 2010). Phosphates were used because the leak tightness between cooling circuits was insufficient and there were many impurities like chlorides in the system. Impurities originated from sea water used for cooling in the ternary circuit. Phosphates decreased the problems caused by these impurities. (Odar & Nordman 2010)

Because of the wastage, plants begun to abandon phosphates, but there were still impurities, because the circuits were not fully isolated from each other, and that resulted in denting corrosion (Odar & Nordman 2010). In denting, the diameter of a steam generator tube is decreased because corrosion products, which are formed onto the tube support plate, have a higher volume than the metal and thus generate a compressive stress (Green & Hetsroni 1995).

These problems were mainly solved when the water chemistry was changed at the end of the 1970s to the all-volatile-treatment, AVT (Odar & Nordman 2010. IAEA 2011, p. 31. Wood 2012 p. 37). Switching to the all-volatile-treatment also decreased problems caused by the deposition of corrosion products onto the tube surfaces and tube support plates. Under the H-AVT, there are 10 times less corrosion products in feed water than under the phosphate treatment. The H-AVT means the all-volatile-treatment with high pH accomplished with hydrazine dosing. Hydrazine decomposes at high temperatures producing ammonia, which is a pH-increasing chemical. In the all-volatile-treatment, all water chemistry chemicals are volatile, so there are no deliberately injected solids in the water. (Schwarz 2001)

While wastage and denting were at least temporarily solved by changing to the AVT chemistry, other problems still persisted. In the 1980s, pitting corrosion was causing problems in the steam generators. Pitting was due to concentrated chloride impurities beneath the magnetite deposits. Pitting can be reduced by reducing the chloride concentration in the feed water but still it can be a problem nowadays. (Odar & Nordman 2010)

Outer Diameter-Integranular Attack (ODIA)/ Stress Corrosion (ODSCC) cracking was a growing issue in the late 1980s and early 1990s (Odar & Nordman 2010). Majority of the steam generator tubes that had had some kind of failure had been made from Alloy 600MA and used in the plants that had low pH (IAEA 2011, p. 33). In the 2000s, the main focus was at replacing Alloy 600MA and preventing flow accelerated corrosion, corrosion product transport and deposition (Odar & Nordman 2010). When Alloy 600MA is replaced with Alloy 690TT or Alloy 800NG the corrosion problems decrease greatly (IAEA 2011, p. 33). There have, of course, been problems also in the primary side of the steam generator, like Primary Water Stress Corrosion Cracking (PWSCC), but they are not in the focus of this work.

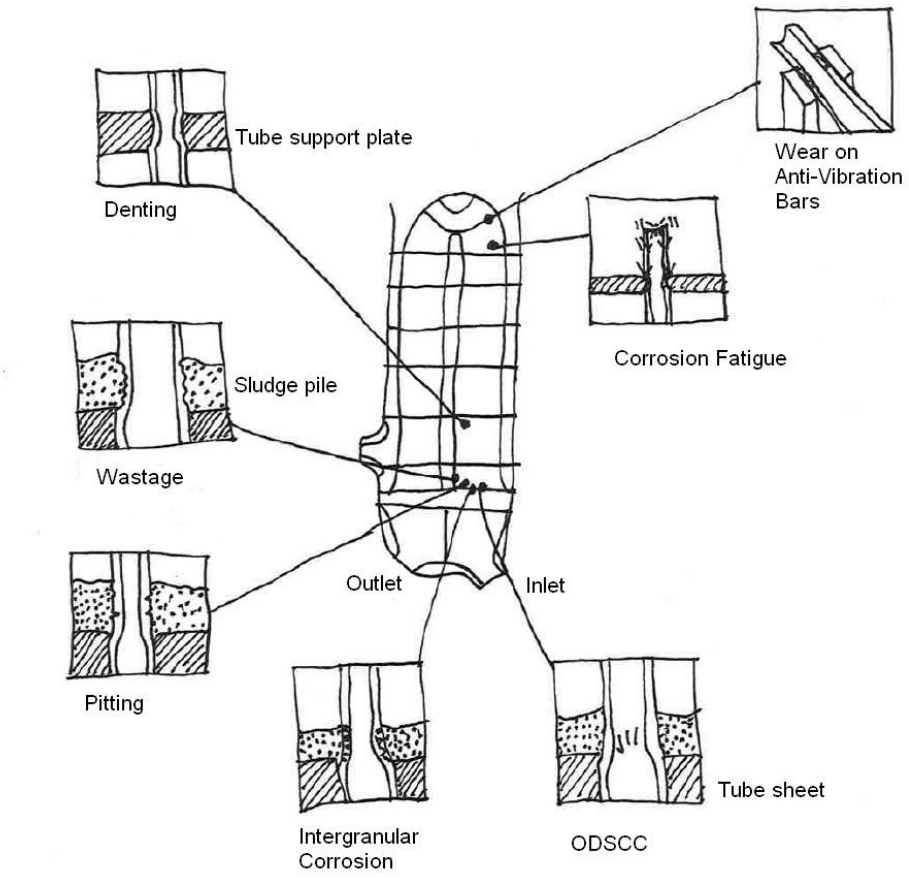

Figure 3: Material degradation processes in the steam generator (re-drawn and altered from IAEA 2011, p. 31, originally from Staehle et al. 2001)

In overall, the corrosion problems have been so severe that worldwide 175 plants have replaced their steam generator (IAEA 2011, p. 31). Figure 4 illustrates how the number of replaced steam generators in the USA has increased over the years. The summary of the occurrence of the different causes of steam generator tube plugging in the history is displayed in Figure 5. The actual numbers of the different corrosion problems are presented in Table 1.

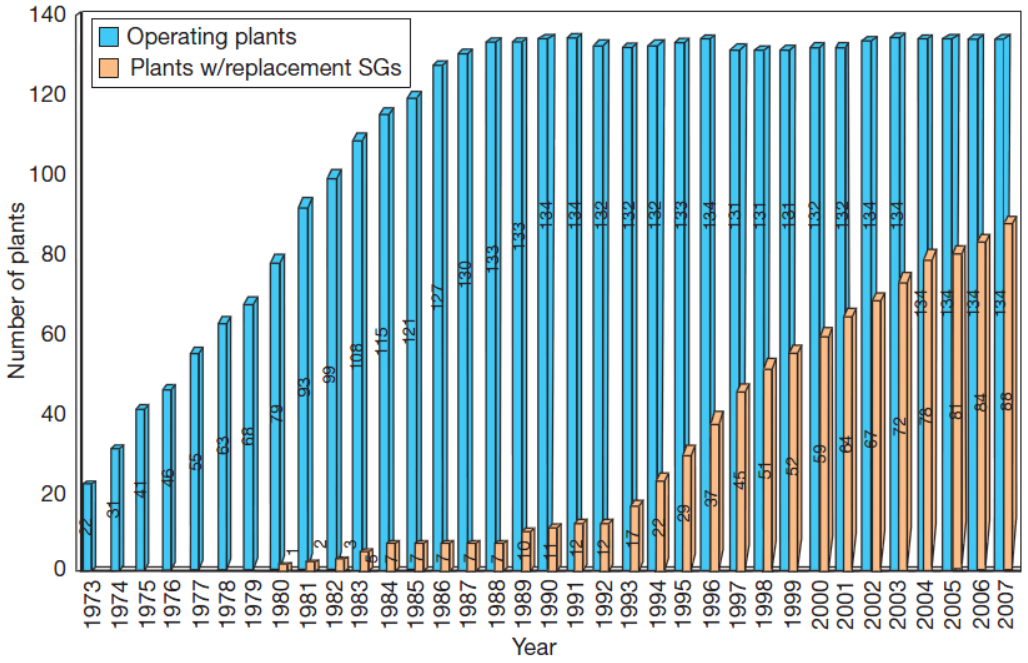

Figure 4: Number of plants with replaced steam generators in the USA (from Wood 2012, p 39, originally from Electric Power Research Institute.)

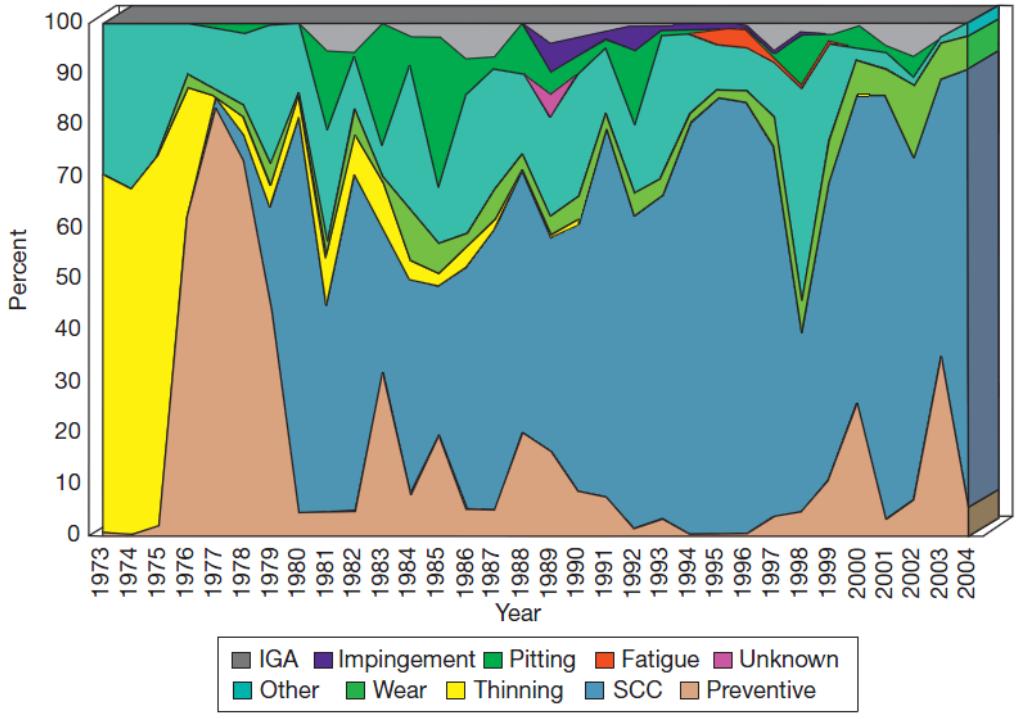

Figure 5 The causes of steam generator tube plugging worldwide (from Wood 2012, p. 39, originally from Electric Power Research Institute.)

Table 1: Reported problems of steam generators from 1977 to 1992 (modified from Green & Hetsroni 1995)

	1977	1982	1992
No. of units total	52	99	205
Reported problems			
Tube support denting	15	30	34
Tube sheet denting	6	12	50
Wastage	19	28	39
Pitting	0	3	14
Inner diameter cracking	1	22	90
Outer diameter SCC/IGA	6	22	74
Fretting	9	15	117
Fatigue cracking	3	4	10
Impingement	0	2	9
No problems	26	32	33
No. of units reporting no problems after five years operation/total number of units with more than 5 years operation	1/14	4/57	13/168
Names of units reporting no problems after five years of operation	Trino	Kewaunee; Mihama 3; Neckarwestheim; Davis Besse	Brokdorf; Chinon B3; Cruas 3; Cruas 4; Genkai 2; Grohnde; Loviisa 1; Loviisa 2; Obrigheim (replacement SGs); Philippsburg 2; Robinson 2 (replacement SGs); Unterweser

Nowadays the steam generators are overall in good condition but also new problems have arisen (Wood 2012, p. 37). It has been observed that lead impurities can cause Pb-assisted stress corrosion cracking (Fruzzetti 2009. Wood 2012, p. 37). There have also been cases of the tubes made of Alloy 600TT having problems of fretting and denting (IAEA 2011, p. 33) and fatigue fracture caused by magnetite deposition changing the flow patterns (Guillodo et al. 2012.). Table 2 summarizes the most important steam generator tube degradation processes, their causes and degradation sites, potential failure modes and method for in-service inspection.

Table 2: Summary of the PWR recirculating steam generator tube relevant degradation processes (IAEA 2011, p. 30)

Rank[a]	Degradation Mechanism	Stressor	Degradation Sites	Potential failure mode	ISI Method
1	ODSCC	Tensile stresses, impurity concentrations, sensitive materials	Tube to tube sheet crevices	Axial or circumferential crack	MRPC
			Magnetite pile	Circumferential crack	MRPC/Cecco5
			Tube support plate	Axial crack	Bobbin coil/Cecco5
			Free span	Axial crack	Bobbin coil (in absolute mode)
2	PWSCC	Temperature, residual tensile stresses, sensitive materials (low mill anneal temperature)	Inside surface of U bend	Mixed crack	MRPC[b]
			Roll transition without kiss rolling	Mixed crack	MRPC
			Roll transition with kiss rolling	Axial crack	MRPC
			Dented tube regions	Circumferential crack	Bobbin coil or MRPC
3	Fretting, Wear	Flow induced vibration, aggressive chemicals	Contact points between tubes and the anti-vibration-bars, or tubes and the preheater baffles	Local wear	Bobbin coil
			Contact between tubes and loose parts	Depends on loose part geometry	Bobbin coil
			Tube to tube contact	Axial wear	Bobbin coil
4	High cycle fatigue	High mean stress level and flow induced vibration, initiating defect (crack, dent, pit, etc.)	At the upper support plate if the tube is clamped	Transgranular circumferential cracking	Leak detection or by detection of precursor
5	Denting	Oxygen, copper oxide, chlorides, temperature, pH, crevice condition, deposits	At the tube support plates, in the magnetite pile, in the tube sheet crevices	Flow blockage in tube, may lead to circumferential cracking, decreases the fatigue resistance	Profilometry, bobbin coil

6	Pitting	Brackish water, chlorides, sulphates, oxygen, copper oxides	Cold leg in magnetite pile or where scale containing copper deposits is found, under deposit pitting in hot leg	Local attack and tube thinning, may lead to a hole	Bobbin coil, ultrasonic
7	Wastage	Phosphate chemistry, chloride concentration, resin leakage	Tubesheet crevices, magnetite pile, tube support plates, anti-vibration-bars	General thinning	Bobbin coil

[a] Based on the operating experience and number of defects (1993)

[b] Multifrequency rotating pancake coil probe

2.3 Dissolution, deposition and the problems caused by the magnetite particles

As it was reviewed earlier, there have been several serious cases of corrosion problems in the steam generators, and the most of the corrosion problems were caused by combination of weak design, wrong material and wrong water chemistry (Odar & Nordman 2010). The condition of the materials in the secondary side of the steam generator must be considered very deeply as 75% of the leaks between the primary and secondary circuits have originated from material degradation on the secondary side (Weeks & Czajkowski 1982). Also nowadays most problems are on the secondary side (IAEA 2011, p. 29-30). The corrosion in the steam generator tubes and support plates is affected by not only the materials and their fabrication, but also the tube installation and the tube support plate design (IAEA 2011, p. 24-27).

The corrosion problems of the steam generator come into existence long before the steam generator itself. They begin when the surface of feed water pipes begins to corrode. At first, oxides will be formed on to the surfaces of the pipes but the water flow removes them as ferrous oxide particulates and carries them to the steam generator. At the steam generator, they start to attach to the surfaces of the steam generator and form deposits. These deposits are typically located on the tube sheet or in the tube to tube support plate crevices (Figure 6) and can grow very large. (Odar & Nordman 2010. IAEA 2011, p. 24-40.) This deposition of the corrosion products is also called fouling, and the deposits are referred also as the crud or the sludge in some literature.

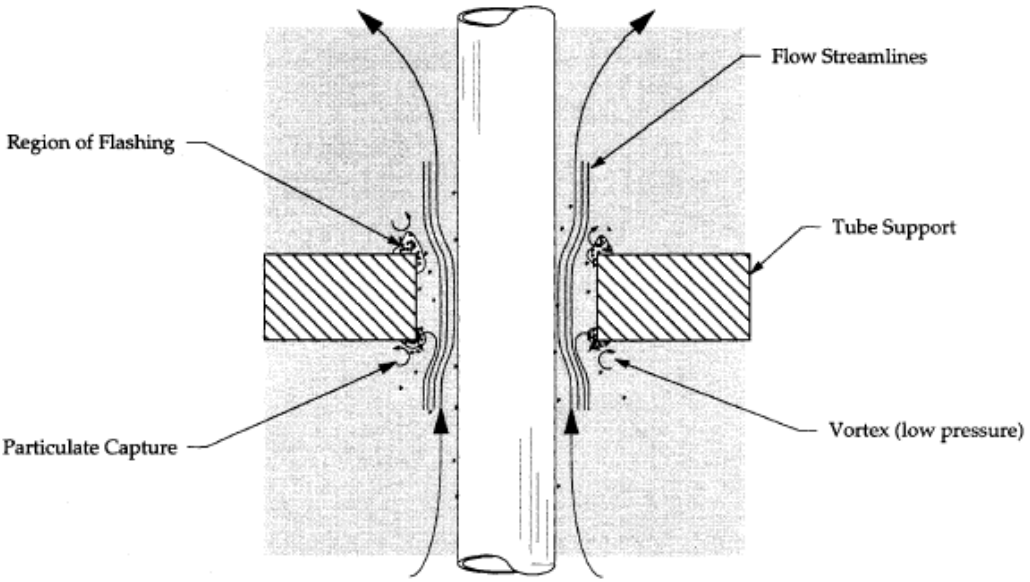

Figure 6: The fluid mechanics on the tube support plate (Varrin 1996)

Deposits decrease the heat transfer of the surfaces, and thus these corrosion product deposits dry out and form a dry-to-wet interface which is constantly boiling and gathering non-volatile impurities (Odar & Nordman 2010. IAEA 2011, p. 39). When the temperature and impurity concentrations increase, numerous corrosion processes will start. This also shifts pH locally which can increase corrosion. (IAEA 2011, p. 40) All in all, corrosion product deposits induce many kinds of material and thermal degradations.

2.3.1 Dissolution and deposition of ferrous oxides

In this sub-chapter we are considering how the corrosion products are released to the system and how they deposit and which mechanisms are affecting to those processes. It is important to understand how these processes work so they can be controlled. Conditions in the different parts of the secondary circuit are rather different from each other. The temperature varies roughly from the room temperature to almost 300°C depending on the power plant. Also the alkalinity, oxygen levels and levels of other substances like hydrazine differ. (Turner 2011) This all affects the formation, transportation and deposition of corrosion products.

Most of the pipes in the secondary circuit are made from carbon and low-alloy steels. General corrosion is not normally a problem in carbon steel and low-alloy steel pipes in the nuclear power plant: the corrosion rate is about a micrometer per year which is an acceptable rate. (Seifert et al. 2012) The most of the corrosion products are instead created by an attack of flow accelerated corrosion (EPRI 2003. Odar & Nordman 2010). In flow-accelerated corrosion (FAC), also known as flow-assisted corrosion or erosion-corrosion in older literature, the protective oxide layer (mostly magnetite, Fe_3O_4) is removed by a high fluid flow rate (Dooley & Chexal 2000. Dooley 2008. Odar & Nordman 2010. Seifert et al. 2012). After removing magnetite layers, FAC attacks the base metal. (Dooley & Chexal 2000) Thus, because the protective oxide layer is destroyed, FAC causes wall thinning (Dooley & Chexal 2000. Wood 2012, p. 45). This can lead to a rupture or a leak (Wood 2012, p. 45).

The flow accelerated corrosion has led to serious problems, not only by producing harmful corrosion products, but mainly due to wall thinning. In 1986, flow accelerated corrosion caused a pipe rupture at the Surry-2 nuclear power plant which led to the death of four plant workers. In 2004, similar accident occurred at the Mihama 3 killing five people. Flow accelerated corrosion has caused many other pipe ruptures, also in the Loviisa-1. (Odar & Nordman 2010) This has led to a deep investigation of the problem.

Flow accelerated corrosion is present in both one-phase flows and two-phase flows (Odar & Nordman 2010). In single-phase regions, flow accelerated corrosion causes horseshoe looking pits that also resemble orange peels. In two-phase regions, the damage looks like tiger stripes. (Dooley & Chexal 2000) Understanding these different phenomena needs a deep knowledge of chemistry.

It has been noticed that magnetite dissolution can be demonstrated as seen in Formula 1, and is controlled by mass transfer

$$Fe_3O_4 + 3(2-b)H^+ + H_2 = 3[Fe(OH)_b]^{(2-b)+} + (4-3b)H_2O \qquad (1)$$

where b can be 0, 1, 2 or 3. (Seifert et al. 2012)

However, magnetite is not the only corrosion product released by flow accelerated corrosion. The great diversity of different environmental factors and reaction kinetics leads to a forming of several iron oxides and oxide hydroxides, like magnetite, hematite, goethite, lepidocrodite, maghemite and ferrihydrate. They are formed in the complicated series of oxidation, hydrolysis, dehydration and transformation reactions. Different environmental factors and different reaction kinetics lead to different corrosion products. The most common phases in the secondary side of the nuclear power plant are lepidocrocite (γ-FeOOH), magnetite (Fe_3O_4) and hematite (α-Fe_2O_3). (Turner 2011) The different iron oxides and oxide hydroxides dominate in the different parts of the secondary circuit as can be seen from Table 3. Crud type has a significant effect also on the fouling rate, which is demonstrated in Figure 7.

Table 3: The occurence of different iron oxides and hydroxides when filtering cooling water in different parts of secondary circuit (Turner et al. 1994)

	Condenser Outlet	High Pressure Heater Outlet	Moisture Separator Drain	Steam Generator Blowdown
lepidocrocite (γ-FeOOH)	30%	20%	35%	-
magnetite (Fe_3O_4)	50%	30%	55%	75%
hematite (α-Fe_2O_3)	20%	50%	10%	25%
Mass transport (g/h)	4-8	3-6	0.5-1	0.3-0.6

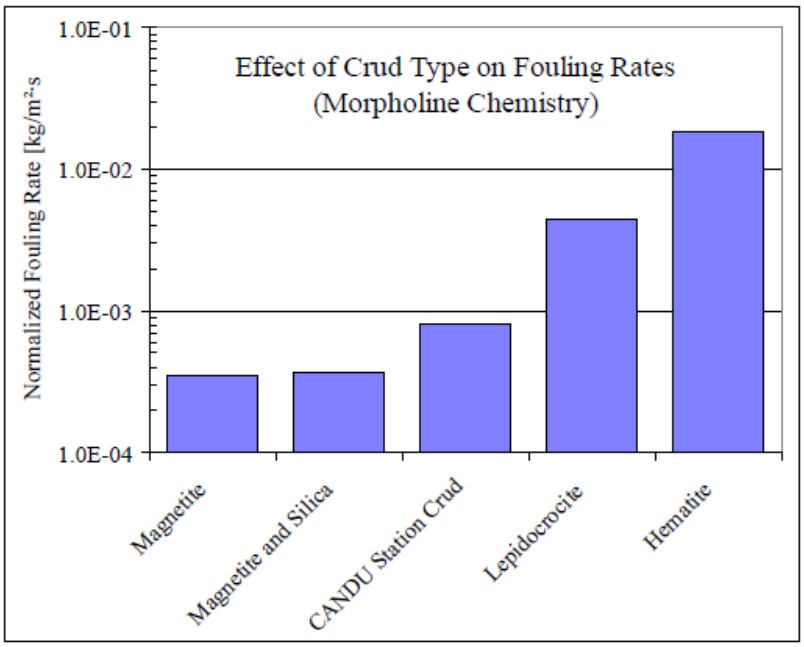

Figure 7: Effect of the crud type on fouling rates in morpholine chemistry (EPRI & AECL 2002)

Decreasing flow accelerated corrosion decreases the amount of corrosion problems and fouling problems in the steam generators. FAC is affected by hydrodynamics, environmental properties and material properties. This includes factors like flow rate, turbulence intensity, temperature, pH and chromium content (Seifert et al. 2012). It has been discovered that FAC can be reduced by elevating pH, injecting oxygen, selecting materials with more chromium and by avoiding turbulence-increasing geometries (Odar & Nordman 2010 Seifert et al. 2012).

The deposition of the corrosion products, like magnetite and hematite, and the problems that it is causing are called fouling (Odar & Nordman 2010). Fouling can be defined as “loss of secondary-side steam pressure at the same primary loop conditions” or as “deposition of corrosion products within the steam generator regardless of their ultimate impact on steam generator performance or integrity” (EPRI 2003). In this thesis, the latter definition is used.

Even though flow accelerated corrosion is well understood, fouling remains as a process that is not quite well known. This is mainly due to the fact that flow accelerated corrosion has caused deaths of power plant personnel while crud deposits have only caused economic losses. (EPRI & AECL 2002) There have been several guesses about the true model of fouling, because there is some uncertainty, whether fouling is purely a chemical process of oxides crystallizing from solutions, or a purely physical process of particles attaching to the surface, or a mixture of both (Varrin 1996).

Chemical fouling is affected by the corrosion product concentration in the solution, the temperature and the similarity of binding energies and lattices between the corrosion products in the solution and in the deposition. Physical fouling is affected by the particle size and concentration, the flow velocity and direction, the temperature, the surface roughness and the surface charges of the particles and the steam generator surfaces. Thus physical fouling is also affected by pH as it affects surface charges. (Varrin 1996)

The maybe most established model, the AECL fouling model describes fouling to be (in a steady state situation) a linear process that contains sub-processes of incubation, initiation, growth, growth limiting, spalling, redeposition and deposit consolidation (Varrin 1996. EPRI & AECL 2002). The incubation stage of fouling happens, when the power plant is pre-oxidized on purpose in order to create a passive layer on surfaces. This passive layer is the base of the oxide deposits. The initiation stage is more complicated. There are several possible mechanisms (Figure 8): inertial or diffusion based particulate deposition, zeta potential attraction, thermophoresis and boiling super-saturation and precipitation. (Varrin 1996)

In inertial deposition, particles are attracted by van der Waals forces and repulsed by the double layer of the surface, which will be discussed later. Inertial deposition is an appropriate idea for larger particles. Zeta potential deposition fits better for smaller particles and is by that, very important model. In zeta potential deposition, the surface of the particle is covered by a layer of ionic sites originated from hydration or dehydration. The net charge is pH dependent. This charge cloud attracts species with opposite charge, like impurity ions, hydroxides and hydronium ions. (Varrin 1996)

Zeta potential deposition consists of two steps; the transport of the particles to the neighbourhood of the surface by inertial forces, eddies, turbulence and diffusion and the attachment of particles to the surface by oppositely charged zeta potentials. It is thought that if the surface and the particle are oppositely charged, the transport limits the process, if they are similarly charged, the attachment limits the process. In the typical steam generator environment, deposition is an attachment limited process. (Varrin 1996)

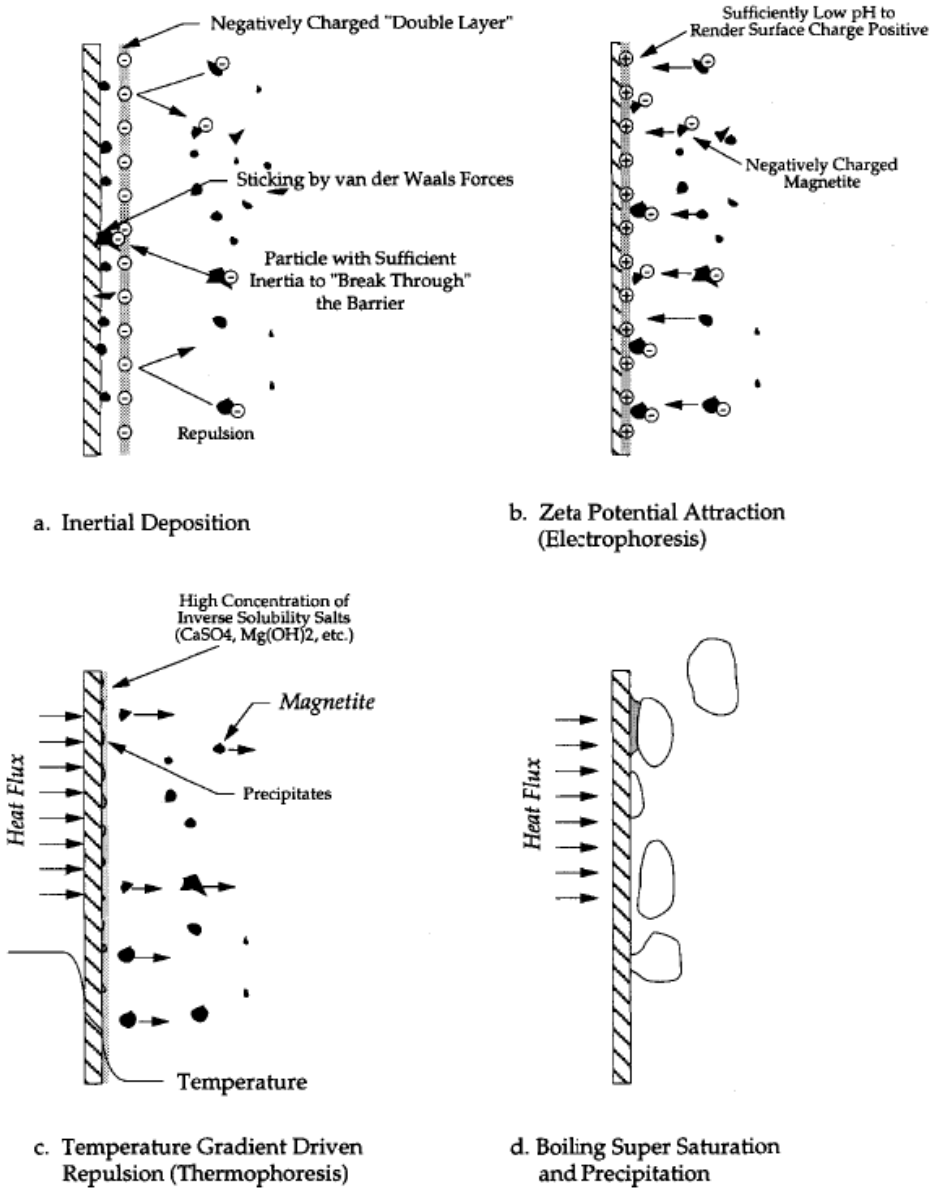

Figure 8: Mechanisms for initiation of oxide deposits (Varrin 1996)

Thermophoresis is a phenomenon where particles are moving from hot surfaces towards colder areas (Zahmatkesh 2008). When the system is not boiling, the deposition is controlled by diffusion and thermophoresis (Basset et al. 2000). According to Varrin (1996) the effect of the thermophoresis on the fouling is still quite small (Varrin 1996). However, thermal-hydraulic conditions affect the fouling rate, e.g. when there is a forced convection situation in single-phase, the fouling rate is low. Subcooled nucleate boiling leads to the moderate fouling. (EPRI & AECL 2002)

Different conditions add different aspects to the consideration. When thinking of isothermal conditions, the deposition process is consisting of the transport of the particles from the bulk liquid to the neighbourhood of the surface and the attachment of the particles to the surface. In steam generator conditions the heat transfer makes conditions non-isothermal and so the thermophoretic effects have to be also considered. Boiling adds the concepts of bubble growth, bubble collapse and effects of film boiling to be also thought of. The trapping of particles by bubbles becomes important when the system is boiling sub-cooled. At this point, the removal of deposition is also happening. Later on, the microlayers start to evaporate and that increases deposition. (Basset et al. 2000)

When the deposit has initiated, it will start to grow. Growing (Figure 9) may happen in the same way as the initiation. However, the surface charges important in this stage are not the ones of the particles and the steam generator wall but the ones of the particles and the already existing deposit. The growth stage is a linear process. The corrosion products are circulated in the neighbourhood of the deposit by inertia, boiling-induced diffusion or concentration-driven diffusion. Then they attach to the deposit by the same mechanisms as at the initiation and pores and chimneys begin to form within the deposit. After that, the magnetite scales start to ripen or undergo crystal growth. At last there will be the precipitation of the consolidating agents like copper, silicates and aluminium. (Varrin 1996)

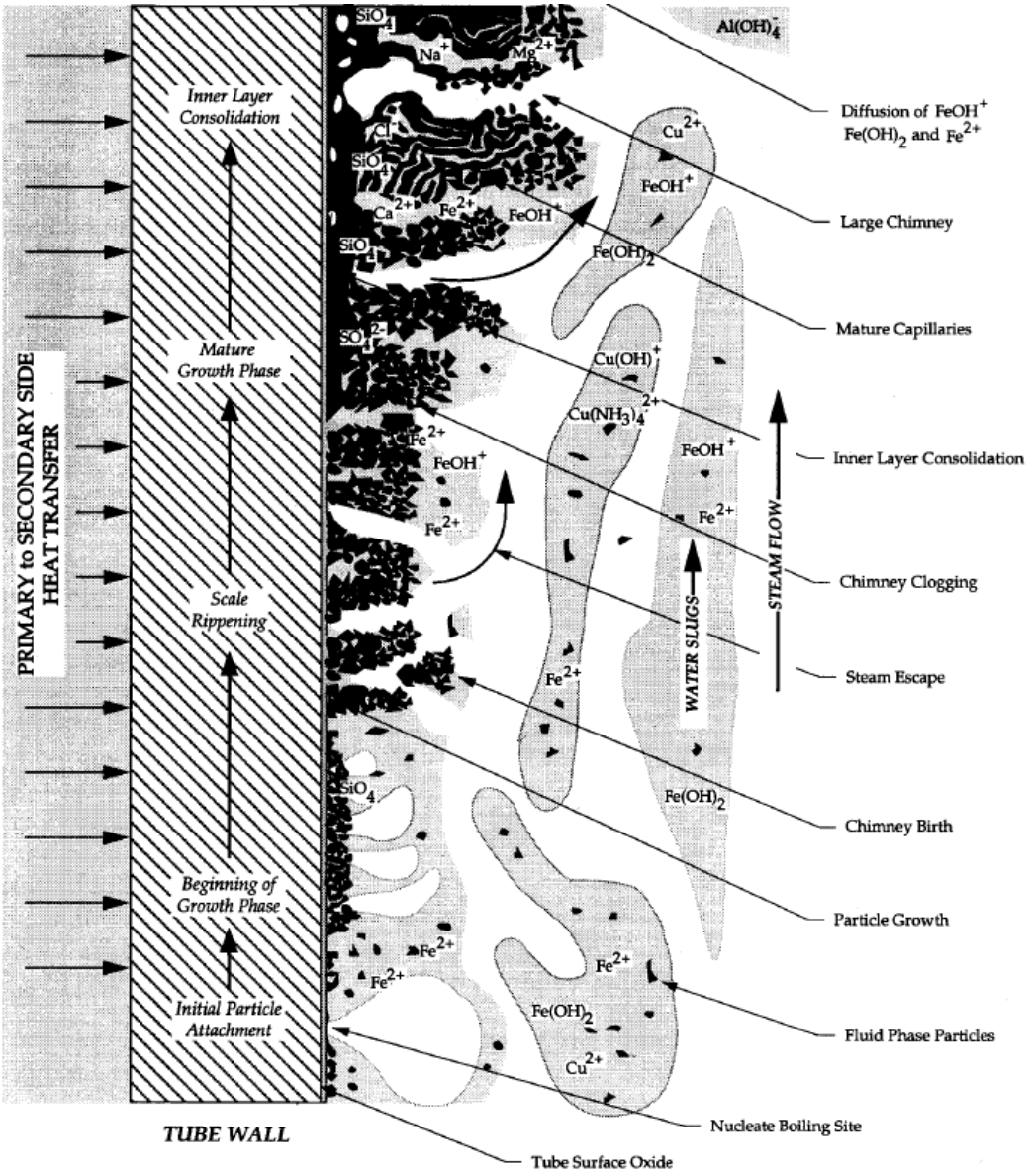

Figure 9: The growth of the deposit (Varrin 1996)

The growing stops after some limit and then begins the growth limiting stage. The reason for that is unclear, but has possibly something to do with thermal hydraulic conditions. In the spalling and re-deposition stage, the flakes of the deposit are removed from the deposit. This may happen because the deposit is unable to withstand the stresses created by thermal cycling and circulating flow. These loose particles and flakes may re-deposit. (Varrin 1996)

The overall steam generator fouling rate (kg/s per boiler) can be presented as:

$$\frac{dm}{dt} = \frac{C_{feed}F_{feed}K_fA}{K_fA+(b+c)F_{feed}} \qquad (2)$$

where *dm/dt* is the overall rate of the steam generator fouling (kg/s), C_{feed} is crud concentration in feed water (kg of crud/kg of water), F_{feed} is feed water flow rate (kg/s), K_f is overall normalized fouling rate (kg/m^{2}s per unit crud concentration), *A* is fouling area (m^2), *b* is the blowdown rate and *c* is carry-over rate. *B* and *c* thus reflect the amount of water and corrosion products removed from the system. (EPRI & AECL. 2002.)

However, the AECL model also predicts that deposits can consolidate so, that no re-entrainment of the particles happens no longer, because deposits become chemically bonded to the metal surface or to the pre-existing deposit (EPRI & AECL 2002). These deposits consolidate over time becoming hard and impermeable. This can take so little time as from 3 to 4 years. (Odar & Nordman 2010). It seems that the fouling rates and the deposit consolidation rates are connected (EPRI & AECL 2002).

Under steady-state operating conditions, Formula 3 applies:

$$m(t) \approx K\rho\frac{\lambda_c}{\lambda}Ct \qquad (3)$$

where *m(t)* is the deposit loading on the fouling surface (kg/m^2), *K*ρ is the normalized deposition rate (kg/m^{2}s), *C* is the crud mass fraction in the steam-water mixture, *t* is the fouling time (s), λ_c is the deposit consolidation rate constant (1/s), λ_r is the deposit re-entrainment rate constant and $\lambda = \lambda_r + \lambda_c$. (EPRI & AECL. 2002.)

The summary of the origin and transport of different fouling species and their consequences is presented in Figure 10. Fouling happens most often at high-heat-flux and low-velocity surfaces. Some deposition can take place at surfaces and crevices with flow restrictions. (EPRI 2003)

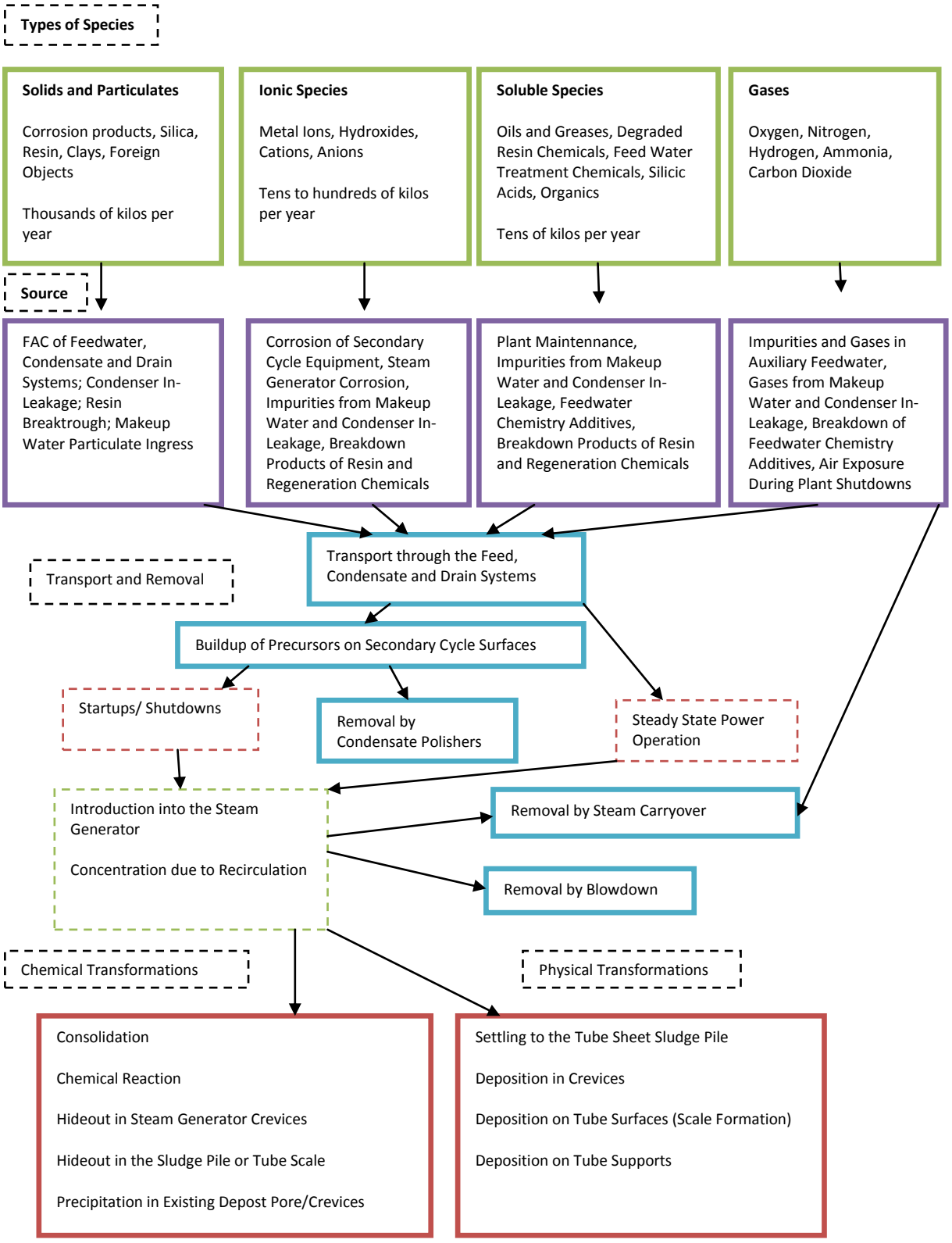

Figure 10: Corrosion product generation and transport (Varrin 1996)

2.3.2 Corrosion degradation

Steam generator tube materials are damaged by numerous phenomena, like primary water stress corrosion cracking (PWSCC) (IAEA 2011, p. 3), outer diameter stress corrosion cracking (ODSCC) (Weeks & Czajkowski 1982. IAEA 2011, p. 3), fretting (Woo & Lu 1981. IAEA 2011, p. 3), pitting (Weeks & Czajkowski 1982. IAEA 2011, p. 3), high cycle fatigue (Woo & Lu 1981. IAEA 2011, p. 29. Turner 2011), vibration (Woo & Lu 1981), wastage (Woo & Lu 1981. Weeks & Czajkowski 1982. IAEA 2011, p. 3), water hammering (Woo & Lu 1981), cracking (Woo & Lu 1981), tube support plate denting (Woo & Lu 1981. IAEA 2011, p. 3) and clogging (IAEA 2011, p. 29).

All these material degradation problems can cause great economic losses, as plugging of leaking steam generator tubes demands shutting down of the power plant. Some of these phenomena are created when tubes are vibrating by water flow, and so they are actually more mechanical problems than typical corrosion problems. Mechanical problems are however increased, when there are more sludge deposits. And on the other hand, all kinds of mechanical stresses make the corrosion problems worse. (Woo & Lu 1981)

The most important phenomenon is maybe the outer-diameter stress corrosion cracking and the intergranular attack (ODSCC/IGA). Stress corrosion cracking of the secondary side is caused by combination of susceptible materials, stress conditions and corrosive conditions. These conditions are met beneath the magnetite deposits typically on the top of tube sheets and in the crevices between tubes and tube support plates. (Diercks et al. 1999. Odar & Nordman 2010)

The most typical reason for corrosion problems in the steam generators are the concentrated impurities beneath the corrosion product deposits. (Odar & Nordman 2010) These impurities can be e.g. sodium, phosphates, lead, sulphate or chlorides (Woo & Lu 1981). Figure 11 shows the situation on the tube sheet with a deposit of corrosion products. The water in the tube has a temperature of about 300˚C but the temperature of the outside is around 250˚C. Therefore liquid evaporates within the pores of the deposit. (Turner 2011)

When the liquid has evaporated it is replaced with a new liquid. While the liquid evaporates, the non-volatile impurities stay in the pore. (Turner 2011) This alternate wetting and drying causes concentration of non-volatile impurities. This also causes a pH change within the pores. Therefore there might be corrosion phenomena which were supposed to be impossible at the overall pH of the system. (Turner 2011) The situation is worst under the deposits, but happens also within deposits (Green & Hetsroni 1995). Concentration of non-volatile impurities can also happen inside the chimneys and capillaries of a deposit (Figure 12).

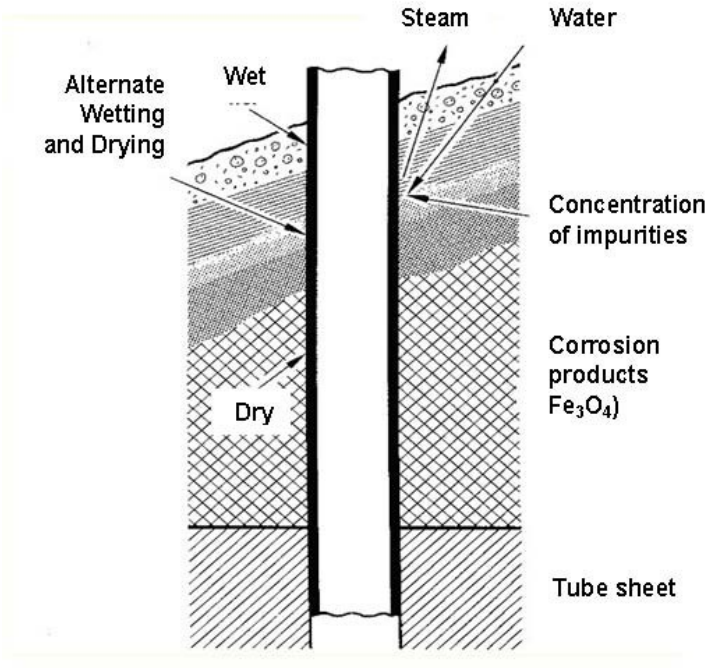

Figure 11: Impurities concentrate on tube sheet (IAEA 2011, p. 39)

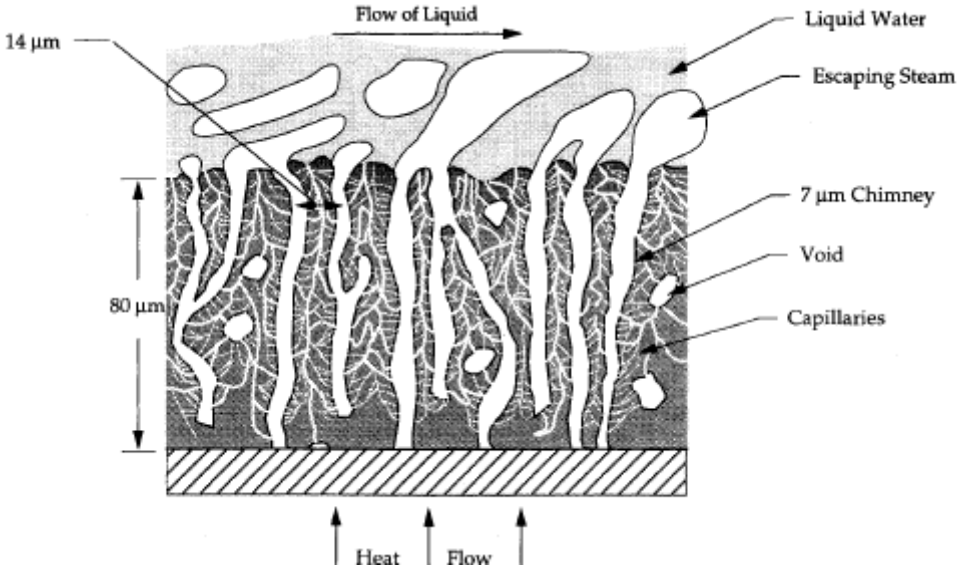

Figure 12: Steam formation in chimneys and capillaries (Varrin 1996)

Green & Hetsroni (1995) present that there is also another process that concentrates impurities. It is based on the fact that any solute raises the boiling point of water. Because water flows to the crevice until it starts to boil, the chemicals concentrate into the crevice. Increasing chemical concentration means higher boiling point and thus longer time for the water to deliver impurity chemicals to the crevice. As water boils, the non-volatile impurities remain in the crevice. This kind of crevice may form under the corrosion product deposition. (Green & Hetsroni 1995) It has been discovered that all steam generator degradation problems are somehow caused by the concentrated impurities and the deposits of the corrosion products (Odar & Nordman 2010. IAEA 2011, p. 39-40).

2.3.3 Thermal degradation

Actual corrosion problems are not the only thing to be concerned about. The corrosion product deposits can not only create relevant environment for corrosion to appear, they also decrease the heat transfer and can block the water flow (Rummens et al. 2004. Turner 2011. Wood 2012, p. 43). Blocking of the tube support plate crevices may induce also vibration (Odar & Nordman 2010). This all can lead to loss of thermal performance and to the appearance of steam generator level oscillations (Turner 2011).

Material degradation leads also to pressure losses in the steam generator. Small pressure losses are caused by tube plugging, primary temperature variations and power increases. Larger pressure losses are caused by large-scale tube plugging, secondary side deposits and the decrease of the primary side temperature. (White et al. 1998)

When these corrosion products deposit, they can reduce the heat transfer, concentrate impurities, restrict the movement of the tubes, block flow passages or form consolidated magnetite piles. A good estimate for the amount of iron oxide accumulation in the steam generator tube bundles is about 70 kg per year. About 10 kg of iron oxides accumulate to the tube sheet, 5 kg to the tube support structures. That amount of deposit has some serious consequences. All in all, 90 % of the corrosion products deposits to the steam generator. (Turner 2011) Typical fouling locations are presented in Figure 13.

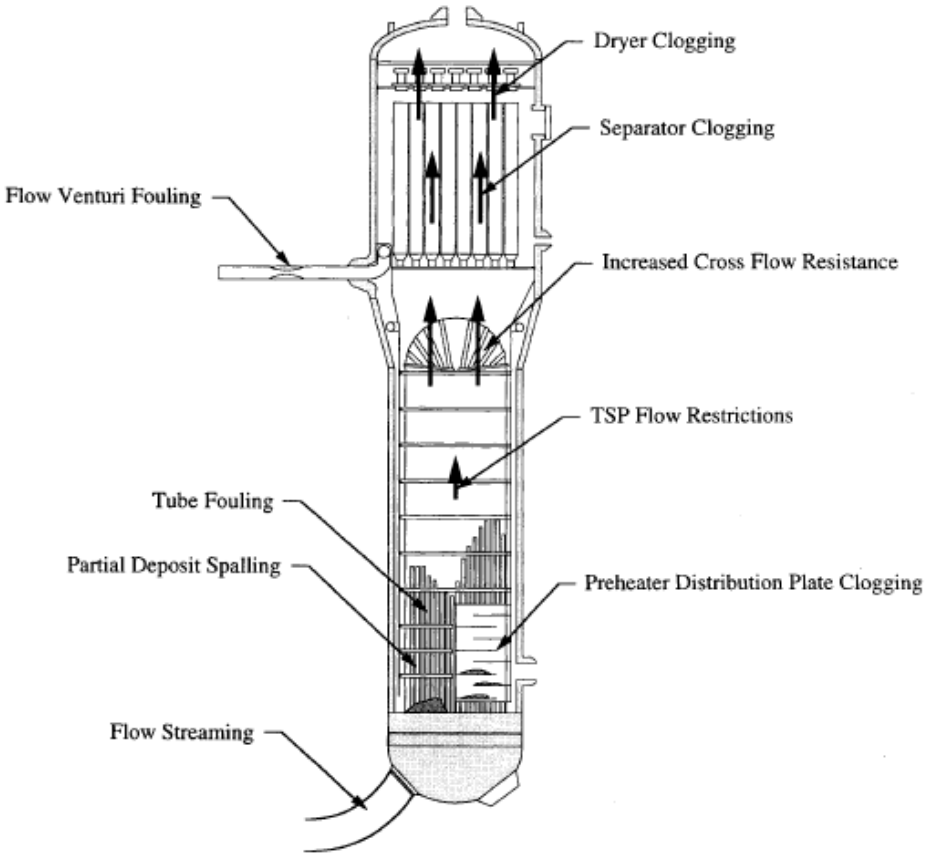

Figure 13: Fouling locations (Varrin et al. 1996)

The type of the corrosion product is not indifferent. Hematite, for example, fouls much more than magnetite on the Alloy 600 MA (Odar & Nordman 2010). In fact, hematite increases fouling by factor of ten when compared to magnetite (EPRI & AECL 2002). This is assumed to be due to the fact that at nuclear power plant operating temperature both Alloy 600MA and magnetite particles have negative surface charge but hematite has a positive surface charge. Thus magnetite deposits grow much slower as there are repulsive forces which hinder the process. (Turner & Klimas 2000. Turner et al. 2002)

2.4 Electrical double layer, electrokinetic phenomena and zeta potential

Colloidal particles have a diameter less than 1 μm. Particles greater than that, are classified as suspended particles. (Elimelech et al. 1995) Magnetite particles typically have a diameter from 0.1 μm to 1 μm. Because magnetite particles are so small, inertial and gravitational forces affecting them are almost zero, and the most important thing affecting them is their surface charge (Varrin 1996). As surface charge has a major impact on steam generator fouling (EPRI & AECL 2003), it is important to become familiar with different electrokinetic phenomena and electrochemistry concepts of surfaces to fully understand fouling.

It has been demonstrated that surface properties are controlled by electrical double layer forces, van der Waals forces, Born repulsion, hydration effects and steric forces (Elimelech et al. 1995). For a simplification, we only consider electrical double layer forces and van der Waals forces. This is called DLVO theory (Israelachvili 2011, p. 326-327). Attractive van der Waals forces can be cancelled by repulsive forces of electrical double layer (Adamson & Gast 1997, p. 240). London-van der Waals forces are created when fluctuating dipole moments interact with each other (Epstein 1997). Electrical double layer is a distribution of charges on a charged surface and it has often more than two layers, but the term 'electrical double layer' is widely used (Delgado et al. 2005).

Colloid particles in water usually have a net charge. This charge can be obtained by three ways. Particles can have a negative charge when the surface groups of a particle become ionized or dissociated. (Israelachvili 2011, p. 291-292) This can be achieved as metal oxide surfaces become hydroxylated when exposed to the water. There will be then possibility of the ionization of the surfaces. (Elimelech et al. 1995) This can be written (4)

$$S - OH_2^+ \rightleftharpoons S - OH \rightleftharpoons S - O^- \qquad (4)$$

where S is a solid surface. (Elimelech et al. 1995 originally from Stumm 1992)

The second option is to adsorb or bind ions from solution onto a surface. The charge depends on the type of the ion. Third option is to exchange charges between different surfaces. This causes an attractive force between the surfaces. (Israelachvili 2011, p. 291-292)

The charge of the surface of the colloidal particle is balanced by the oppositely charged counter-ions of the solution. Counter-ions are attracted to the surface by electrostatic interaction but repelled by the demand of diffusion, driven by the Gibbs free energy. (Elimelech et al. 1995) The repulsive force between similarly charged surfaces in a solvent with counter-ions is due to the osmotic pressure between the counter-ions. Actually, the electrostatic forces are attractive, but the osmotic pressure dominates, so the net force is repulsive. So essentially, the interaction between two surfaces is more about entropy than electric forces. (Israelachvili 2011, p. 298-299)

The outcome of the interaction between two planes may have several results. If the electrolyte is dilute and the surfaces are highly charged, there is a strong repulsion with a long range. This repulsion has interaction energy maximum at the distance of 1 to 5 nm. When the electrolyte has a higher concentration, the so called secondary minimum of interaction energy will form at the distance of 3 nm. The colloidal particles may then remain in that secondary minimum or be dispersed in the solution, if the energy barrier between the secondary minimum and the primary minimum of the surface is too high. If the energy barrier is lower, particles will coagulate or flocculate to the surface. When a surface charge is really small, the system is considered to only be affected by van der Waals forces and then the interaction is strongly attractive. (Israelachvili 2011, p. 326-327) Figure 14 presents these barriers. V_R describes the situation when there is only a strong repulsion caused by the double layer interaction. V_A shows the situation when there is only a strong attraction caused by the van der Waals interaction. V_T shows the combination of these two, which also shows the preferable states of the system, the two minimums of the interaction energy.

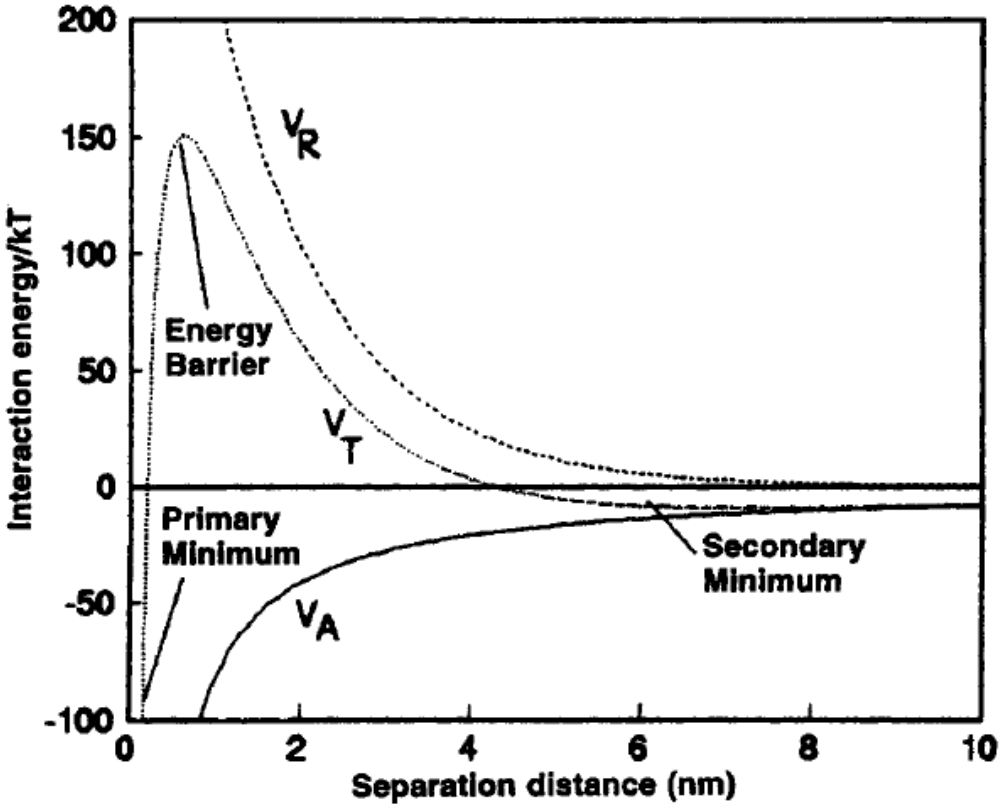

Figure 14: The interaction energy in the neighbourhood of the electric double layer (Elimelech et al. 1995)

The electrical double layer can be pictured as one layer being a fixed charge bound on a solid surface of some kind, and the other layer surrounding it within the solution and having a net charge opposite of the fixed charge. In a more advanced model, the hydrated ions, which have a charge opposite of the solid surface, are called the diffuse-layer or Gouy-Chapman layer. The charge distribution and the structure of the electrical double layer according to the Gouy-Stern-Grahame model are clarified in Figure 15. There is an uncharged region between the solid surface and the diffuse layer. It is called the Stern layer. It can be divided into inner Helmholtz layer, inner Helmholtz plane, outer Helmholtz layer and outer Helmholtz plane. The outer Helmholtz plane has the potential called diffuse-layer potential ψ^d or Stern potential. Inner Helmholtz potential is marked with ψ^i. (Delgado et al. 2005)

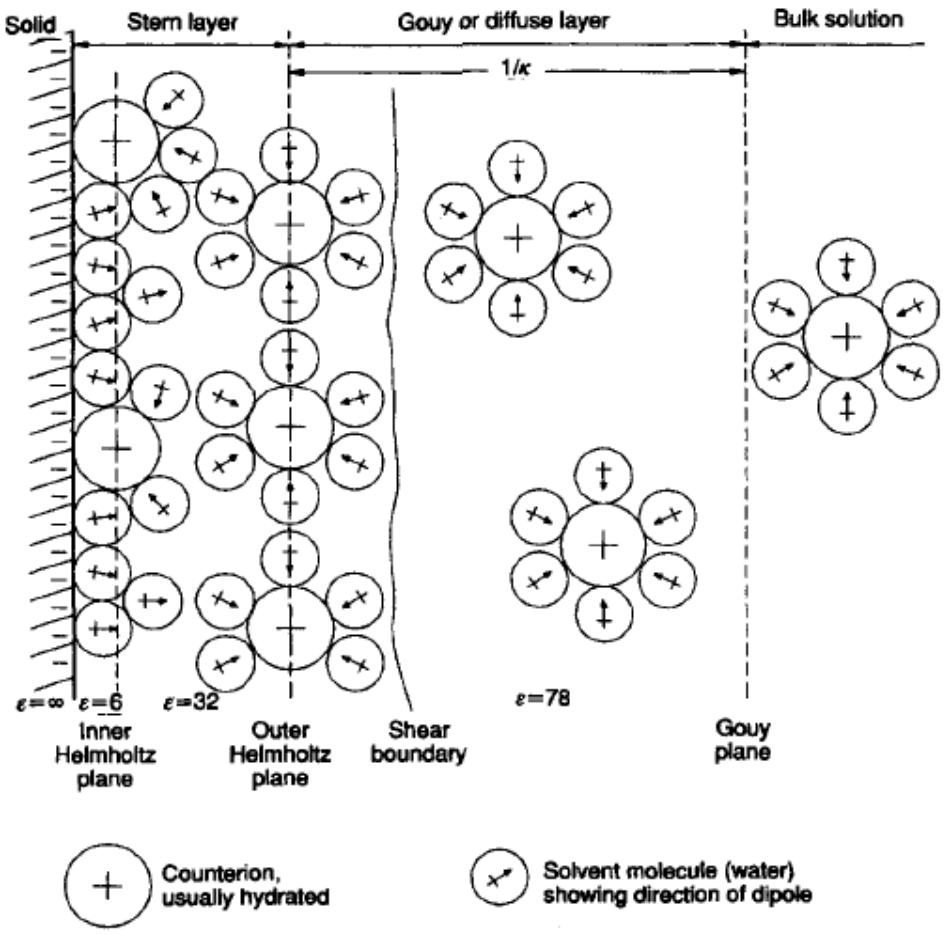

Figure 15: Gouy-Stern-Grahame model (Elimelech et al. 1995)

The inner Helmholtz surface is located the nearest to the surface and the outer Helmholtz plane the nearest of the diffuse layer. The schematic presentation of the inner and the outer Helmholtz plane and the slip plane, their location and potential is presented in Figure 16. Specifically adsorbed ions are located in the inner Helmholtz plane. Specifically adsorbed ions are affected by not only the Coulomb interaction, but also chemical bonds and specific adsorption forces. Of course all these planes and layers are theoretical models of the reality. (Delgado et al. 2005)

The slip plane is an imaginary plane near the solid surface, in which the fluid is considered to be stationary, so that electric charges move with this packet of fluid within the flow of liquid (Hunter 1981, p. 4-6. Delgado et al. 2005). In literature, also terms the surface of a shear, the shear boundary and the shear plane are used for the slip plane. That region inside the slip plane is called the stagnant layer, and despite its motionless nature, it can still conduct charges. The potential at $x=d^{ek}$ (slip plane) is called the electrokinetic or zeta potential (ζ potential).

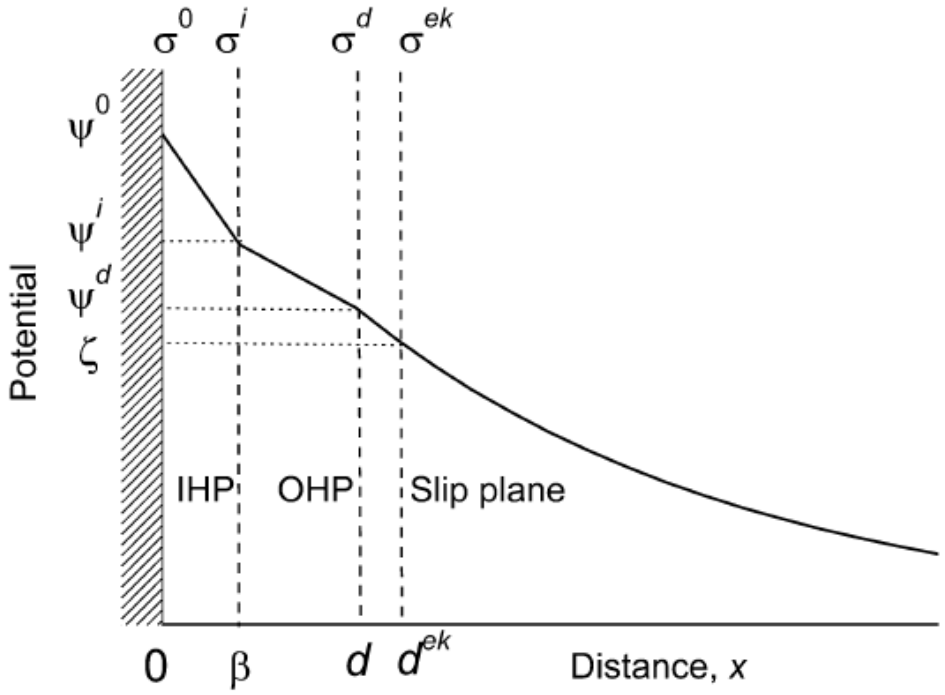

Figure 16: The potential and distance of the important planes of the electrical double layer. (Delgado et al. 2005)

The zeta potential is thus the potential of the point, which is on the border of the stagnant liquid packet surrounding the solid surface or the solid particle. (Delgado et al. 2005) When particles move in fluid under the effect of an electric field, i.e. they experience electrophoresis, the slip plane covers the particle with itself. This packet includes a small amount of the surrounding solution and its charge. By measuring the electrophoretic mobility, it is possible to obtain the net surface charge of the solid particle. It is also possible to measure the electrostatic potential in the slip plane instead of the actual charges. (Hunter 1981, p. 4-6)

The deposition of the particles is dependent on the zeta potential and the zeta potential is dependent on the nature and charge of the surface, the electrolyte concentration in the solute and the nature of the electrolyte and of the solvent (Delgado et al. 2005). For example, increasing pH changes positive zeta potential values to the negative direction (Epstein 1997). The isoelectric point is the point, where the slip plane has the zero charge, e.g. the zeta potential is zero (Adamson & Gast 1997, p. 190). The deposition rate is at greatest when pH values are between the isoelectric point of the particle and e.g. the isoelectric point of the tube support plate. (Epstein 1997) The reason for this can be seen in Figure 17, though the pH values presented in that figure must be ignored as they are purely imaginary.

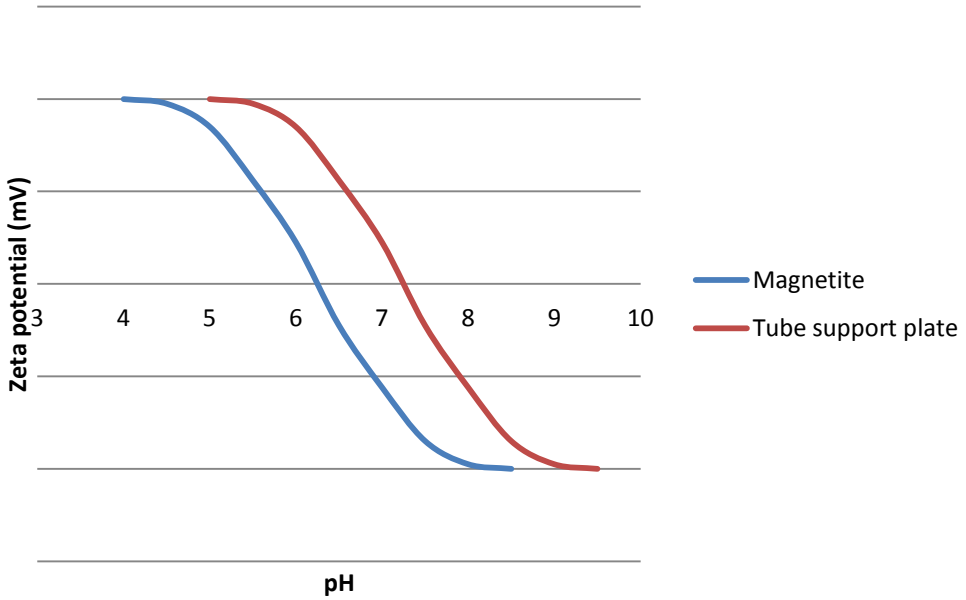

Figure 17: Zeta potentials of magnetite and tube support plate in an imaginary situation

In Figure 17, the isoelectric point of the magnetite is somewhere in the neighbourhood of pH=6.25 and the isoelectric point of the tube support plate (TSP) is at approximately pH=7.25. So when the pH is under 6.25, both the particles and the plate have a positive zeta potential. If the particles and the surface have a similar charge, the deposition needs more energy in order to occur. (Epstein 1997. EPRI 2003) Thus the more acidic the conditions are, the harder it is for the particles to deposit. The same situation is for pH values over pH=7.25. In those conditions, both the particles and the plate have a negative zeta potential.

Usually the acidic conditions are not acceptable due to the fact that they increase other material degradation mechanisms (Varrin 1996.) When the zeta potential difference between the corrosion products and the steam generator surfaces is large, also the particles tend to be carried to the surface in great amounts (EPRI 2003). So the deposition is at greatest between pH values of 6.25 and 7.25, because the magnetite particles and the tube support plate have the zeta potential of the different sign. It must be remembered that those were purely imaginary values, and real isoelectric points are dependent of many factors, including the temperature.

The location of the slip plane, or the accuracy of the zeta potential as a describer of the double layer, is uncertain and under debate. Nonetheless, the zeta potential seems to be the best alternative available for estimating the structure and the properties of the electrical double layer and the behaviour of the particles. (Elimelech et al. 1995) The method used in this thesis for zeta potential determination is streaming potential measurement. Streaming potential is suitable for experiments with magnetite particles in high temperatures (Jayaweera & Hettiarachchi 1992) and is the most common method used for the measurement of the zeta potential of granular materials (Elimelech et al. 1995). Streaming potential is one of the four elektrokinetic phenomena.

IUPAC defines electrokinetic phenomena as “all those phenomena involving tangential fluid motion adjacent to a charged surface” (Delgado et al. 2005). There are several electrokinetic phenomena, and the most important ones are electrophoresis, electro-osmosis, streaming potential and sedimentation potential. Usually, they are phenomena where a fluid moves with respect to a solid surface. (Hunter 1981, p. 1-4) The electric charges in the electrokinetic phenomena are affected by the electrical potential, the diffusion force and the convection of the fluid. The fluid itself is affected by the pressure gradients, the electrical charges and the shear forces of the liquid. (Hunter 1981, p. 1-4)

In the electrophoresis, an applied electric field moves solid particles in a fluid or gas phase. In the electro-osmosis, an applied electric field instead moves the fluid through a solid capillary or a porous plug. (Hunter 1981, p. 1-4) So in the electro-osmosis and the electrophoresis, the electric force causes the mechanical motion to occur (Delgado et al. 2005). In the case of the streaming potential, the situation is the opposite: the mechanical force leads to the electric current (Delgado et al. 2005). IUPAC defines the streaming potential as "the potential difference at zero electric current, caused by the flow of liquid under a pressure gradient through a capillary, plug, diaphragm, or membrane" (Delgado et al. 2005). In the sedimentation potential, solid particles are moved by gravity or a centrifugal field. (Hunter 1981, p. 1-4)

The streaming potential is created by the interaction between a streaming current and a conduction current. The streaming current I_s appears, when the charges of the double layer are moving inside of a capillary. This movement is induced by forcing the liquid to move through the capillary. The streaming current generates an electric field, thus inducing a conduction current I_c, which is opposite to the fluid flow. When these currents balance each other, the steady state is accomplished. Finally, there will be an electrostatic potential difference between the ends of the capillary, which is called the streaming potential. The streaming potential is dependent on the pressure difference between the ends of the capillary, the zeta potential of the capillary, the viscosity of the solution, the bulk liquid conductivity and the absolute permittivity of the solution. (Hunter 1981, p. 64-68)

The streaming current can be presented as (5)

$$I_{str} = -\frac{\varepsilon_{rs}\varepsilon_0 a^2}{\eta}\frac{\Delta p}{L}\zeta \qquad (5)$$

where a is the radius of the circular cross section of the capillary, and L is the length of charged walls, $\varepsilon_{rs}\varepsilon_0$ is the absolute permittivity of solution, Δp is the pressure difference between the ends of the capillary, η is the viscosity of the solution and ζ is the zeta potential of the capillary. (Delgado et al. 2005).

The conduction current, which is induced to the system, can be presented as (6)

$$I_c = K_L a^2 \frac{U_{str}}{L} \qquad (6)$$

where K_L is the bulk liquid conductivity (S m^{-1}) (Delgado et al. 2005)

The streaming current only appears if there is a short circuit. If the circuit is not short, the streaming current can't be observed as there appears the conduction current. When the conduction current and the streaming current are equal, there is no net current and the streaming potential is (7)

$$U_{str} = \frac{\varepsilon_{rs}\varepsilon_0 \zeta \Delta P}{\eta K_L} \qquad (7)$$

This is valid, when the curvature radius of the particle is much greater than the Debye length and the electrical conductance of the surface is small. (Delgado et al. 2005)

Zeta potential is thus (8)

$$\zeta = \frac{U_{str}\eta K_L}{\Delta p \varepsilon_{rs}\varepsilon_0} \qquad (8)$$

(Delgado et al. 2005)

In this thesis Formula (9) is used, as it takes into the consideration also the size of the column. Formula (9) has also already been used successfully in similar measurements than measurements in this thesis (Pat. US 5280250 1994. Väisänen 2012).

$$\zeta = \frac{U_{str}}{\Delta p} \frac{4\eta l}{\varepsilon_{rs}\varepsilon_0 a^2 R} \qquad (9)$$

Here *l* is the length of the magnetite column and *a* is the radius of the magnetite column. *R* is the inverse of the conductivity of the flow path, referred in this thesis as the resistance of the magnetite column. (Pat. US 5280250 1994)

2.5 Methods for preventing material degradation in steam generators

There are several methods for reducing magnetite dissolution and deposition and the material degradation that they cause. These methods include preventive actions accomplished by altering water chemistry, designing and selecting better materials and structures, and restorative actions accomplished by cleaning and repairing. There is also the possibility of eliminating already existing problems (leakage) by plugging the heat exchanger tubes or changing the whole steam generator.

There are several procedures for avoiding corrosion problems. These are e.g. using high pH chemistry (high ammonia or amine concentration) (Woo & Lu 1981. Tapping et al. 2000. IAEA 2011, p. 42), reducing oxygen content (Woo & Lu 1981) and using a copper free secondary circuit (Tapping et al. 2000. IAEA 2011, p. 42). Also great effect can be made by avoiding impurities as much as possible, by controlling the molar ratio of strong cations to strong anions, or by using hydrolysable substances like phosphate or boric acid, although phosphate treatment is no longer in use because it forms wastage (IAEA 2011, p. 42- 44). The steam generator blowdown rate can also be increased (Woo & Lu 1981. Tapping et al. 2000), but that is not very economically effective (IAEA 2011, p. 43). Furthermore, titanium-based inhibitors and boric acid are used for controlling the corrosion processes (Wood 2012, p. 39). Most power plants use several of these methods (IAEA 2011).

Correspondingly, the power plant designing and the balance of the plant design are important when thinking of corrosion problems in the steam generator. Material degradation can be minimized by using low alloyed Cr/Mo-carbon steels, when there is possibility of flow accelerated corrosion, avoiding the turbulence of feed water (which increases FAC) and decreasing the amount of the make-up water (which contains impurities). (IAEA 2011, p. 49-55) Chemical cleaning of the pipes is also possible (Woo & Lu 1981).

Corrosion problems can have a huge economic impact (Klimas et al. 2003). Therefore the last options are plugging or sleeving tubes, or replacing tubes or the whole steam generator (Woo & Lu 1981). The replacement of the steam generator costs $200 million on average. Even the cleaning of the steam generator is expensive, the chemical cleaning of the crud deposits costing $3,200/kg. (Klimas et al. 2003)

Material degradation has a strong influence on radiation safety as well. The personnel of the nuclear power plant get the greatest part of their radiation exposure during the maintenance works. Thus reducing corrosion problems and the time spent on maintenance is desirable. (EPRI 1997a)

2.5.1 Water chemistry

Secondary side water chemistry is controlled in order to minimize the corrosion rate of the steam generator tubes and to decrease the rate of flow accelerated corrosion and deposition of corrosion products in the secondary side. At the same time, operating costs should be minimized, still maintaining the safety of the plant, and minimizing the amount of the waste released to the environment. (Odar & Nordman 2010) The most important point about secondary side water chemistry control is to prevent impurities from forming and transporting, and to decrease fouling and other corrosion damages in the steam generator tubes (Wood 2012, p. 37). Besides, water chemistry must be chosen so that it does not damage steam generators, turbines, condensers, feed water heaters, moisture separator reheaters or the piping of the secondary circuit (Odar & Nordman 2010).

Earlier there were several problems caused by impurities, like chlorides and sulphates. Soon it became clear that it is not enough to control impurities, but it is also necessary to modify water chemistry by controlling oxygen levels and pH in the nuclear power plants. Nowadays new requirements for material integrity and thus water chemistry have arisen as the plant owners want to increase the life time of their power plants. (Wood 2012, p. 18) Efforts for making water chemistry better have not been useless, as improvements in the water chemistry of the secondary side of the nuclear power plant have led to an increase of over 20 years in the life time of the steam generators (EPRI 1997a).

As it was concluded earlier, surface chemistry has a great effect on the deposition of particles. The surface charge of corrosion products can be altered by water chemistry and by using amines for pH control (EPRI & AECL 2002). Optimum pH is selected in order to avoid flow accelerated corrosion. It is selected so that the iron solubility in the secondary circuit environment is at its lowest (Figure 18). Then also the FAC is at its lowest, as it is the hardest to the flow to dissolve iron to the solution (Figure 19). Optimum pH would be somewhere in the range 9.7-10.1 (Nordmann & Fiquet 1996. Varrin 1996. EPRI 1997b). Sometimes lower pH (9.2-9.6) is used, because there are copper parts in the circuit (Saddler et al. 1989).

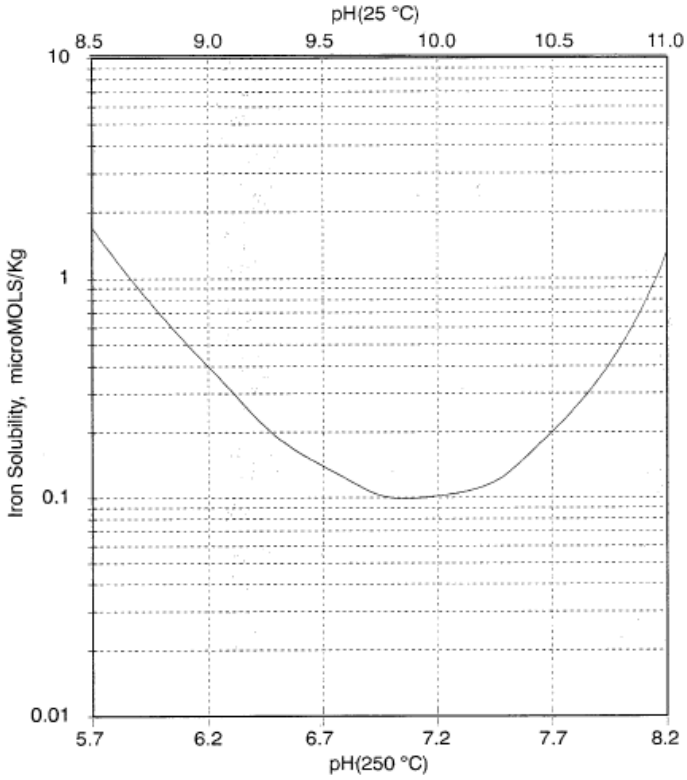

Figure 18: The solubility of iron as a function of pH in the temperature of 250˚C (EPRI 1997b)

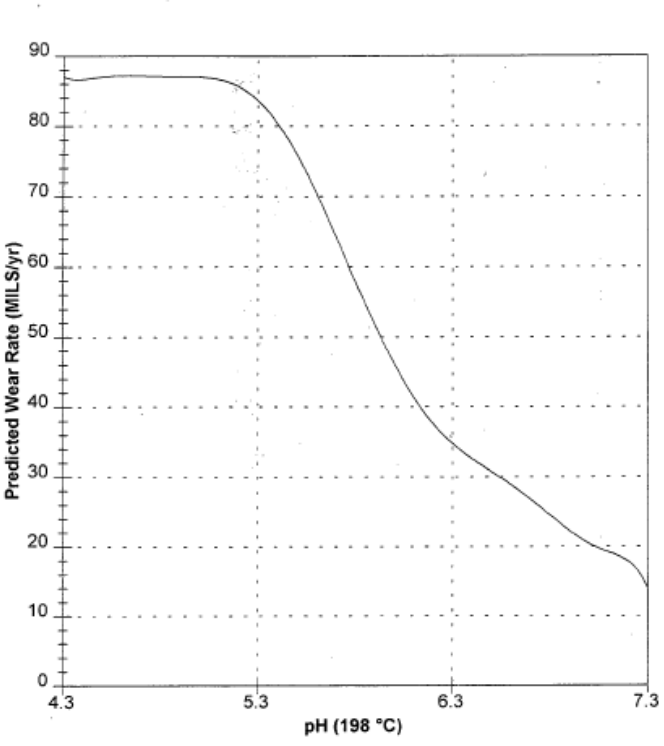

Figure 19: Flow accelerated corrosion in carbon steel as a function of pH in the temperature of 198˚C (EPRI 1997b)

Nowadays there are several options for water chemistry procedures in addition to all-volatile treatment (EPRI 1997a). These include high hydrazine treatment (EPRI 1997a), adding morpholine or advanced amines (EPRI 1997a), using boric acid (EPRI 1997a) or other corrosion inhibitors (EPRI 1997a), optimizing oxidation-reduction-potential to minimize iron transport (EPRI 2004), eliminating specific impurities (EPRI 2004), and combinations of all of these methods (EPRI 1997a). It is also possible to control the molar ratio of ions (EPRI 1997a). Significance of molar ratio control has been lowered and no plants with replaced or new steam generators are using it. Only ten plants were using molar ratio control in 2007 and they all have old steam generators. (Wood 2012, p. 37) It must be emphasised that controlling water chemistry is not easy as it must be suitable for all parts of the water circuit. (EPRI 1997a)

In conventional power plants, there is a rather long history of using amines like cyclohexylamine and morpholine. Amines were first tried in the conventional power plants in the 1930s. Amines have been tested and used in the nuclear power plants for a quite long time as well. This history extends back to the 1960s. (Saddler et al. 1989) For commercial use, amines and their mixing for controlling pH were introduced in the 1990s (Wood 2012, p. 41-42).

The main reason to use amines is to prevent flow-assisted corrosion and to decrease corrosion products transport by increasing pH (Nordmann & Fiquet 1996). Typical amines for that are monoethanolamine (ETA) and morpholine (MPH). Ammonia (NH_3) is not an amine, as it has no carbon atoms, but is used like an amine. Figure 20 shows the structures of ammonia, ethanolamine and morpholine. There are also more rare amines, so called advanced amines, like 2-amino-2-methyl-propanol (AMP), dimethylamine (DMA) and 3-methoxypropylamine (3MPA). (Klimas et al. 2003)

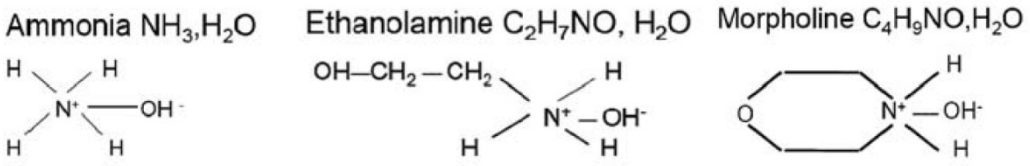

Figure 20: Molecule structures of ammonia, ethanolamine and morpholine (Odar & Nordman 2010)

The most commonly used amine in the nuclear power plants of the USA is ethanolamine. Over 70% of US plants are using ETA alone or with other amines. About 11% of the plants are using morpholine, or morpholine and other amines to control the secondary circuit chemistry. (Wood 2012, p. 42) The percentage of different amines used in the nuclear power plants in the USA is presented in Figure 21.

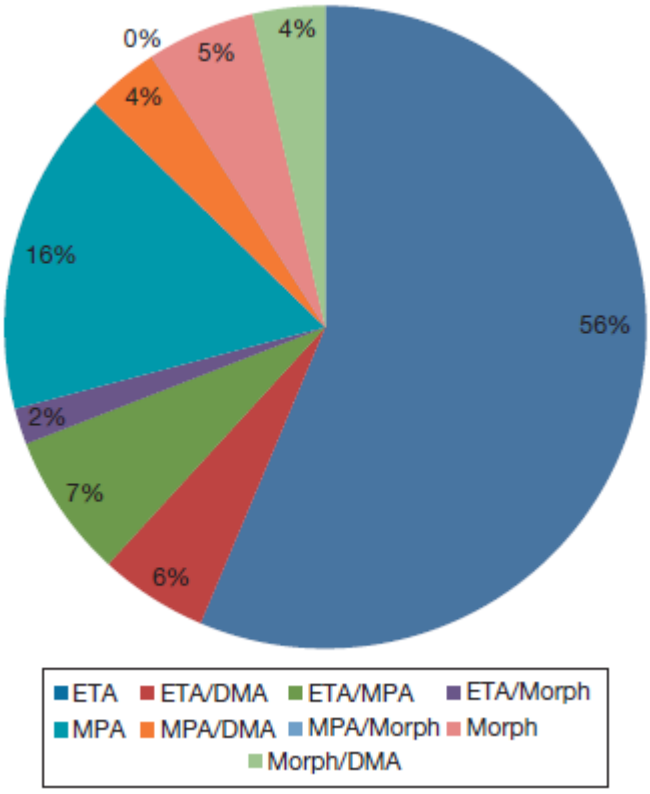

Figure 21: Different amines used in the secondary systems of the nuclear power plants in the United States of America (Wood 2012, p. 42)

There are several selection criteria for amines used in the secondary side (Klimas et al. 2003). Amines must e.g. be strong base (Saddler et al. 1989. Klimas et al. 2003) and have low volatility (Saddler et al. 1989. Klimas et al. 2003), they must not increase corrosion rates (Klimas et al. 2003) and preferably result in a low deposition rate for magnetite particles (Klimas et al. 2003). They must have certain thermal stability (Saddler et al. 1989) and compatibility with circuit materials (Saddler et al. 1989), they must have a rather low price (Saddler et al. 1989. Klimas et al. 2003) and they must be commonly used (Klimas et al. 2003). Furthermore, they must not cause any serious environmental hazards (Saddler et al. 1989).

The concentration of the amines in the circuit water can be measured by measuring the direct conductivity of the circuit water. There are also colorimetric on-line instruments for measuring the amine levels. Moreover, it is possible to measure the levels with ion-chromatography. (Saddler et al. 1989)

It has been demonstrated that amines reduce flow accelerated corrosion and iron transport (Saddler et al. 1989) and they affect both the particle deposition and the deposit consolidation (Odar & Nordman 2010). The change from ammonia treatment water chemistry to amine treatment is rather easy (Saddler et al. 1989), so there should be no problem. However, amines can contaminate the system by decomposing at higher temperature producing e.g. organic acids and amine treatment is more expensive than ammonia treatment. Less common amines may also have health hazards, which should be investigated in advance. (Saddler et al. 1989)

Ammonia has been used for elevating pH for a long time. Ammonia has well known properties also in environmental and health aspects (Odar & Nordman 2010). Ammonia can be added to the system, by adding hydrazine, as hydrazine decomposes producing ammonia. Ammonia itself has high stability so there are no decomposition products that could damage the system. Amines, on the contrary, decompose rather easily. It must be noticed that ammonia in higher concentrations is not compatible with copper alloys. (Odar & Nordman 2010).

Moreover, ammonia does not prevent flow accelerated corrosion in two-phase situations (Saddler et al. 1989). Therefore condensate lines can suffer from corrosion when using ammonia. This is due to the fact that ammonia has high volatility and thus does not stay in liquid phase in sufficient quantity. (EPRI & AECL 2002) Also the pH which is achievable in high temperatures with ammonia is not sufficient to minimize corrosion product transport in feed water and is not sufficient to prevent flow-accelerated corrosion of carbon steel components (Nordmann & Fiquet 1996). Thus there is a need for strong, volatile alkali that has a low steam-water partition coefficient, i.e. it distributes both to the water and to the steam (Saddler et al. 1989).

Morpholine has greater alkalinity in high temperatures than ammonia when thinking of a situation where both have the same alkalinity in the room temperature (Odar & Nordman 2010). This means that in e.g. above 200 °C morpholine is a stronger base than ammonia (Saddler et al. 1989). Besides, morpholine is quite cheap (Saddler et al. 1989). Also the volatility of morpholine is less than that of ammonia (Saddler et al. 1989), so it decreases the rate of flow accelerated corrosion in two-phase situations and in the whole secondary system (Odar & Nordman 2010). Indeed, morpholine has nearly constant concentration in the whole secondary system, both in the areas of steam and water, while ammonia concentration decreases in liquid. Contrary to ammonia, the concentration of ethanolamine decreases in steam. This is due to their different steam-water distribution factors, originating from their different volatilities (Odar & Nordman 2010).

However, a higher concentration of morpholine than NH_3 is required in order to accomplish the same pH at room temperature. A higher concentration may reduce the life time of the condensate polishers. (Odar & Nordman 2010) Morpholine also generates nitrogen (Odar & Nordman 2010) and increases the concentrations of organic acids, acetates and formiates (Nordmann & Fiquet 1996).

ETA produces less organic acids than morpholine but has a lower steam-water distribution factor. The required ETA concentration is smaller than that of morpholine so the burden to the condensate polishers is smaller. (Odar & Nordman 2010) Ammonia, morpholine and ethanolamine are compared in Table 4.

Table 4: Properties of ammonia, morpholine and ethanolamine (Nordman 2006)

Amine	Chemical formula	Molecular mass	pK_b=-logK_b			Steam-water distribution factor, Kd		
			25°C	150°C	300°C	25°C	150°C	300°C
Ammonia	NH_3	17	4.76	5.13	6.83	30.20	10	3.23
Morpholine	C_4H_8ONH	87	5.50	5.30	6.63	0.12	0.77	1.29
ETA	$C_2H_4(OH)NH_2$	61	4.50	4.83	6.40	0.004	0.11	0.489

There are also amines which tend to form a protecting film on the pipe surfaces (Saddler et al. 1989). One of these filming amines is octadecylamine (Saddler et al. 1989). These filming amines reduce the rate of flow accelerated corrosion and fouling. It is even reported that filming amines seem to have greater effect on flow accelerated corrosion and fouling than pH altering amines. (EPRI 2003)

Besides amines, it is possible to apply dispersants which prevent deposition. However, they must not have any harmful impurities. (Wood 2012, p. 43) Pure polyacrylic acid PAA has been observed to be a good dispersant for nuclear applications (Fruzzetti 2009. Wood 2012, p. 43). The history of the different water chemistry altering methods is demonstrated in Figure 22. Figure 23 illustrates how common different methods of the water chemistry altering are in the secondary side of the nuclear power plants in the USA.

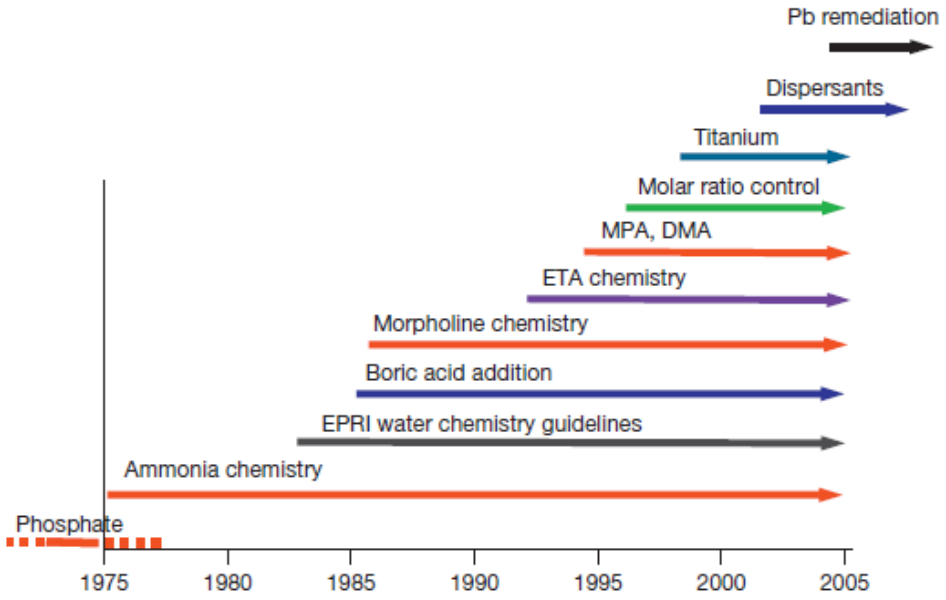

Figure 22: History of different water chemistry altering methods. (Wood 2012, p. 41)

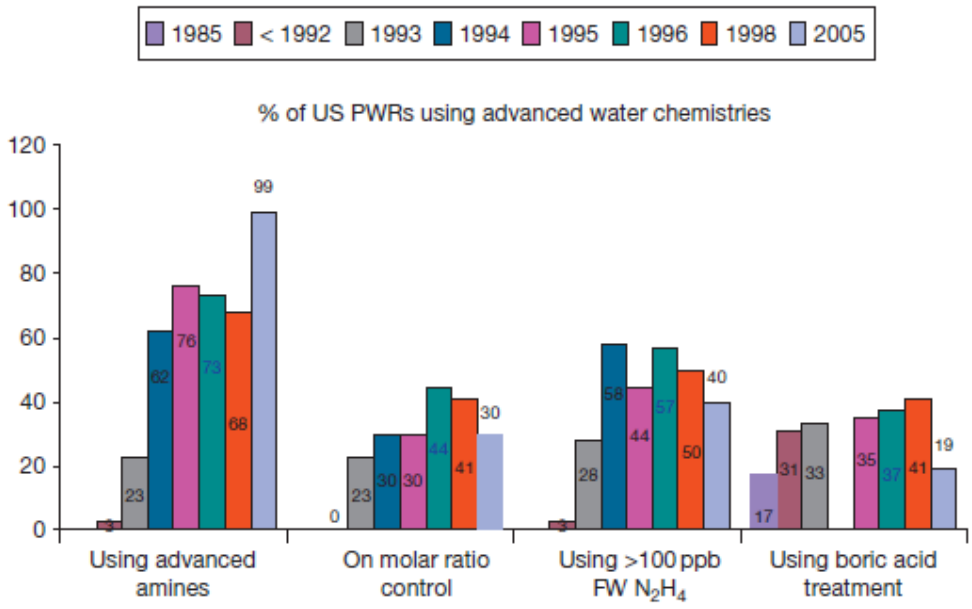

Figure 23: Advanced water chemistries in the US (Wood 2012, p. 43)

2.5.2 Chemical and mechanical cleaning

There are several chemical and mechanical cleaning methods and purification systems in the nuclear power plant. Even though there are impurities in the whole secondary system, the concentration of non-volatile impurities rises in the steam generators because of the boiling. Therefore the cleaning of the steam generator is important. The process that contains directing part of the water from the steam generator through the purifying system and returning it to the system is called the blowdown (Saddler et al. 1989). The blowdown is one of the most important purification systems. However, the blowdown removes only corrosion products that are suspended the liquid, not the particles that have already deposited (Green & Hetsroni 1995). The amount of water blowdowned is typically 1 to 2 % of the whole amount water going through the steam generator (Klimas et al. 2004.).

Condensate Polishing System (CPS) purifies water coming from the condenser and going to the steam generator. CPS has multiple Ion Exchange Resin (IER) filters or beds. CPS allows running the plant even when the condenser is leaking, but CPS is expensive and restricts the pH and the reagent selection of the secondary circuit. Steam Generator Blowdown Demineralizer (SGBD) also has ion exchange resin filters or beds and is used for purifying the blowdown water. (Odar & Nordman 2010)

Corrosion problems can be decreased by removing the particle deposits by chemical cleaning. This also increases the heat transfer rate. (Schwarz 2001) Chemical cleaning is effective when executed in the whole tube bundle (White et al. 1998). In Hard Chemical Cleaning processes solvents are used for removing copper and iron deposits from the secondary circuit. In the maintenance chemical cleaning processes, dilute chemicals are used for removing some of the deposits.

There are also mechanical cleaning processes. (Odar & Nordman 2010) There are two gas pressure methods that are designed to remove magnetite deposits in the once-through steam generators. In these methods, a large amount of nitrogen gas is fast released to the steam generator thus replacing water, which then flushes all the crevices and holes removing corrosion product deposits. When the deposits are detached, they can be removed from the steam generator by filters or a blowdown. Third option is sludge lancing, where deposits are removed with high-pressure water sprays (Green & Hetsroni 1995).

2.5.3 Repairing, plugging and replacement

The options, in the case of severe material degrading in the steam generator, are to change the steam generator, to reduce the power of the reactor due to the heat transfer problems or to shut down the plant. Especially, if the reactor is near the end of its life, it becomes appealing to shut down the plant or to reduce the power, as the plant would not pay back the investment of a new steam generator. (EPRI 1997a) Steam generator replacement is not easy, not from the radiation, economy or engineering point of view (Tipping 1996).

Ruptured steam generator tubes can be sleeved or plugged (Tipping 1996). Tube bends that are prone to corrosion problems can be shot peened to reduce susceptibility to stress corrosion cracking (Tipping 1996). Most tube plugging is caused by outer-diameter secondary side stress corrosion cracking (Diercks et al. 1999).

2.5.4 Other methods

It is important to estimate the condition of steam generator tube materials so that material degradation prevention actions can be planned. There are several methods for that. They include mathematical modelling, non-destructive testing and chemistry monitoring.

The safety and the condition of steam generator tubes can be estimated with mathematical models. These models give information about the probability of a tube rupture, the number of tubes to be plugged or repaired, and the estimation about the maximum amount of water that can be leaked between the secondary and the primary side in the case of an accident. All these models give a picture about the total safety of the steam generator. (Dvoršek et al. 1998)

Location of deposits can be estimated with mathematical models as well (Srikantiah & Chappidi 2000). The ATHOS3 software can be used to calculate fouling regions and fouling factors on the vertical and horizontal surfaces in the steam generator (White et al. 1998. Srikantiah & Chappidi 2000). It has been calculated that fouling happens most often in the hot side upper bundle and on the top of the tube sheet (Srikantiah & Chappidi 2000). SLUDGEM is another computer program that models the behaviour of the deposits in the pressurized water reactor (Green & Hetsroni 1995).

Non-destructive testing methods are required for examining the condition of materials and components in the nuclear power plant. Eddy current testing is widely used for the periodic inspection of the steam generator tubing. Also visual inspection techniques and ultrasonic techniques are being used. (Woo & Lu 1981)

In order to determine the right chemistry and to evaluate the possibility of problems, it is necessary to somehow monitor the chemistry. This is accomplished by on-line monitoring and by grabbing samples. In steam generators, the parameters to be monitored are e.g. specific conductivity, cation conductivity, redox potential and the levels of sodium, chloride, sulphate, oxygen, hydrazine and copper. (Odar & Nordman 2010) For example, corrosion rates can be estimated by measuring the amount of hydrogen in the system as hydrogen is produced in most corrosion processes under reducing conditions (Woo & Lu 1981).

3. Materials and methods

The purpose of the experiments presented in this thesis was to measure the zeta potential of colloidal magnetite particles in the environment simulating the secondary circuit of the pressurized water reactor while using different amines to increase pH. As mentioned earlier zeta potential can be used to evaluate the behaviour of magnetite particles in the secondary circuit and thus help to minimize the problems caused by magnetite deposits and impurities.

Streaming potential was chosen to be the method for these zeta potential measurements, as it had been earlier used successfully for evaluating zeta potential at high temperatures. Even though there are several automated instruments for zeta potential measuring, they could not been used in this experiment as they could only be used up to 90°C. (Jayaweera & Hettiarachchi 1992) Therefore special customized equipment was needed. This equipment was for a great part the same used in the Master's thesis written before by Saija Väisänen (Väisänen 2012). However, equipment was modified in order to increase operating temperatures from 143˚C to 248˚C.

The measurements were performed by circulating oxygen-free water through the magnetite column. The flow velocity of circulating water was changed in order to achieve a change in pressure difference over the magnetite column. The streaming potential over the column was measured continuously so that the change in the potential difference caused by the flow velocity change could be recorded. After the measurement, the impedance of the magnetite column was measured in order to obtain the resistance of the magnetite particles in that particular environment. The pH in measurements was 9.2 ± 0.25 and the temperature was varied from 23 to 248˚C. The equipment had not been used in such high temperatures before so a lot of effort and time was used to modify the equipment for those temperatures and to learn how the system reacts in those environments.

3.1 Chemicals and substances used

The measurements were performed with commercial magnetite powder (99.5%) produced by Ventron GmbH. The diameter of particles was roughly 0.5 µm (Väisänen 2012) The magnetite powder was suction filtrated through a polypropylene membrane filter (Pall Life Sciences GH Polypro, 0.45 µm) in order to minimize the amount of the magnetite flowing through the ceramic filter. The filtered powder was dried before weighting it with an analytic scale (Mettler AE 163). The amount of magnetite used was mainly 2.5 g but also 4 g was used in a couple of measurements with the purpose of resolving how the amount of magnetite possibly affects the results.

The amine solutions used in measurements were diluted from ammonia (Merck 25%), 2-aminoethanol (Aldrich 99+%) and morpholine (Aldrich 99+%).

3.2 Methods of the measurements and description of the testing equipment

3.2.1 Measuring streaming potential

The amine water solution was circulated in the measurements between the water loop shown in Figure 24 and the test loop of Figure 25. The conductivity (inlet and outlet), the pH (inlet) and the oxygen level (inlet) of solution going to the test loop were measured on the water loop. The solution in the water loop was circulated with a mixing pump. Oxygen was removed from the solution by bubbling nitrogen (99.999%) through it. Nitrogen was delivered by Oy AGA Ab. The water loop was equipped with a feed water tank of 60l, a Hach Lange sc200 pH meter, ABB Ax400 conductivity meter and Orbisphere 3660 dissolved oxygen meter.

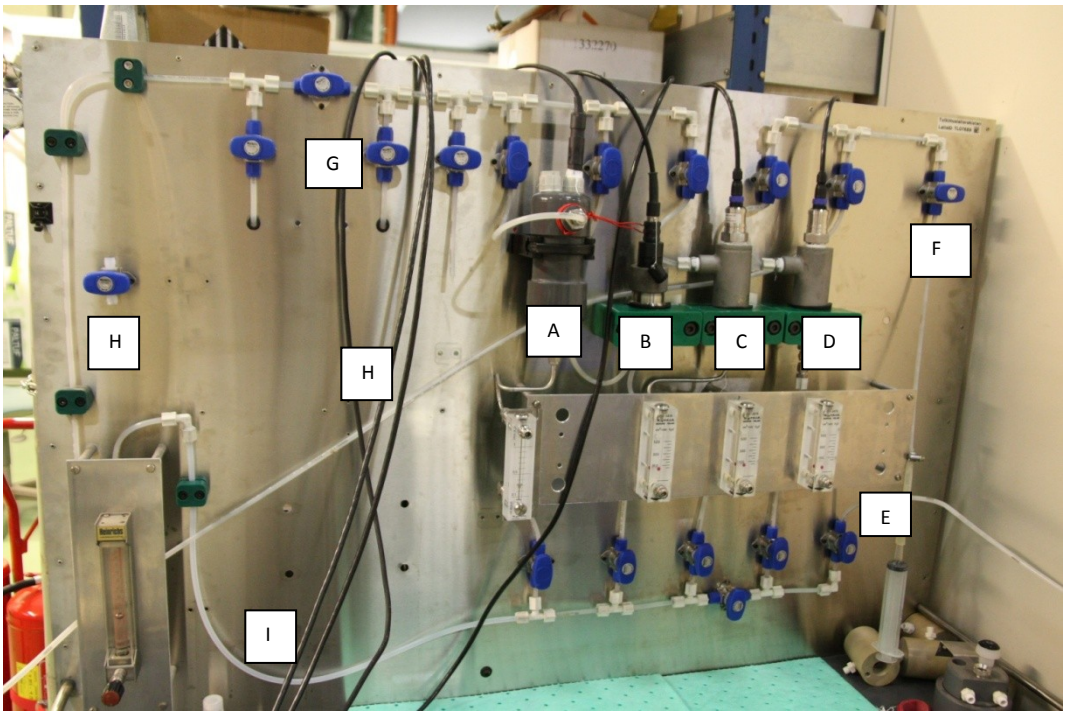

Figure 24: Water loop. A=pH (inlet), B=O_2 (inlet), C=Conductivity (inlet), D=Conductivity (outlet, E=Water from the test loop, F=Chemical insertion, G=Inlet and outlet of the ion exchanger used for the removing the chemicals, H=Water to the water tank and I= Water from the water tank. The mixing pump, the water tank, the nitrogen bottle and the piping from the water loop to the test loop are not to be seen here.

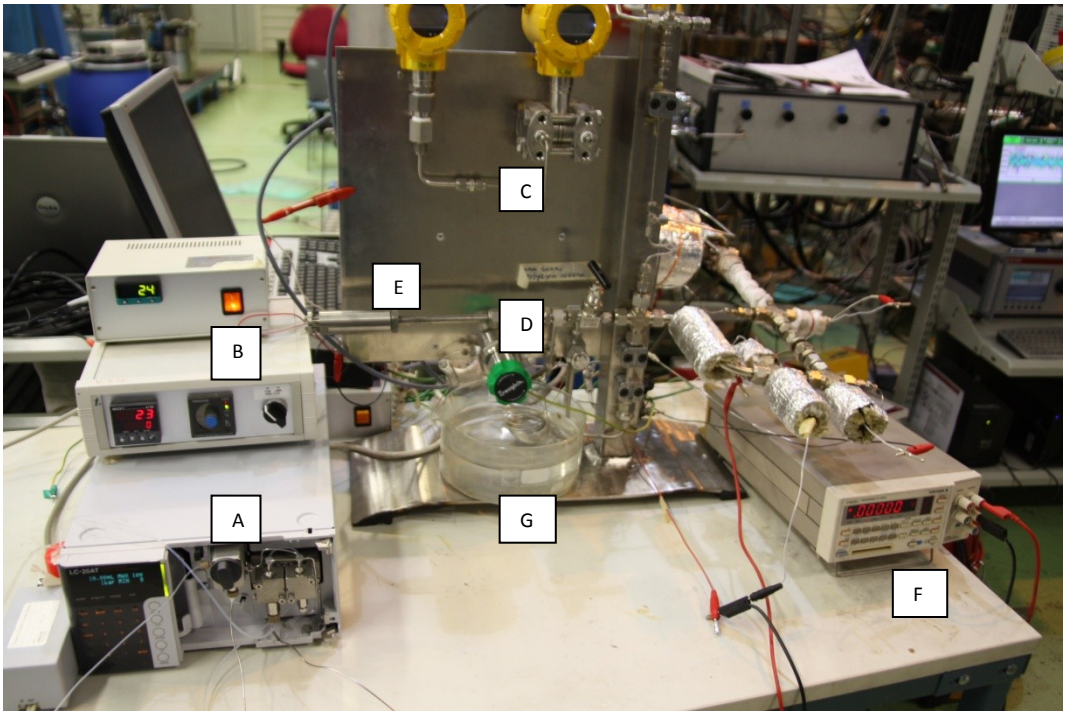

Figure 25: Test loop. A=LC pump, B=Temperature controlling, C=Pressure gauges, D=Back pressure valve, E=Reference electrode, F=Power supply for polarizating of the Pd electrode, G=Water cooling

From the water loop solution was pumped to the test loop with a LC-pump (Shimadzu Corporation LC-20AT). The test loop was pressurized to 7 MPa. The solution was heated to the measuring temperatures by a cartridge heater controlled by West 6100 temperature controlling equipment and two heating tapes controlled by Meyer-vastus temperature controlling equipment. The test loop itself was made of AISI 316 stainless steel tubes and connectors manufactured by Swagelok. The power supply of the circuit for the polarization of the Pd electrode was Yokogawa 7651. The results of the measurements were transferred to the computer by Agilent 34970A Data Acquisition/Switch Unit. The results were saved by the HP BenchLink Datalogger program.

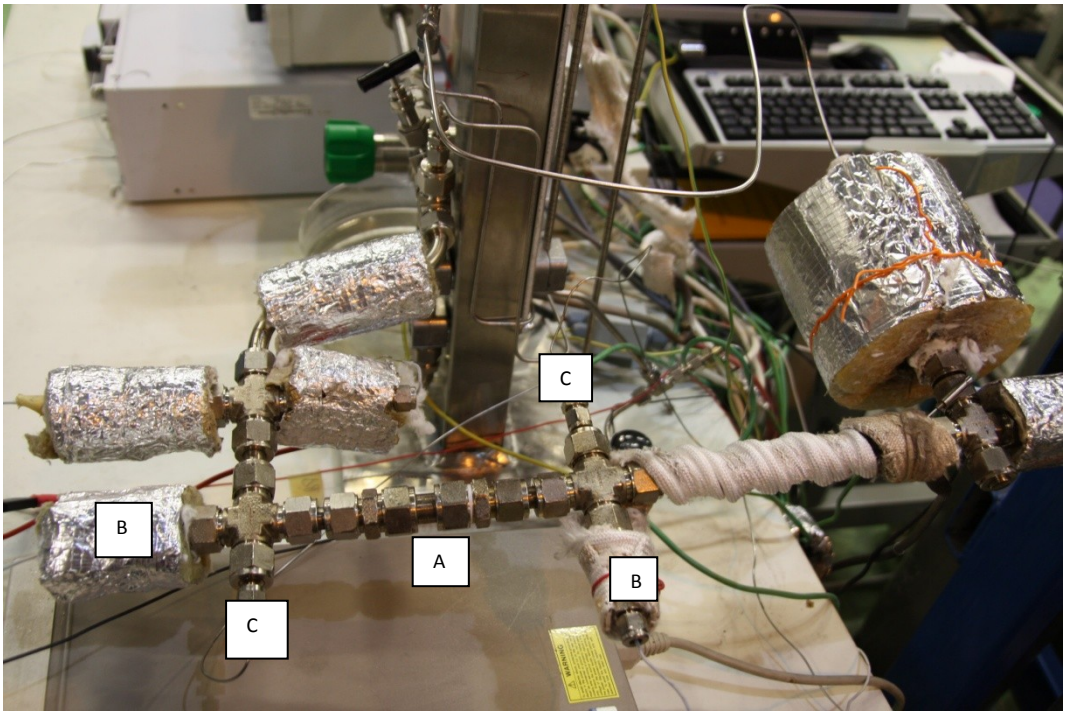

Figure 26: Part of the test loop. A=Magnetite column, B=Pt electrodes, C=Temperature measuring

The test loop details are shown in Figures 26-28. The most important part of the test loop is the magnetite column (Figure 27, and bullet no. 1, in Figure 28), which is kept in place by a stopper, made of oxidized zirconium, and a ceramic membrane filter. The ceramic membrane filter (Sterlitech, cut at Finnish Specialglass) is at the end of the magnetite column and it prevents magnetite leaving the test loop. The zirconium stopper upwards the stream is used to keep magnetite column in a proper shape. The zirconium stopper had holes in it for not preventing the flow of the solution. The magnetite column is isolated from the metallic pressure bearing tubes with an inner PTFE pipe. The PTFE tube and the ceramic membrane filter are compressed to their place with a PTFE seal. Also numerous other sealing materials were tested but they all lacked in temperature, amine or pressure endurance or they clogged the pores of the ceramic membrane filter as they deformed during operation.

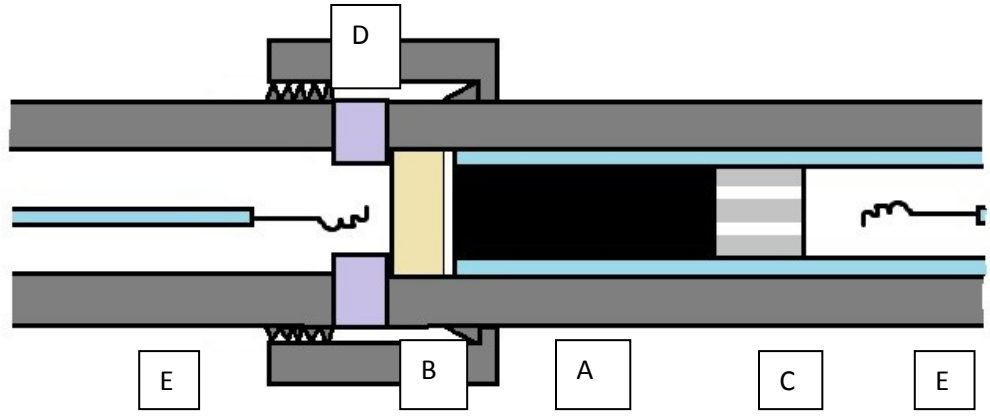

Figure 27: The magnetite column and its surroundings. A=Magnetite column, B=Ceramic membrane filter, C=Zirconium stopper, D=PTFE seal, E=Pt electrodes.

The potential difference needed in the zeta potential measurements was measured between the ends (2) of the magnetite column with platinum electrodes. The electrode wires were isolated from metallic surfaces with small PTFE tubes.

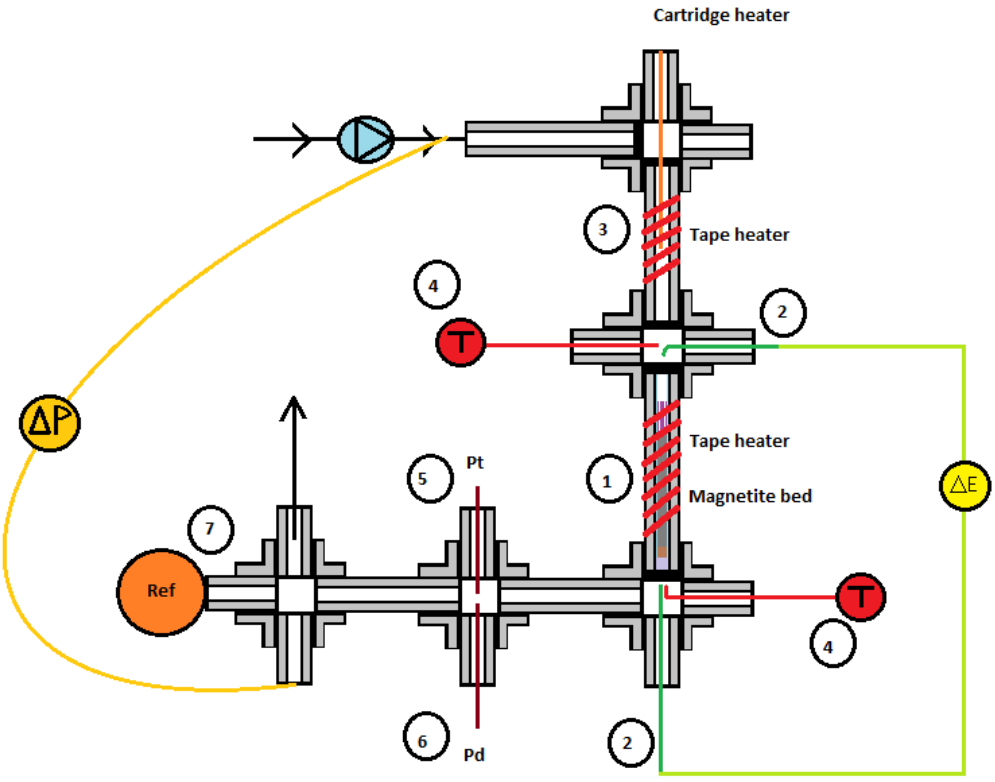

Figure 28: Principle of test loop (modified from Väisänen 2012). 1=Magnetite column, 2=Platinum electrodes, 3=Cartridge heater, 4=Thermocouples for temperature measuring, 5=Platinum electrode, 6=Palladium electrode, 7=Reference electrode.

Heating of the test loop was accomplished with two tape heaters and a cartridge heater (3). The cartridge heater and the first tape heater were used to pre-heat solution before entering the magnetite column area, and the second tape heater was directly surrounding the magnetite column area thus heating the column effectively. Two thermocouples, positioned under the tape heaters touching the metal pipe itself, were used for measuring the temperature next to the heaters in order to control the heating. There were also two thermocouples inside the loop (4), one right before the magnetite column and one after the seal of the ceramic membrane filter. The temperature of the magnetite column was defined as the average of two temperatures measured at these thermocouples. The cartridge heater was controlled with the temperature gained from the first (upstream) thermocouple inside the circuit (4). The whole test loop was insulated with glass wool tubes and plates tied to the pipes. The water loop with insulation is seen in Figure 29. The water was cooled after the magnetite column before it entered back to the water loop.

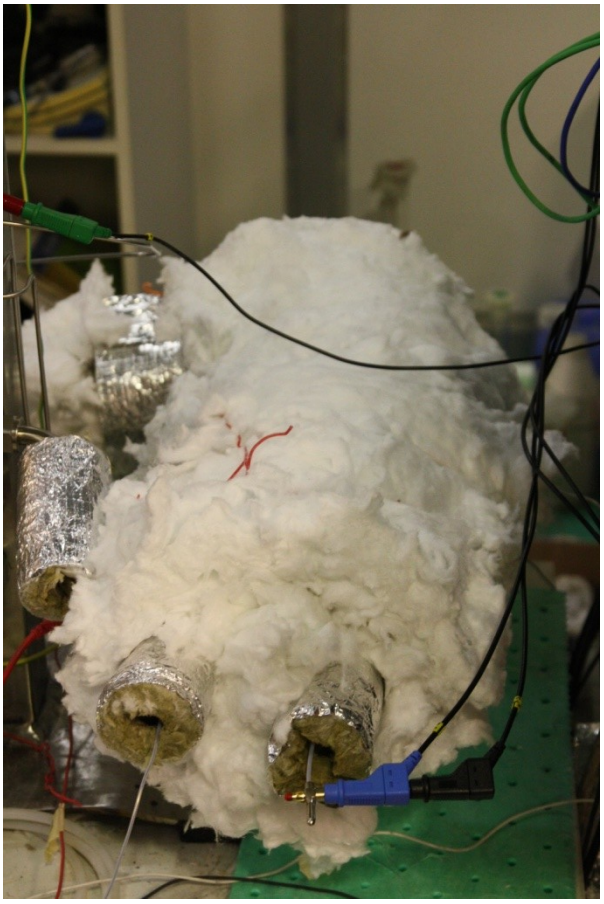

Figure 29: Insulated test loop

Total pressure was measured at the inlet of the test loop. Also the pressure difference between the ends of the test loop was measured as it was important part of the zeta potential measurements. The total pressure gauge was calibrated to the maximum pressure of 7 MPa and the pressure difference gauge to the maximum pressure difference of 0.4 MPa. The total pressure of the system was controlled by a Swagelok back pressure valve.

Even though there was pH measurement equipment in the water loop, there was also an alternative high temperature pH measuring system in the test loop. The Pd electrode (6) was polarized against the Pt electrode (5) until hydrogen begun to form on its surface. After that the palladium potential could be compared with the Ag/AgCl reference electrode (7) and thus acquire the acidity of the solution. Also the Pt electrodes (2) were measured against the Ag/AgCl reference electrode (7).

3.2.2 Measuring the impedance of the magnetite particles

Electrochemical impedance spectroscopy is an electrochemical measuring method where the stationary state of the system is interrupted slightly with a periodic signal that has small amplitude. Then the response in the output induced by the input is measured as a function of the frequency. The input is a potential signal with angular frequency ω and amplitude $\hat{E}$ ($E = \hat{\mathrm{E}}\, sin(\omega t)$). It generates an output with amplitude $\hat{I}$, angular frequency ω and phase shift δ ($I = \hat{\mathrm{I}}\sin(\omega t + \delta)$). (Murtomäki et al. 2010)

In polar coordinate system input (10) and output (11) can be presented as

$$E = \hat{\mathrm{E}}e^{j\omega t} \quad (10)$$

and $I = \hat{\mathrm{I}}e^{j(\omega t+\delta)}$ (11).

As the impedance by the law of the Ohm is $Z = \frac{E}{I}$ (12),

we obtain $Z = \frac{\hat{\mathrm{E}}e^{j\omega t}}{\hat{\mathrm{I}}e^{j(\omega t+\delta)}} = \frac{\hat{\mathrm{E}}}{\hat{\mathrm{I}}}e^{-j\delta} = \hat{\mathrm{Z}}e^{-j\delta}$ (13),

where j is an imaginary unit. (Murtomäki et al. 2010)

In an electrochemical system, there is always a resistor *R*. But the phase boundaries can also store an electric charge. Thus there will be not only a resistance but also capacitive impedance, $Z_C = \frac{1}{j\omega C}$, (14) in a system. (Murtomäki et al. 2010)

The total current over the phase boundary is $I_T = \frac{E}{R} + j\omega CE = \left(\frac{1}{R} + j\omega C\right)E$. (15)

So the admittance of the phase boundary is $Y = \frac{1}{R} + j\omega C$. (16)

And because admittance is the inverse of the impedance,

is total impedance $Z = R + \frac{1}{j\omega C}$. (17)

(Murtomäki et al. 2010)

The impedance between the upper and lower electrode was measured in order to gain the resistance of the magnetite column for the zeta potential calculations. The impedance was measured right after the streaming potential measurements at the same temperature, pressure and pH. The impedance was measured using Autolab potentiostat/galvanostat equipment and Autolab Nova software. The software presented impedance both as the Bode diagram and the Nyquist diagram. In the Bode diagram, the amplitude and the phase angle of the impedance is presented as a function of the logarithm of the frequency. In Nyquist diagram, the real part of the impedance *Z'*, the resistance, is presented in x-axis and the additive inverse of the imaginary part of the impedance *-Z''*, the capacitance is presented in the axis y. (Murtomäki et al. 2010)

In the impedance measurements, frequency area was between 1000 Hz and 0.01 Hz. The amplitude of the input signal was 30 mV. The resistance of the magnetite column was obtained from Nyquist diagram by reading the value of the real part of the impedance from the x-axis at the moment when the imaginary part of the impedance was zero.

3.3 Measurements

At the beginning of each measurement, it was checked that the oxygen levels were low enough for the measurements. The reasonable maximum level was defined at 130 ppb as the leak tightness of the system was not as good as hoped for. It was confirmed through potential measurements and Pourbaix-diagrams that this amount of oxygen does not change magnetite to hematite. Also the colour of the magnetite column was examined after the measurements in order to make sure that magnetite has not changed to hematite. The oxygen level was controlled by nitrogen bubbling (99.999% N_2) and the bubbling was used also during the measurements.

The water loop was pressurized to 7 MPa by pumping the water through the water loop and adjusting the back pressure valve. The system was checked for water leaks. When the loop was confirmed not to be leaking, the heating was started. When the measuring temperature was over 100°C the insulation was used, at lower temperatures the heating losses were insignificant. Some of the measurements were conducted with both tape heaters and a cartridge heater but some only with a cartridge heater, because the tape heaters lost their ductility and became unusable after certain amount of measurements. However, the heating with only the cartridge heater was successful, and the temperature difference between the ends of the magnetite column was reasonably low for almost all measurements (1-10°C), except for the ones measured at T> 200°C (max 60°C). In all cases the temperature reported was the average of inlet and outlet temperatures.

When the temperatures and the potentials of the electrodes had been settled at a constant level, the measurement was started. The pH, the oxygen level and the conductivities of the inlet and outlet water were written down and compared with the acceptable levels. The potentials of the measuring electrodes versus the ground, the reference electrode versus the ground and the potential of the reference electrode versus the palladium electrode were measured with a Fluke multimeter, written down and compared with the values measured by Agilent 34970A Data Acquisition/Switch Unit in order to ensure that the values sent to the computer were correct.

The LC-pump was programmed to change the velocity of the circulating water between three different velocities that followed each other continuously. First the highest velocity was used for a constant time, then it was instantly changed to the constant middle velocity for the same amount of time, then to the lowest velocity correspondingly and then changed back to the highest velocity and this was repeated to the end of the measurement. The time used for one velocity varied from 5 to 10 minutes so that with higher temperatures longer times were used in order to have enough time for the system to stabilize. The whole measurement lasted from 1 hour to 1.5 hours, so that two to three whole cycles of the velocity changing were conducted.

The velocity of the water flow was varied from 10 ml/min to 1 ml/min, the most typical velocities being 10, 7 and 4 ml/min. The velocities were chosen so that at the highest velocity the pressure difference did not exceed 0.4 MPa, the maximum pressure difference that could be measured by the sensor. At velocities lower than about 1ml/min the back pressure valve seized to function properly. When there was enough data (after two or three velocity changing cycles), the measurement was ended, and the impedance of the magnetite column was measured at the same conditions and written down.

Measurements were conducted for ammonia, ethanolamine and morpholine solutions at several temperatures. The conditions of the system varied slightly between the measurements. The details of the measurements are summarized in Tables 5-7.

Table 5: Details of the measurements in ammonia solution

Temperature (˚C)	pH	Amount of magnetite (g)
23	9.25	2.5
55	9.21	2.5
128	9.18	2.5
176	9.19	2.5
209	9.18	2.5
233	9.18	2.5

Table 6: Details of the measurements in ethanolamine solution

Temperature (˚C)	pH	Amount of magnetite (g)
23	9.40	2.5
52	9.45	2.5
84	9.41	2.5
136	9.36	2.5
179	9.40	2.5
210	9.33	2.5
236	9.30	2.5

Table 7: Details of the measurements in morpholine solution

Temperature (˚C)	pH	Amount of magnetite (g)
23	9.18	2.5
66	9.16	2.5
72	9.48	4
119	9.10	2.5
186	9.10	2.5
218	9.32	4
249	9.10	2.5

4. Results

4.1 Analyzing the results

The pressure difference and the potential difference gained from the measurements were plotted against time (Fig 30), so that areas where the system had not reached its stationary state could be omitted from the zeta potential calculations. In Fig 30, there are several areas, where the system was not stable. It must be pointed out that in high temperatures the system was not always stable because the change in the velocity of the circulating water changed rather drastically the lower temperature.

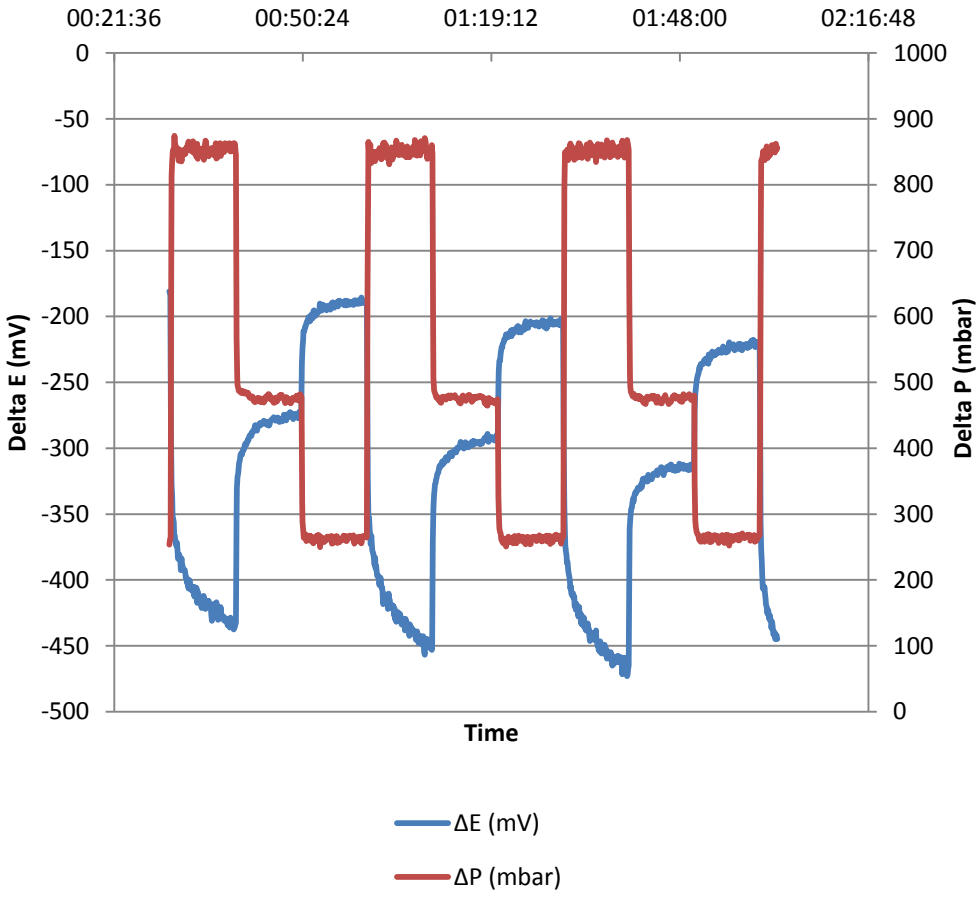

Figure 30: The original graph of ΔE and ΔP as a function of time for ethanolamine solution in 23˚C

After excluding the values where the system was not stable, the results from the zeta potential measurements were plotted as a graph that showed the potential difference as a function of the pressure difference (Fig 31).

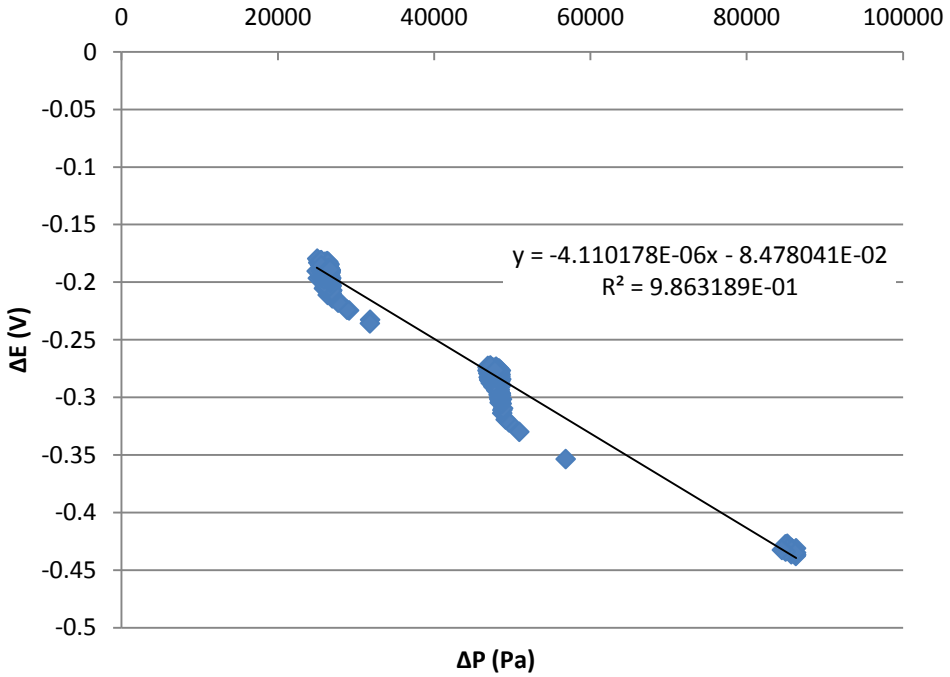

Figure 31: ΔE as a function of ΔP for ethanolamine solution in 23 ˚C with a linear slope fitted to data

The slope of that graph was then multiplied with certain constants, according to the Formula 9 (repeated here from page 40).

$$\zeta = \frac{U_{str}}{\Delta p}\frac{4\eta l}{\varepsilon_{rs}\varepsilon_0 a^2 R} = \frac{\Delta E}{\Delta P}\frac{4\eta l}{\varepsilon_{rs}\varepsilon_0 a^2 R} \qquad (9)$$

For ethanolamine solution at 23 ˚C, $\frac{\Delta E}{\Delta P}$ was $-4.110178 \cdot 10^{-6}\ \frac{V}{Pa}$, η was $0.00095\ \frac{Ns}{m^2}$, *l* was 0.026 m, ε_{rs} was 79, ε_0 was $8.854\ \cdot\ 10^{-8}\frac{F}{m}$, *a* was 0.005 m and *R* 800 000 Ω. When inserted to the equation above, one arrives at

$$\zeta = -4.110178 \cdot 10^{-6}\frac{V}{Pa} \cdot \frac{4 \cdot 0.00095\frac{Ns}{m^2} \cdot 0.026m}{79 \cdot 8.854 \cdot 10^{-8}\frac{F}{m} \cdot 0.005^2 m^2 \cdot 800000\Omega}$$

Unit for this is

$$\zeta = \frac{V}{Pa}\frac{\frac{Ns}{m^2}\cdot m}{\frac{F}{m}\cdot m^2\cdot\Omega} = \frac{V}{Pa}\frac{\frac{Ns}{m}}{Fm\Omega} = \frac{V}{Pa}\frac{Ns}{Fm^2\Omega} = \frac{V}{Pa}\frac{Ns}{\frac{s}{\Omega}m^2\Omega} = \frac{V}{\frac{N}{m^2}}\frac{N}{m^2} = V$$

and the result is $\zeta = -0.0290\,V = -29.0mV$

The resistance for the calculation was gained from impedance measurements. Figure 32 shows the measured resistance for all the experiments. Results were analysed with Microsoft Office Excel 2010 programme.

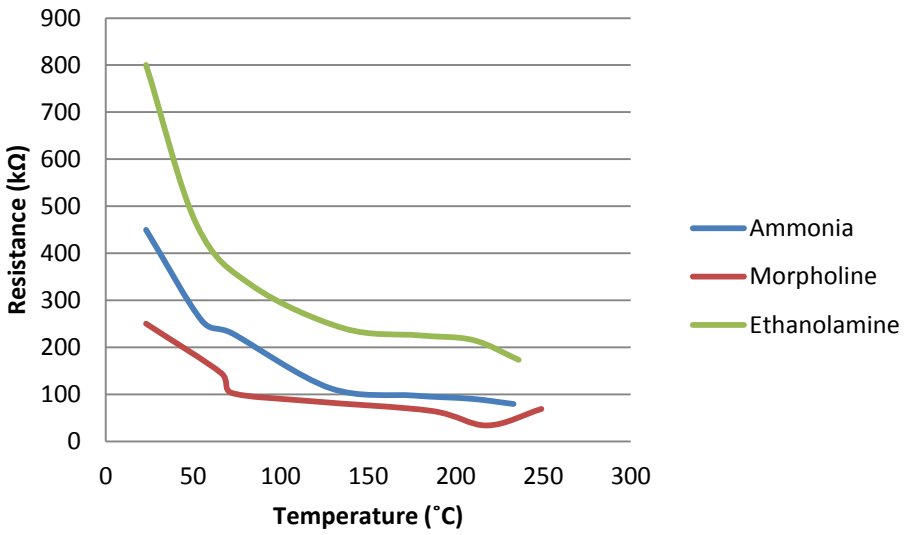

Figure 32: The resistance of magnetite column in different solutions as a function of temperature. In the morpholine curve, the effect of two measurements with the longer magnetite column can be seen at T=72˚C and T=218˚C.

4.2 The zeta potential of magnetite as a function of temperature in ammonia solution

The amount of the magnetite in the ammonia solution measurements was 2.5 g in all measurements and the length of the magnetite column was measured to be 26 mm after the measurements. It must be emphasized that the column of magnetite compresses during the measurements so the length of the magnetite column is not certain as there is possibility that the magnetite was not as compressed in the first measurement at room temperature as it was in the last measurements with T>200˚C.

In order to understand the effect of temperature on the zeta potential of magnetite in the solutions, both the calculation constant (Formula 10 without $\Delta E/\Delta P$) (Fig 33) and the slope of the $\Delta E/\Delta P$ graph (Fig 34) were plotted as a function of temperature. Both show an increasing trend, but it is hard to say whether the trend is linear or exponential.

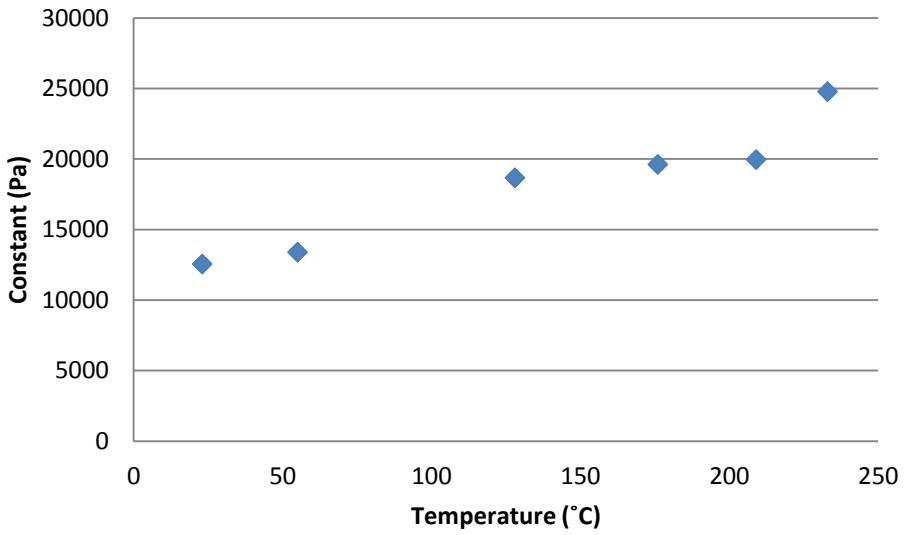

Figure 33: The calculation constant in ammonia solution

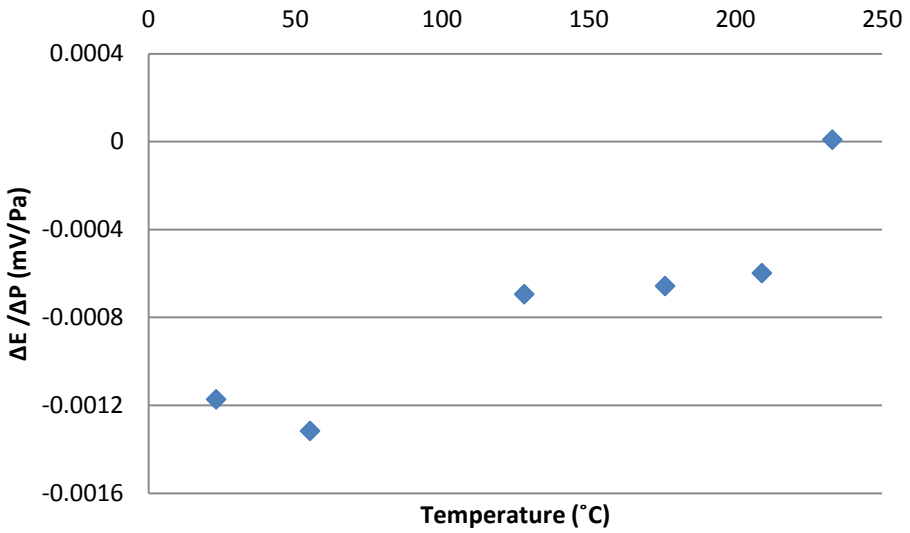

Figure 34: The *ΔE/ΔP* in ammonia solution

When these terms are multiplied to achieve the zeta potential (Fig 35), it seems that the zeta potential of magnetite in ammonia solution is slightly increasing from -16 mV to -12 mV in the temperature range of 20-200˚C. When approaching 250˚C the zeta potential quickly approaches zero. There is some uncertainty of the zeta potential value at the highest temperature, because the reduction of water velocity at high temperatures induced a maximum drop of 30˚C in the outlet temperature. This unbalanced the steady state of the lower electrode creating disruption to the measurement.

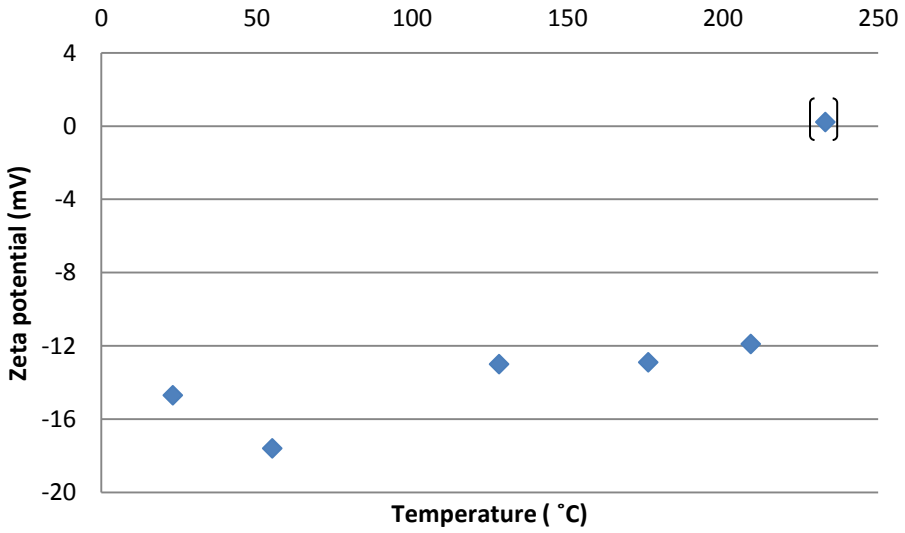

Figure 35: The zeta potential in ammonia solution as a function of temperature

Nevertheless, while the exact zeta potential value at high temperature might have greater percentage error than at lower temperatures, it can still be said that the value is near zero, because the change of the potential of the electrodes is really small (Fig 36). The exact zeta potential results for ammonia solution can be seen in Table 8.

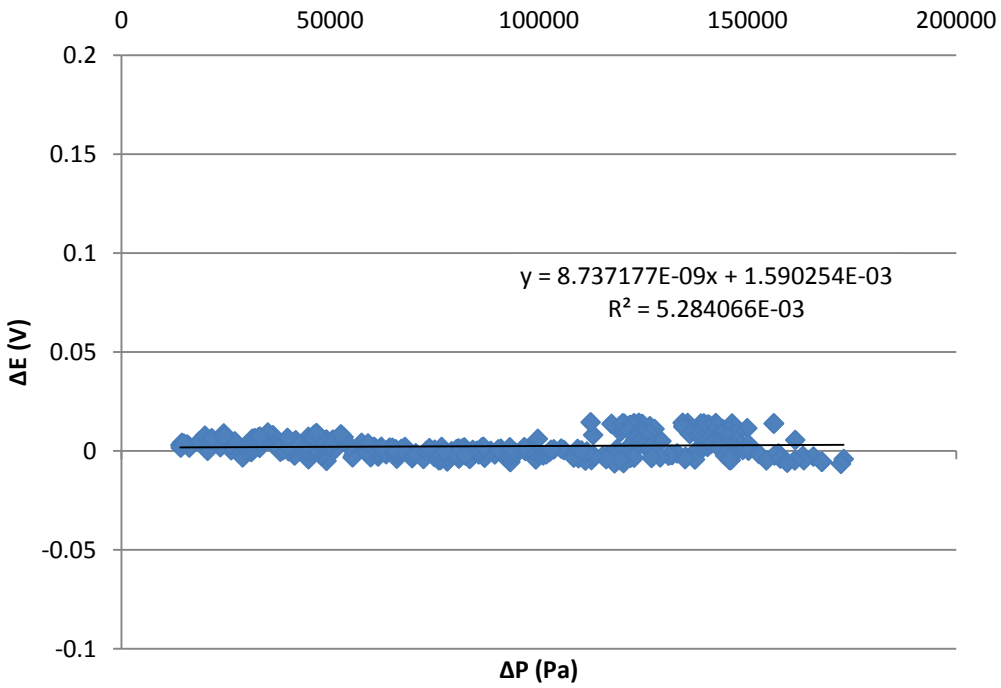

Figure 36: *ΔE* as a function of *ΔP* for ammonia solution in 233 ˚C with a linear slope fitted to data

Table 8: The zeta potential of magnetite in ammonia solution

Temperature (°C)	Zeta potential (mV)
23	-14.7
55	-17.6
128	-13.0
176	-12.9
209	-11.9
233	(0.22)

4.3 The zeta potential of magnetite as a function of temperature in ethanolamine solution

The amount of the magnetite in the measurements in ethanolamine solution was the same 2.5 g in all measurements and the length of the magnetite column was measured to be 26 mm after the measurements.

The results were processed similarly than to those in the case of ammonia. The calculation constant (Fig 37) increased when the temperature increased, in a similar fashion to the ammonia case. However, the absolute values were only about half of those for ammonia. This was due to the about twice higher resistance (Figure 32) in comparison to the case with ammonia.

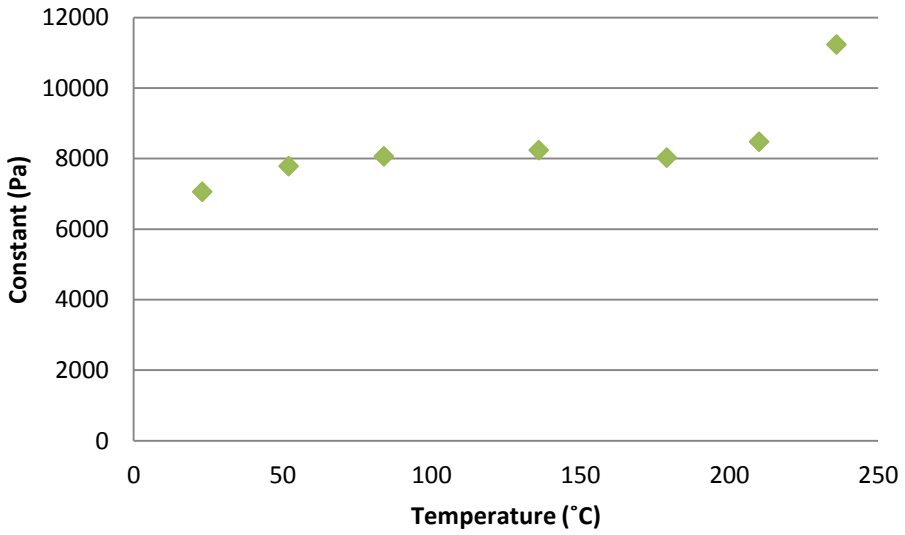

Figure 37: The calculation constant in ethanolamine solution

The absolute value of the *ΔE/ΔP* (Fig 38) decreased slowly as a function of temperature up to about T=180˚C and much faster above that, approaching zero at about T=250˚C.

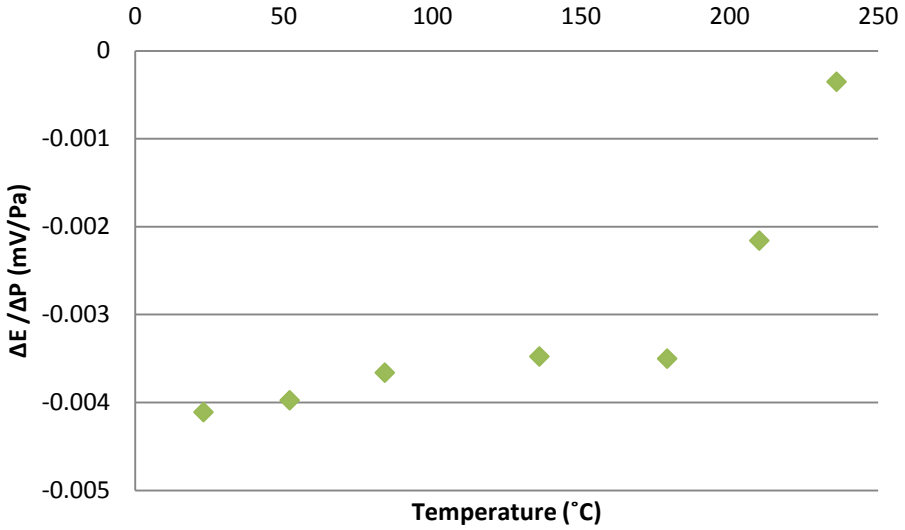

Figure 38: The *ΔE/ΔP* in ethanolamine solution

The absolute value of the zeta potential of magnetite in ethanolamine solution, Figure 39, is rather stable at roughly ζ=30 mV to about T=180˚C, after which a steady decrease is evident. The numerical values of zeta potential of magnetite are shown in Table 9.

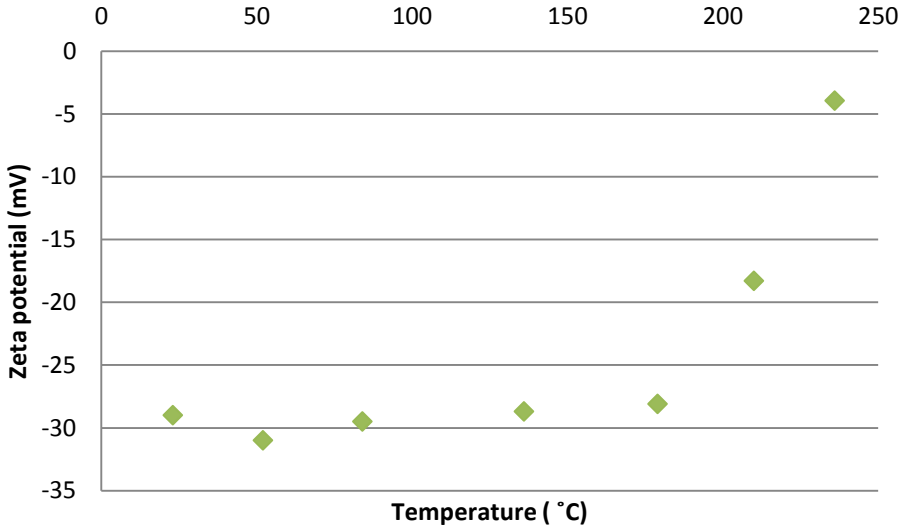

Figure 39: The zeta potential in ethanolamine solution as a function of temperature

Table 9: The zeta potential of magnetite in an ethanolamine solution

Temperature (°C)	Zeta potential (mV)
23	-29.0
52	-31.0
84	-29.5
136	-28.7
179	-28.1
210	-18.3
236	-3.95

In this case also the zeta potential value obtained at the highest temperature seems quite reliable, as the potentials of the electrodes appeared to be stabilized during the measurement. This is because the period for stabilization between the pressure changes was increased to 10 minutes.

4.4 The zeta potential of magnetite as a function of temperature in morpholine solution

The amount of the magnetite was 2.5 g for all measurements in the morpholine solution except the ones conducted at T=72 ˚C and T=218 ˚C. For those temperatures the amount of the magnetite was increased to 4 g in order to determine whether the amount of the magnetite affects the results, although it is supposed to not affect. The length of the magnetite column for 2.5 g was 26 mm and 35 mm for 4 g.

The increase in the magnetite amount can be seen in Figure 40, where the calculation constant increases slightly with increasing temperature but there are clear spikes at temperatures measured with 4 g of magnetite. This is due to the change in resistance of the magnetite columns with different amounts of magnetite.

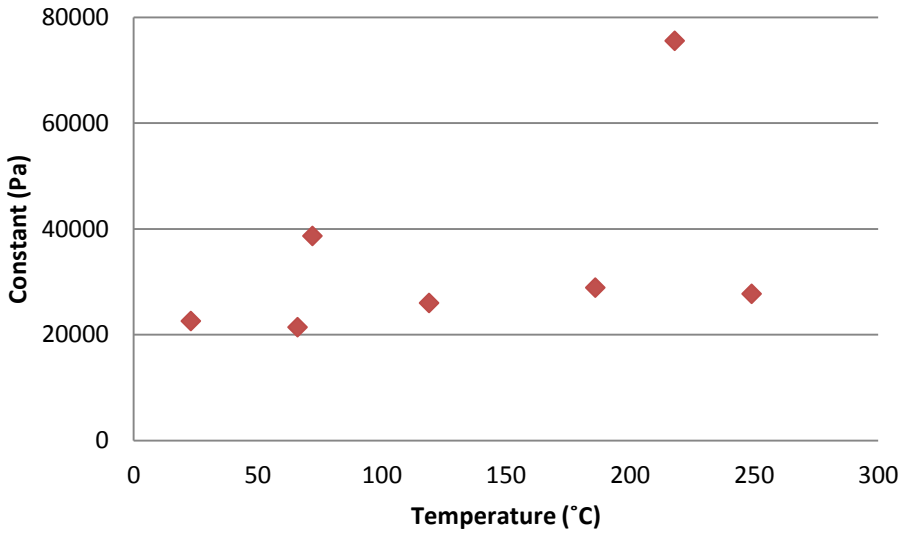

Figure 40: The calculation constant in morpholine solution

Figure 41 shows the *ΔE/ΔP*, for magnetite in morpholine solution as a function of temperature. The data points with larger amount of magnetite do not appear to deflect from the overall trend. It must be noticed that the absolute value of the *ΔE/ΔP* of magnetite decreases quite linearly in the case of morpholine solution.

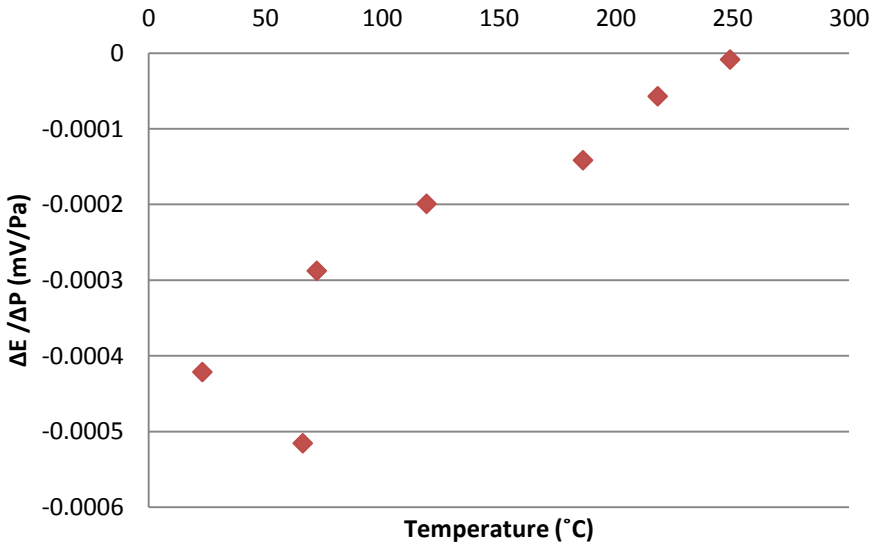

Figure 41: The *ΔE/ΔP* in morpholine solution

In the zeta potential graph (Fig 42), it seems that there is no clear effect of the length of the magnetite column on the zeta potential as the zeta potential at T= 66˚C with 2.5 g of magnetite is 11.0 mV and the zeta potential at T= 72˚C with 4 g of magnetite is 11.1 mV.

The exact values of zeta potential at the two highest temperatures have greater uncertainty, because of the stabilization problem described earlier with ammonia results. They still can show the trend of the zeta potential with increasing temperature, which seems quite linear. The exact numeric results are shown in Table 10.

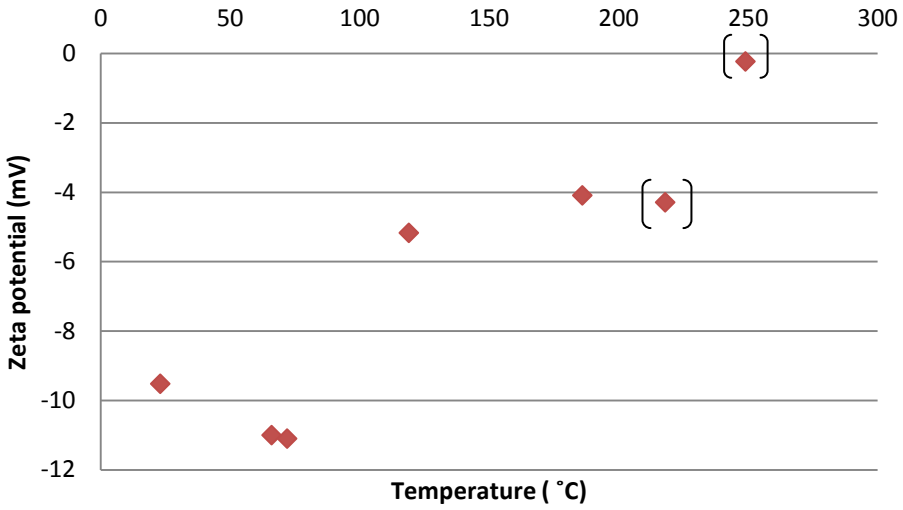

Figure 42: The zeta potential in morpholine solution as a function of temperature

Table 10: The zeta potential of magnetite in a morpholine solution

Temperature (°C)	Zeta potential (mV)
23	-9.52
66	-11.0
72	-11.1
119	-5.17
186	-4.09
218	(-4.29)
249	(-0.23)

5. Discussion

5.1 The effect of amines on the zeta potential of magnetite

The purpose of this thesis was to compare ammonia, morpholine and ethanolamine in the effectiveness of keeping magnetite particles colloidal at different temperatures, by measuring their zeta potential with the streaming potential technique. It was found out that, in the temperature range from the room temperature to 233-249˚C, the zeta potential of ammonia changed from -17.6 mV to 0.22 mV, the zeta potential of ethanolamine from -31 mV to -3.95 mV and the zeta potential of morpholine from -11.1 mV to -0.23 mV. Thus, in all cases the absolute value of the zeta potential decreased when temperature increased.

The measured zeta potential of ammonia at room temperature was compared with the zeta potential values obtained by the same equipment before (Väisänen 2012) and by values measured with commercial Zetasizer equipment before (Väisänen 2012) (Figure 43). Within the resources of this thesis, unfortunately only one data point could be produced. The measured value is seen to be somewhat lower in absolute terms than those measured by Väisänen (2012).

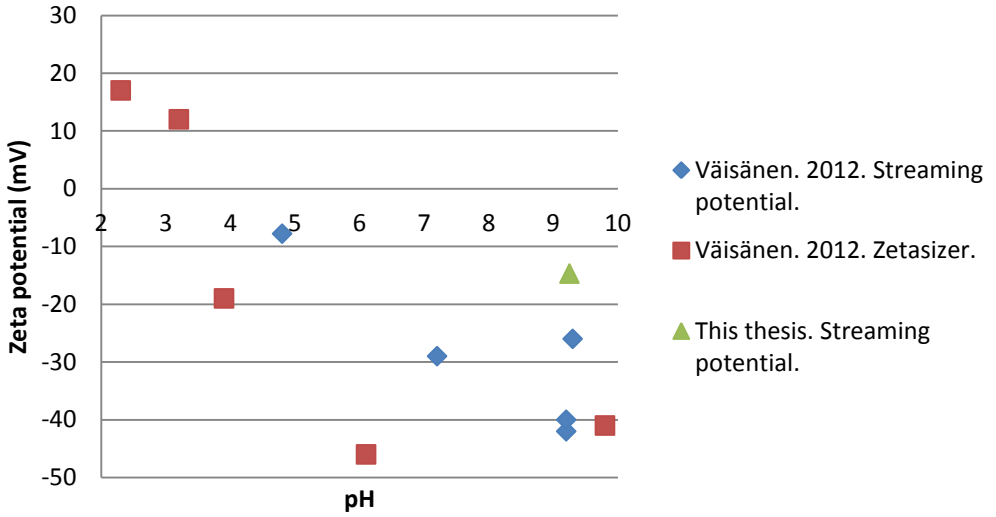

Figure 43: The zeta potential of magnetite in ammonia solution in the room temperature (Väisänen 2012)

Other data to compare with was rather scarce. There have been several measurements of the zeta potential of magnetite at room temperature (Erdemoğlu & Sarıkaya 2006. Pang et al. 2007. Vereda et al. 2008.), but the data obtained at elevated temperatures has been rare. This is because the maximum measuring temperature of the commercial zeta potential equipment is about 90˚C. The measuring principle of this equipment is to measure zeta potential with electrophoretic light scattering. (Malvern. 2013.)

Few measurements have been made at higher temperatures (Wesolowski et al. 2000. Barale et al. 2008. Vidojkovic et al. 2011). They utilized potentiometric titration (Wesolowski et al. 2000.), mass titration (Barale et al. 2008.) and particle electrophoresis technique (Vidojkovi et al. 2011.) to understand how the temperature affects to the isoelectric point of magnetite. There is one study conducted at high temperatures with streaming potential apparatus, resembling one presented in this thesis (Jayaweera et al. 1994.) but it had only one measuring temperature. The isoelectric point obtained in that measurement was 6.2, for 235˚C. That differs a little from other studies that suggest that the isoelectric point at higher temperatures is 5.31 for 250˚C (Wesolowski et al (2000), 5.2 for 250˚C (Barale et al. 2008), and 5.05 for 200˚C (Vidojkovi et al. 2011.). At room temperature, the isoelectric point was measured to be 6.5 (Pang et al. 2007.), 6.6 (Vereda et al. 2008) and 6.35 (Vidojkovi et al. 2011.).

Determining the isoelectric point has been the major focus in most of the studies and only a few give actual numbers of the zeta potentials at different temperatures. Vidojkovic et al (2011) measured that the zeta potential at T=25˚C and at pH 9.51 was -140.9 mV and the zeta potential at T=200˚C at pH 7.3 was -76.6 mV. The KNO_3 10^{-4} mol kg^{-1} solution was used for the background electrolyte. (Vidojkovic et al. 2011). The isoelectric point was not determined in this thesis, because all measurements were conducted at constant pH. It was noticed that for justifying the usage of the measuring method and equipment used in this thesis, the measuring of the isoelectric point in high temperatures should be done. It would also be interesting to see how the isoelectric point changes as a function of temperature.

Comparing different studies has turned out to be difficult, because the zeta potential of magnetite has been measured in several measuring medium and background electrolytes (KNO_3, NaTr, NaOH, HNO_3 etc.), which have been used to change the pH of the solution and to make the measurement possible by increasing the conductivity of the water. Only a few measurements (Bénézeth et al. 2009.) have been conducted to measure the zeta potential of magnetite in solution used in this thesis, but they also used other measuring mediums at the same time. In their study, Bénézeth et al (2009) found out that the measuring medium affected to the zeta potential of magnetite so much that it was impossible to say whether the morpholine or ethanolamine had any influence on the zeta potential of magnetite.

One aim in this thesis was to find out how temperature affects the zeta potential values of magnetite in water treated with different amines. It was found out that an increase in the temperature induces a decrease in zeta potential magnitude in case of all additives studied. However, in case of both ammonia and ethanolamine, Figures 35 and 39, the zeta potential value was essentially constant until T ≈200˚C, after which a rapid decrease in magnitude was observed. In the case of morpholine, the zeta potential magnitude increased with a rather constant rate from T=23˚C to T=249 ˚C. Clearly, more data points would be needed to rule out the effect of variability in the trend.

Figure 44 presents the pH of ammonia, morpholine and ethanolamine solution and the pH of pure water as a function of temperature. It can be seen that pH decreases dramatically as a function of temperature in all cases (for the temperature range in question). As discussed earlier (page 37) decreasing pH changes negative zeta potentials to the positive direction. Thus, it is difficult to discern between the effect of the decreasing pH on the zeta potential and the direct influence of the temperature. All in all, it seems certain that temperature affects zeta potential also by decreasing pH.

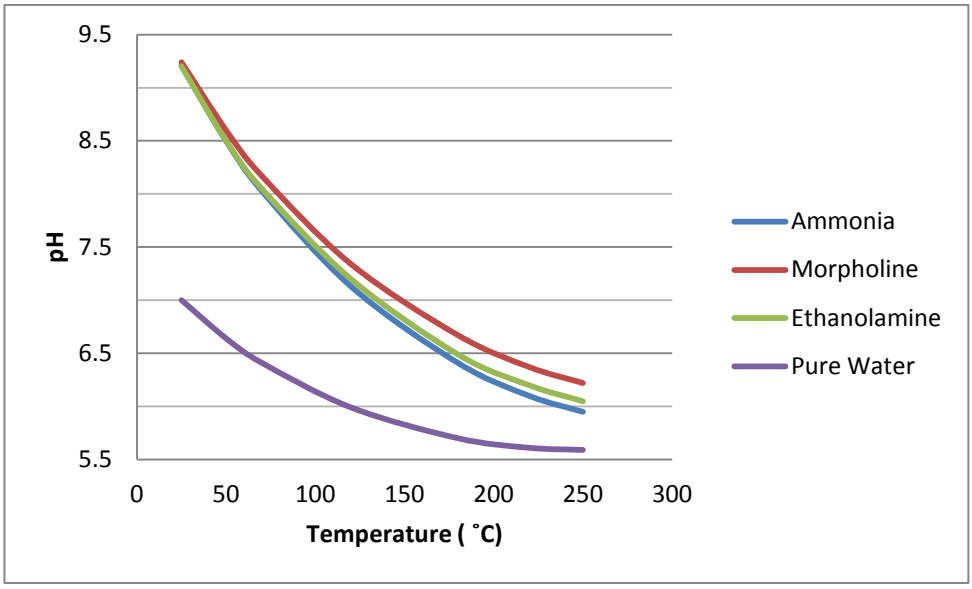

Figure 44: The pH of the ammonia, morpholine and ethanolamine solutions and the pH of pure water as a function of temperature. Ethanolamine values from EPRI 1997b, other values from EPRI Multiple Equilibria Program Multeq-Redox 2.1

Reppert & Morgan (2003) brought some clarification by declaring that the streaming potential changes over temperature and this change can't be explained purely by the change in water viscosity, permittivity and conductivity but the zeta potential is also dependent on temperature. They also claim that the negative zeta potential values increase with temperature and this is controlled primarily by the surface charge density. (Reppert & Morgan 2003) The results obtained in this thesis are similar to this statement. Nonetheless, it seems clear that the subject is not fully studied as there is some disagreement between different studies, and so this study was clearly needed, even though the certainty was still not reached. For example, Varrin (1996) states that the increase in temperature induces always a decrease in the zeta potential, also with the negative values.

In order to resolve whether the magnetite particles will attach to the surfaces or not, it is essential to know also the zeta potential values of the surfaces. According to Guillodo et al (2012), Type Z10C13 stainless steel has a zeta potential of +4250 mV at pH of 6.45 measured at 275˚C at morpholine solution. In ethanolamine solution, its zeta potential in the same conditions was -125 mV. (Guillodo et al. 2012.) It must be emphasized that amines and ammonia not only change the zeta potential of magnetite particles but also the zeta potential of the steel surfaces, and already existing deposits (Varrin 1996). From values presented by Guillodo et al (2012) it seems that ethanolamine would be a better fouling inhibitor than morpholine. Varrin (1996) presents that the reason why tube surfaces usually have negative zeta potential is their propensity to collect hydroxyl groups at various temperatures and pressures. Varrin (1996) continues that surfaces will attract magnetite particles, if the secondary side pH at high temperature is between 5.3 and 6.0 (Varrin 1996), which according to Figure 44, is the case in the ammonia treatment with pH_{RT}=9.2. It would be important to measure the zeta potential for steel particles with the equipment used in this thesis to broaden the knowledge upon the zeta potential of the steam generator construction materials.

It is most likely, that if the zeta potential of the magnetite particles and the zeta potential of the steam generator surfaces are too different to each other, the particles will attach to the surfaces. However, if the zeta potential of the magnetite particles is too close to zero, the particles will attach to each other. In this thesis, it was found out that the zeta potential of magnetite is zero in ammonia solution at approximately T=232˚C, in ethanolamine solution at T=238˚C, and in morpholine solution at T=251˚C. Temperatures were gained by the extrapolation of the result curves. Those temperatures are all still quite low in the steam generator scale, and should be higher, if these compounds really inhibit fouling in the steam generator. With these values, it is highly possible that magnetite particles attach to themselves in the steam generator. It is still unclear, whether amines decrease fouling by affecting particles in the steam generator, or do they simply only reduce flow accelerated corrosion so much that also fouling rates decrease. It might even be possible that amines are doing harm in the steam generator. Varrin (1996) states that amines may decrease the amount of corrosion product transport but increase the fouling (Varrin 1996).

Fouling rates with different amines have been studied reasonably much, as there are many nuclear power plants with a large variety of different amines used especially in the USA. In those studies, it appears that the highest fouling rates are obtained when using pyrrolidine and monoethanolamine. The lowest fouling rates are achieved when using a combination of dodecylamine and monoethanolamine. Morpholine is a better fouling inhibitor than ethanolamine. (EPRI & AECL 2002. Klimas et al. 2003) This can be seen in Figure 45. When compared with water with the same pH but no amines, both morpholine and ETA are actually increasing the fouling rate. (EPRI & AECL 2002)

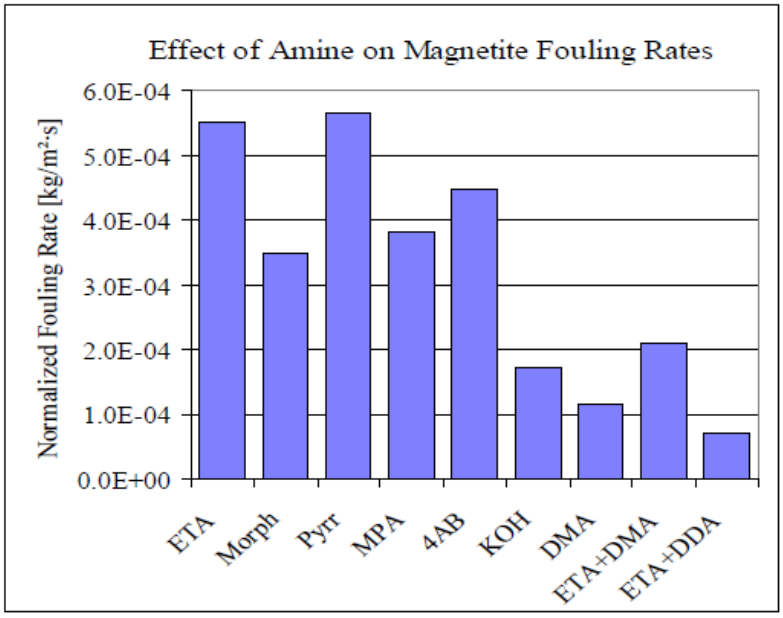

Figure 45: Effect of amine on magnetite fouling rates. (EPRI & AECL 2002)

There have been also other studies concerning the superiority of different amines. In the study of Delaunay et al. (2010) it was found that in one-phase flow conditions at 220 ˚C, morpholine and ethanolamine prevented magnetite deposits better than ammonia. (Delaunay et al. 2010.) EPRI & AECL (2003), on the contrary, declare that ammonia might be a better fouling inhibitor that ethanolamine or morpholine. The superiority between morpholine and ethanolamine is not so obvious either as EPRI & AECL (2002) and Klimas et al. (2003) have come to the conclusion that morpholine is better, whereas Olmedo et al. (2012) found out that combination of hydrazine and ethanolamine prevented fouling and corrosion product release slightly better than hydrazine and morpholine in degassed conditions (Olmedo et al. 2012). Also Guillodo et al (2012) suggest using ETA. (Guillodo et al. 2012.)

There is also the third opinion as Bénézeth et al. (2009) declare that amines have no effect on the magnetite surface charge at 200 and 250°C in 0.03 mol·kg^{-1} NaTr (sodium trifluoromethanesulfonate) and come to the conclusion that pH and ionic strength are controlling the surface charge, not the properties and nature of the amine itself. (Bénézeth et al. 2009) It must be remembered that fouling and the surface charge are not directly related, but surface charge probably has a remarkable effect on fouling.

During the measurements of this thesis, it was noticed that the magnetite column must be changed between the different solutions, because at least morpholine attached to the magnetite particles so well, that results obtained in the following ammonia measurements were values typical for zeta potentials of magnetite in morpholine solution. This might suggest that the mechanism how the amines affect particles is not entirely controlled by pH, but the properties of the amine itself are important too.

Also Varrin (1996) states that amines affect the magnetite particles by other mechanisms than strictly only by changing pH. ETA and morpholine treatments have been observed to produce more magnetite particles with a diameter of 0.1 to 0.5 µm, whereas ammonia treatment produces larger particles with a diameter of 1 to 3 µm. This can lead to the result of thicker tube deposits with ETA or morpholine. However, the effect on pH of ETA and morpholine is greater than that of ammonia, which can cancel the effect of the particle size. Then again, higher pH can cause the formation of more soluble ferrous hydroxides which can act like “glue” for deposit formation. But on the other hand, there is reason to believe that high pH lowers both the zeta potential of the particle and the zeta potential of the steam generator surface, so that particle-surface attraction will be stronger. Because ETA and morpholine induce smaller particles, it may mean that with ETA and morpholine, magnetite particles will repulse each other stronger than with ammonia solution. (Varrin 1996)

There is also a problem with testing fouling in laboratory conditions. The laboratory measurements cannot fully predict the fouling phenomena in a real system as the synthetic deposit has not exactly the same porosity, density, particle size or zeta potential as a real deposit (EPRI 2003). The real deposit also consists of different species which are suggested to have different zeta potentials (Table 11).

Table 11: Zeta potential for several species in the steam generators (Varrin 1996)

Material	Approximate Zeta potential at pH 10 and 25 ˚C (mV)
Magnetite	-170
Ferrous Hydroxide	+120
Hematite	-90
Nickel Oxides and Hydroxides	+80
Aluminium Oxide	-50
Copper Oxides and Hydroxides	-30
Chromium Oxide	+50

5.2 Error analysis

One possible source of error in the measurements conducted in this thesis was the measurement of the change in the potentials of the platinum electrodes and the change in the pressure difference between the ends of the magnetite column if the system is not stable. The data ranges where the potentials were clearly not stabilized were eliminated from zeta potential measurements, but especially at high temperatures, it seemed that the system never reached a fully stable stage. The error originating from the instability of the system was attempted to analyze by derivation (19, 20) of the zeta potential formula (18).

$$\zeta = \frac{\Delta E}{\Delta P} \cdot constant \qquad (18)$$

$$\frac{d\zeta}{d\Delta E} = \frac{1}{\Delta P} \qquad (19)$$

$$d\zeta = \frac{1}{\Delta P} \cdot d\Delta E \qquad (20)$$

From formula 20 it is evident that the error in the electrode potentials induces the greatest error in the zeta potential when the pressure difference is small, and the error in the pressure difference induces the greatest error in the zeta potential when the electrode potentials are small. This means that the error in the electrode potentials is meaningful at small water velocities and thus possibly minimized by using reasonably high water velocities. The error in the pressure difference, which was estimated to be quite small, is thus a source of scatter especially at high temperatures.

Surprisingly, the error resulting from the short-timed shifting of the potentials was measured to be usually lower than 2 %. This was obtained by calculating zeta potential values of the same measurement either after removing the data ranges where the system was not stable or letting the data go untouched. The error created by potentials shifting for the whole measurement at high temperatures was found to be hard to evaluate, and thus the most uncertain high temperature zeta potential values were left to brackets. It was furthermore noticed that increasing the stabilizing time resulted as more stable potentials. High temperature measurements should thus be redone in order to achieve more reliable data, with stabilizing time of 30 minutes or more.

It was estimated that one of the greatest sources for error is the measuring of the length of the magnetite column, which was done after the measurement. The magnetite column compressed differently in each measurement and the length of the magnetite column was thus slightly different in each measurement. Sometimes the magnetite column was also noticed to be in two separate sections, or be consisting of a solid column and a more slurry-like border area. It was also noticed that the stopper, supposed to keep the column in its place, stayed steadily in its place while the magnetite column compressed. Thus, in order to measure the length of the magnetite column, it was necessarily to move the stopper nearer the column and then there was the danger of pressing the column itself. This was a problem, because it was found very difficult to get the whole magnetite column out of the tube without breaking it, so it had to be measured still in the tube. All the magnetite columns were measured, but it was clear that some of the column length measurements were not valid, as e.g. in one case the length of the magnetite column of 2.5 g was nearly the same or even larger than the one with 4 g.

This was solved by doing some careful measurements to columns both in the tube and out of the tube, evaluating the truthfulness of several different results, and applying two heights, 26 mm for 2.5 g and 35 mm for 4 g, to all of the results, which were thought to be the most correct. This means that there is some error in the length of the column. However, since all measurements were conducted with one column for one solution (except two for morpholine), the trend in measured zeta potentials is valid, because the possible error in column length is systemic within the measurements with each chemical. On the other hand, it is possible that the column compressed more after several measurements in the same solution, so the length of the magnetite column might be greater for lower temperatures and lesser for higher temperatures. The length of the 26 mm long magnetite column was 34 mm before the measurement, but it is unclear if all the compressing happened during the first pressure increasing period. The maximum differences in the lengths of magnetite columns were in the order of 10 mm, which means a maximum error of 25%. This means that the length of the magnetite column is indeed a great source of error that must be minimized if possible.

There was also possibility of error by electrical disturbance in the electrodes or electrical measuring equipment. One data point with ammonia solution was discarded because it was thought that there was some kind of contact failure between the electrodes and the measuring equipment.

In the measurements of zeta potential, it must be remembered that the impedance measurement contains the impedances of the magnetite column, the solution, the zirconium stopper and the ceramic filter. In Figure 32, at room temperature the difference between the measured impedance in the case of ethanolamine is about double to that of ammonia, even though the measured solution conductivity was almost the same. This result indicates that the solution resistance does not play an important role in the measured impedance. As the only variable between these two experiments was the chemical used, it can also be concluded that the role of the zirconium stopper and the ceramic filter are negligible. Also the actual zeta potential values contain the zeta potential of the magnetite column, the zeta potential of the zirconium stopper and the zeta potential of the ceramic filter. Most likely the greatest effect on those values origins from the magnetite column, but the other components should be evaluated as well. It was noticed, for example that ceramic filter has to be changed at times, because it was obstructed by the smallest of magnetite particles and consequently pressure difference increased.

In order to improve the reliability of the measurements, the number of repetitions should be increased and the measurements should be repeated not only with the equipment used in this thesis but also with other facilities working with the same or different measuring principle. This way it could be convinced that accurate zeta potential values can be measured at high temperatures with the streaming potential method. The amount of data points in this thesis was too small to make any definite conclusions about the superiority between the amines. There should have been several data points for every solution and every temperature, but because of the limited time, there is only one data point at each temperature.

6. Conclusions

Magnetite deposition causes severe material degradation and thermal degradation problems in the steam generators. Deposition of the magnetite particles is at least partly affected by the surface charge of the particles. The magnitude and the sign of the surface charge can be described with the zeta potential. Within this thesis, the zeta potential measurement equipment based on streaming potential measurement was successfully updated to allow for measurements up to T=250˚C. The zeta potential values of magnetite particles in ammonia, morpholine and ethanolamine containing solutions with pH=9.2 were determined as a function of temperature. There are no previous studies concerning the effect of ammonia, morpholine and ethanolamine on the zeta potential of magnetite at high temperatures, even though they are widely used chemicals in the nuclear power plants.

It was found that in the temperature range from the room temperature to about T=248˚C, the zeta potential of ammonia changed from -17.6 mV to 0.22 mV, the zeta potential of ethanolamine from -31 mV to -3.95 mV and the zeta potential of morpholine from -11.1 mV to -0.23 mV. Thus in all cases the magnitude of the zeta potential decreased as temperature increased. As the pH of water decreases with increasing temperature, it could be at least partially the reason for increasing zeta potential. Nonetheless, Reppert & Morgan (2003) declare that the change in the streaming potential with increasing temperature is dependent also purely on temperature as the change can not be exclusively explained with changes in water viscosity, permittivity and conductivity.

The room temperature result for ammonia solution was the only one that could be strictly compared to the literature. Väisänen (2012) presents that the value for zeta potential of magnetite in ammonia solution of pH=9.2 is between -26mV and -42mV when measured with streaming potential method and -41mV when measured with Zetasizer. The value for zeta potential measured in this thesis under similar conditions was -14.7 mV, which is clearly smaller. This may be due to the fact that the data point measured in this thesis was measured in de-oxygenated solution and the results reported by Väisänen (2012) were measured in solution where oxygen was present. Nonetheless, it seems clear that repeated measurements should be conducted.

Sources

Adamson, Arthur W. Gast, Alice P. 1997. Physical Chemistry of Surfaces. Sixth edition. John Wiley & Sons, Inc. ISBN 0-471-14873-3

Barale, M. Mansour, C. Carrette, F. Pavageau, E.M. Catalette, H. Lefèvre, G. Fedoroff, M. Cote, G. 2008. Characterization of the surface charge of oxide particles of PWR primary water circuits from 5 to 320 ˚C. Journal of Nuclear Materials, Vol. 381. pp. 302-308.

Basset, Mark. McInerney, Jeff. Arbeau, Norm. Lister, Derek H. 2000. The Fouling of Alloy-800 Heat Exchange Surfaces by Magnetite Particles. The Canadian Journal of Chemical Engineering, Volume 78.

Bénézeth, Pascale. Wesolowski, David J. Palmer, Donald A. Machesky, Michael L. 2009. Effect of Amines on the Surface Charge Properties of Iron oxides. J Solution Chem, 38. pp. 925-945.

Delaunay, Sophie. Pavageau, Ellen-Mary. Mansour, Carine. Cote, Gérard. Fédoroff, Michel. Bretelle, Jean-Luc. 2010. Comparison of ammonia, morpholine and ethanolamine as conditioning agent on the formation and deposition of iron oxides on stainless steel and carbon steel in conditions of PWR secondary circuits. Nuclear Plant Chemistry Conference 2010. October 3-8. Quebec City, Canada.

Delgado, A. V. González-Caballero, F. Hunter, R. J. Koopal, L. K. Lyklema, J. 2005. Measurement and interpretation of elektrokinetic phenomena. IUPAC Technical Report. Pure Applied Chemistry, Vol. 77, No. 10. pp. 1753-1805.

Diercks, D. R. Shack, W. J. Muscara, J. 1999. Overview of steam generator tube degradation and integrity issues. Nuclear Engineering and Design, 194. pp. 19-30.

Dooley, R. B. Chexal, V. K. 2000. Flow-accelerated corrosion of pressure vessels in fossil plants. International Journal of Pressure Vessels and Piping, 77. pp. 85-90.

Dooley, R. Barry. 2008. Flow-Accelerated Corrosion in Fossil and Combined Cycle/HRSG Plants. PowerPlant Chemistry, 10(2).

Dvoršek, T. Cizelj, L. Mavko, B. 1998. Safety and availability of steam generator tubes affected by secondary side corrosion. Nuclear Engineering and Design, 185. pp.11-21.

Elimelech, M. Gregory, J. Jia, X. Williams, R. A. 1995. Particle Deposition and Aggregation: Measurement, Modelling and Simulation. Butterworth-Heinemann. ISBN 0-7506-7024-X

EPRI, Electric Power Research Institute. 1997a. Plant-Specific Optimization of LWR Water Chemistry. Millet, Peter. Wood, Chris. Frattini, Paul. Ocken, Howard. Gaudreau, Tina. TR-107329.

EPRI, Electric Power Research Institute. 1997b. Advanced Amine Application Guidelines, EPRI, Palo Alto, CA. TR-102952.

EPRI, Electric Power Research Institute. 1999. Effects of Morpholine on the Surface Charge Properties of Magnetite. Palo Alto, CA.

EPRI, Electric Power Research Institute. 2003. Multivariable Assessment of Flow Accelerated Corrosion and Steam Generator Fouling: Literature Review. Technical Report.

EPRI, Electric Power Research Institute. 2004. Pressurized Water Reactor Secondary Water Chemistry Guidelines – Revision 6. Technical report. Palo Alto, CA.

EPRI, Electric Power Research Institute. AECL, Atomic Energy of Canada Limited. 2002. Identification and Testing of Amines for Steam Generator Chemistry and Deposit Control. Technical Report.

EPRI, Electric Power Research Institute. AECL, Atomic Energy of Canada Limited. 2003. Identification and Testing of Amines for Steam Generator Chemistry and Deposit Control, Part 2. Technical report.

Epstein, Norman. 1997. Elements of Particle Deposition onto nonporous solid surfaces parallel to suspension flows. Experimental Thermal and Fluid Science, 14. pp. 323-334. Elsevier Science Inc.

Erdemoğlu, Murat. Sarıkaya, Musa. 2006. Effects of heavy metals and oxalate on the zeta potential of magnetite. Journal of Colloid and Interface Science, Vol 300. pp. 795-804.

Fruzzetti, Keith. 2009. Operating Experience Driven Advancements in Plant Chemistry Practices and Standards. 6th CNS International Steam Generator Conference, November 8 – 11, 2009. Toronto, Ontario, Canada.

Green, S. J. & Hetsroni, G. 1995. PWR steam generators. International Journal of Multiphase Flow, Vol 21, suppl. pp. 1-97.

Guillodo, Michaël. Guingo, Mathieu. Foucault, Marc. Ryckelynck, Natacha. Chahma, Farah. Mansour, Carine. Alos-Ramos, Olga. Corredera, Géraldine. 2012. Experimental and numerical study of deposit formation in secondary side SG TSP by electrokinetic approach. Nuclear Plant Chemistry Conference 2012. September 23-27. Paris, France.

Harrod, D. L. Gold, R. E. Jacko, R. J. 2001. Alloy Optimization for PWR Steam Generator Heat-Transfer Tubing. Journal of Materials, Jul 2001, 53, 7. pg. 14.

Hunter, Robert J. 1981. Zeta Potential in Colloid Science, Principles and Applications. Academic Press inc. London. ISBN 0-12-361960-2. ISSN 0305-9723.

IAEA, International Atomic Energy Agency. 2011. Assessment and Management of Ageing of Major Nuclear Power Plant Components Important to Safety: Steam Generators. 2011 Update. International Atomic Energy Agency, Vienna. IAEA-TECDOC-1668. ISBN 978-92-0-121410-2. ISSN 1011-4289.

Israelachvili, Jacob N. 2011. Intermolecular and surface forces. Third edition. Academic press, Elsevier. United States of America. ISBN 978-0-12-375182-9.

Jayaweera, P. Hettiarachchi, S. 1992. Determination of zeta potential and pH of zero charge of oxides at high temperatures. Rev. Sci. Instrum. 62 (2). American Institute of Physics.

Jayaweera, P. Hettiarachchi, S. Ocken, H. 1994. Determination of the high temperature zeta potential and pH of zero charge of some transition metal oxides. Colloids and Surfaces. Vol 85. pp. 19–27.

Klimas, S.J. Fruzzetti, K. Turner, C. W. Balakrishnan, P. V. Strati, G. L. Tapping, R. L. 2003. Identification and Testing of Amines for Steam Generator Corrosion and Fouling Control. Refereed proceedings, Heat exchanger fouling and cleaning: fundamentals and applications. Engineering conferences international.

Malvern. 2013. Zetasizer Nano series. Product Brochure. available: http://www.malvern.com/common/downloads/MRK1839.pdf, cited 25th November 2013.

Murtomäki, Lasse. Kallio, Tanja. Lahtinen, Riikka. Kontturi, Kyösti. 2010. Sähkökemia. 2. ed. Kopijyvä Oy. Jyväskylä, 2010.

Nordmann F. 2006. IAEA Workshop on Optimizing the Chemistry Model of the Secondary Circuit with ETA. Tianwan NPP, China. 4 – 7 September 2006.

Nordmann, Francis. Fiquet, Jean-Marie. 1996. Selection criteria for the best secondary water chemistry. Nuclear Engineering and Design, Vol 160. pp. 193-201.

Odar, Suat. Nordmann, Francis. 2010. PWR and VVER secondary system water chemistry report. Advanced Nuclear Technology International.

Olmedo, A.M. Bordoni, R. Strack, M. 2012. Characterization of the oxide films grown at 260 ˚C in a simulated secondary coolant of a nuclear reactor. 11th International Congress on Metallurgy & Materials SAM/CONAMET 2011. Procedia Materials Science. Vol. 1. pp. 528-534.

Pang, Suh Cem. Chin, Suk Fun, Anderson, Marc A. 2007. Redox equilibria of iron oxides in aqueous-based magnetite dispersions: Effect of pH and redox potential. Journal of Colloid and Interface Science, Vol 311. pp. 94-101.

Pat. US 5280250. 1994. Method and apparatus for measuring ζ potential of a substance at high temperature. Electric Power Research Institute, Inc., Palo Alto, California. Jayaweera, P. Hettiarachchi, S. Appl. No. 769174, 30.9.1991. 18.1.1994. 10p.

Reppert, Philip M. Morgan, Frank Dale. 2003. Temperature-dependent streaming potentials: 1. Theory. Journal of Geophysical Research. Vol. 108, No. B11.

Rummens, Helena E. C. Rogers, J. T. Turner, C. W. 2004. The thermal hydraulics of tube support fouling in nuclear steam generators. Nuclear Technology, vol. 148.

Saddler, M. A. Tittle, K. Wetton, E. A. M. Lewis, G. G. 1989. The application of amine conditioning to PWR secondary steam-water circuits. Central Electricity Generating Board. Operational Engineering division Scientific and Technical Branch, Northern Area. Report No. OED/STN/88/0766/R. Job No. ZE 271.

Schwarz, Thomas. 2001. Heat transfer and fouling behaviour of Siemens PWR steam generators – long term operating experience. Experimental Thermal and Fluid Science, 25. pp. 319-327.

Seifert, H.-P. Hickling, J. Lister, D. 2012. Corrosion and Evironmentally-Assisted Cracking of Carbon and Low-Alloy Steels. In Comprehensive Nuclear Materials, ed. Konings, R. J. M. Elsevier. ISBN: 978-0-08-056033-5

Srikantiah, G. Chappidi, P. R. 2000. Particle deposition and fouling in PWR steam generators. Nuclear Engineering and Design, 200. pp. 285-294.

Staehle, R.W., et al., 2001. Progress in understanding and mitigating corrosion on the secondary side in PWR steam generators, Proceedings of the 10th International Symposium on Environmental Degradation of Materials in Nuclear Power Systems, Lake Tahoe.

Stumm, W. 1992. Chemistry of the Solid-Water Interface, John Wiley, New York

Tapping, R. L. Nickerson, J. Spekkens, P. Maruska, C. 2000. CANDU steam generator life management, technical note. Nuclear Engineering and Design, 197. pp. 213-223.

Tipping, Philip. 1996. Lifetime and ageing management of nuclear power plants: a brief overview of some light water reactor component ageing degradation problems and ways of mitigation. International Journal of Pressure Vessels and Piping, 66. pp. 17-25.

Turner, C. W. Liner, Y. Carver, M.B. 1994. Modelling magnetite particle deposition in Nuclear Steam Generators. 2nd International Steam Generator and Heat Exchanger Conference, Toronto, Ontario, 1994 June 13-15.)

Turner, Carl W. 2011. Implications of Steam Generator Fouling on the Degradation of Material and Thermal Performance. 15th International Conference on Environmental Degradation of Materials in Nuclear Power Systems – Water reactors. Colorado Springs, USA, August 7 – 11, 2011.

Turner, Carl W. Klimas, Stan J. 2000. Deposition of Magnetite Particles from Flowing Suspensions under Flow-Boiling and Single-Phase Forced-Convective Heat Transfer. The Canadian Journal of Chemical Engineering, Vol. 78.

Turner. Klimas. Guzonas. Frattini. Fruzzetti. 2002. New insights into controlling tube-bundle fouling using alternative amines. International Conference on Water Chemistry in Nuclear Reactor System.

Väisänen, Saija. 2012. Magnetiitin zeta-potentiaali painevesivoimalaitoksen sekundääripiiriä vastaavissa olosuhteissa. Master's Thesis. Tampereen teknillinen yliopisto, teknis-luonnontieteellinen koulutusohjelma.

Varrin, R. 1996. Characterization of PWR Steam Generator Deposits. EPRI, Palo Alto CA. TR-106048.

Vereda, F. de Vicente, J. Hidalgo-Álvarez, R. 2008. Colloidal characterization of micron-sized rod-like magnetite particles. Colloids and Surfaces A: Physiochem. Eng. Aspects. Vol. 319. pp. 122-129.

Vidojkovic, Sonja. Rodriguez-Santiago, Victor. Fedkin, Mark V. Wesolowski, David J. Lvov, Serguei N. 2011. Electrophoretic mobility of magnetite particles in high temperature water. Chemical Engineering Science, Vol. 66. pp. 4029-4035.

Weeks, John R. Czajkowski, Carl J. 1982. The degradation of steam-generator tubing and components by operation of pressurized-water reactors. Brookhaven National Laboratory, New York.

Wesolowski, David J. Machesky, Michael L. Palmer, Donald A. Anovitz, Lawrence M. 2000. Magnetite surface charge studies to 290 ˚C from in situ pH titrations. Chemical Geology, Vol 167. pp. 193-229.

White, G. A. Kreider, M. E. Varrin, R. D. 1998. A Global Fouling Factor Methodology for Analyzing Steam Generator Thermal Performance Degradation. KAPL Atomic Power Laboratory. KAPL-P-000065

Wilam, M. Čermáková, I. 1995. Integrity of VVER steam generator tubes. Theoretical and Applied Fracture Mechanics, Vol 23, Issue 2. pp. 151-153

Woo, H. H. Lu, S. C. 1981. Worldwide Assessment of Steam-Generator Problems in Pressurized-Water-Reactor Nuclear Power Plants. Lawrence Livermore Laboratory. UCRL-53032.

Wood, C. J. 2012. Water Chemistry Control in LWRs. In Comprehensive Nuclear Materials, ed. Konings, R. J. M. Elsevier. ISBN: 978-0-08-056033-5